論文 / 著書情報
Article / Book Information

題目(和文)	赤外分光法を用いたZSM-5ゼオライト上で進行するメタノールからの炭化水素生成に関わる炭素-炭素結合の形成機構に関する研究
Title(English)	Infrared study on mechanisms of C-C bond formation during methanol-to-hydrocarbons reaction over ZSM-5 zeolite
著者(和文)	山崎弘史
Author(English)	Hiroshi Yamazaki
出典(和文)	学位:博士(理学), 学位授与機関:東京工業大学, 報告番号:甲第9412号, 授与年月日:2014年3月26日, 学位の種別:課程博士, 審査員:野村　淳子,北村　房男,酒井　誠,馬場　俊秀,原　亨和
Citation(English)	Degree:Doctor (Science), Conferring organization: Tokyo Institute of Technology, Report number:甲第9412号, Conferred date:2014/3/26, Degree Type:Course doctor, Examiner:,,,,
学位種別(和文)	博士論文
Type(English)	Doctoral Thesis

Doctor thesis

Infrared study on mechanisms of C-C bond formation during methanol-to-hydrocarbons reaction over ZSM-5 zeolite

(和訳: 赤外分光法を用いた ZSM-5 ゼオライト上で進行するメタノールからの炭化水素生成に関わる炭素-炭素結合の形成機構に関する研究)

This thesis was submitted to Tokyo Institute of Technology for the degree of Doctor of Science.

Hiroshi Yamazaki (11D27050)

Department of Electronic Chemistry

Interdisciplinary Graduate School of Science and Engineering

Tokyo Institute of Technology

Contents

Chapter I General introduction

Chapter II Experimental

Chapter I

General Introduction

1. Zeolites

Zeolites and related zeotypes are microporous crystalline materials that play important roles in catalysis, ion exchange, and adsorption sciences, and the molecular-sieving properties of zeolites are exploited in many industrial applications [1-5]. Proton-form zeolites have been used in several hydrocarbon conversion reactions. The excellent activity of these materials is due to two main properties: shape selectivity associated with the well-defined porous structure and a strong acidity of acidic OH groups generated by the presence of aluminum inside the silicate framework.

1.1. Structure of zeolites

Zeolites and related zeotypes are crystalline microporous materials with well-defined pores and cavities of molecular dimensions. Their frameworks are composed of TO_4 tetrahedra (with T = Si, Al, P, Ti, Sn etc.), which is called "primary building units", connected by oxygen atoms (Figure I-1). However, this bulding units solely does not characterize the zeolite framework. "Secondary building units (SBU)", shown in Figure I-2, is widely used to characterize the zeolite framework [6]. These SBU's, which contain up to 16 T-atoms, are derived assuming the entire framework is made up one type of SBU only. The number of observed SBU's has increased from 16 in 1992 to 23 at 2013 [6].

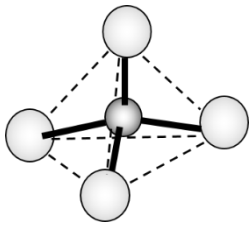

Figure I-1. TO4 (T = Si, Al etc.)

The system of channels and/or cavities of zeolites make the solids with very high surface area and pore volume, which are able to absorb a great amount of molecules. Furthermore, because of both crystalline structures and microporous structures in molecular dimensions, which provide

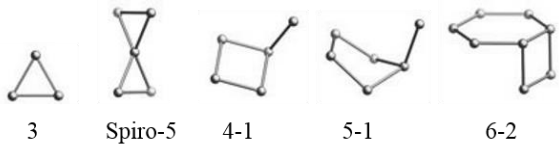

Figure I-2. A partial example of secondary building units of zeolite framework.

nano-sized reaction field to reactants, zeolites can be regarded as "uniform heterogeneous catalysts" that will act as model catalysts [7].

Pure silicate materials (SiO_2) do not contain framework charge since silicon is tetravalent. However, substituting a part of Si sites by Al atoms, the zeolite framework has a net negative charge equal to the number of aluminum sites. This negative charge is balanced by either metal cations (metal-cation-exchanged zeolites) or protons (H-form zeolites). Existence of these counter ions in zeolites cages make zeolites very useful as functional materials, such as ion exchangers, sorbents, gas separator and catalysts especially. The general formula of aluminosilicate zeolite is, then, expressed as follows:

$$\mathrm{M}_{n/a}{}^{a+}\,(\mathrm{SiO}_2)_m(\mathrm{AlO}_2)_n \cdot x\mathrm{H}_2\mathrm{O}$$

Here, M is an *a*-valent cation that balances the negative charge, and H_2O is zeolitic water housed within the microporous network [7].

Structure types of zeolites have been compiled by Meier et al. [8,9]. These structure types are designated by three capital letters, which is called "structure type codes", whose rules have been set up by an IUPAC Commission on Zeolite Nomenclature [10]. Since the pore size of zeolites plays an important role in their sorptive and catalytic properties, it is convenient to classify zeolites with the smallest number of O atoms that limit the pore aperture of their largest channel: ultra-large (>12-), large (12-), medium (10-) or small (8-membered ring) pore zeolites. There are more than 200 different zeolites acknowledged the International Zeolite Association (IZA) [6].

Zeolites are generally synthesized under hydrothermal conditions at temperatures ranging between 373 and 473 K from mixtures of the required sources of framework atoms (Si, Al, Ti, Sn, Ge, etc), mineralizing agents (such as hydroxyl or fluoride anions), and inorganic and/or organic cations that act as structure-directing agents (SDAs) [11-14]. Since the synthesis of high-silica zeolites, with Si/Al ratios higher than 10, provides high hydrothermally stable materials with strong Brønsted acidities (protons are placed close to aluminum atoms after removing the organic moieties by calcination). In fact, three of the most successful acid zeolites used today in industry, Y (**FAU**),

ZSM-5 (**MFI**) and Beta (***BEA**). ZSM-5 and Beta were synthesized in the 1960s by Mobil researchers by using tetrapropylammonium and tetraethylammonium cations, respectively, as organic SDAs [15,16].

ZSM-5 (structure type code: **MFI**) is a member of silicon-rich pentasil zeolites which represent a series of medium-pore molecular sieves. ZSM-5 crystallizes in the idealized orthorthombic system with lattice constants a = 2.01 nm, b = 1.99 nm and c = 1.34 nm [17,18]. The unite cell contents of the Na form are

$$Na_nAl_nSi_{96-n}O_{192} \cdot 16H_2O$$

where $n < 27$ [19]. Its skeletal diagrams along the [010] and [100] directions are shown in Figure I-3. ZSM-5 has a tree-dimensional channel system where straight channels run along the [010] direction and have opening of 0.54 nm x 0.56 nm, defined by 10-membered rings of tetrahedral as shown in Figure I-4. Intersecting these channels, at right angles, there is a second type of sinusoidal channels running parallel to the [100] direction with opening of 0.51 x 0.55 nm as shown in Figure I-4. Its schematic three dimensional channel structure is presented in Figure I-5. The elliptical 10-membered ring openings controlling the channels have a medium-sized open aperture between erionite (0.38 x 0.52

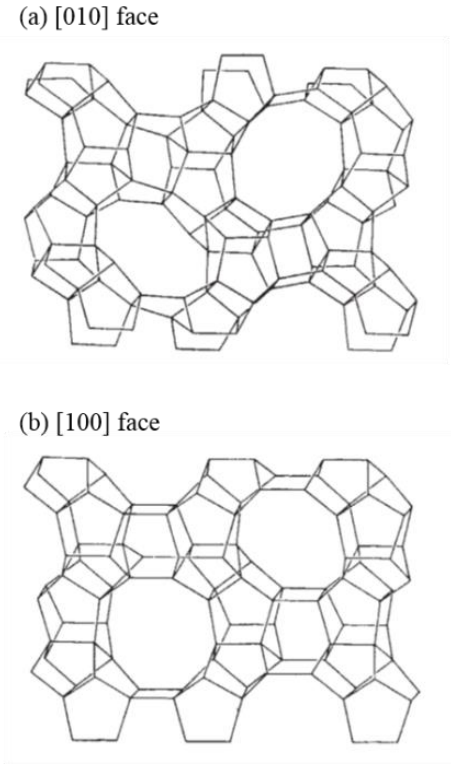

Figure I-3. Skeletal diagram of ZSM-5: (a) [010] and (b) [100] face [17].

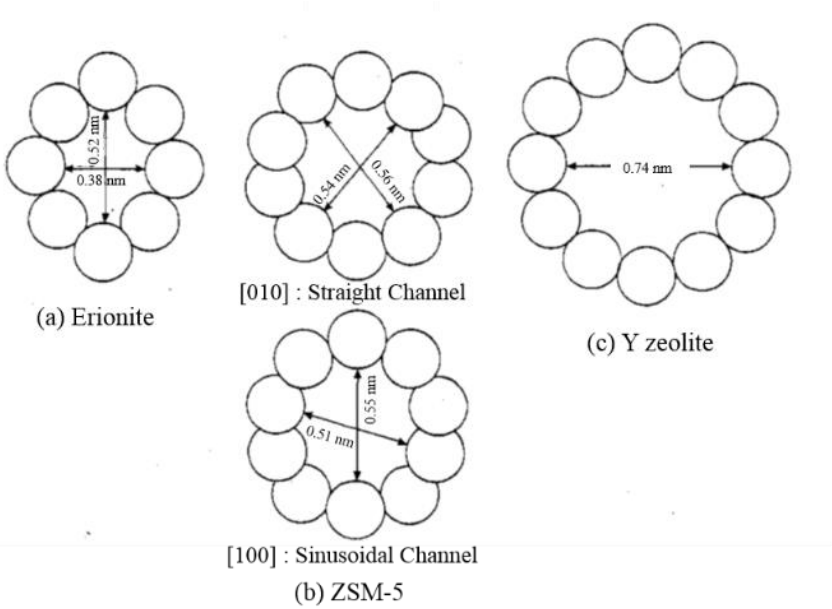

Figure I-4. Comparison of pores of (a) erionaite, (b) ZSM-5 and (c) Y zeolite [18].

nm) and faujasite (0.74 nm). This medium-sized open aperture gives H-ZSM-5 unique properties in shape selectivity as solid-acid catalyst [20-22]. ZSM-5 has 12 topologically different T-sites and 26 different O-sites. Of these 26 different oxygen atoms, 22 atoms bridge crystallographically different T-atoms; 4 atoms bridge T-atoms that are symmetry-related. This yields a total of 48 different possibilities for Al-OH substitution [23].

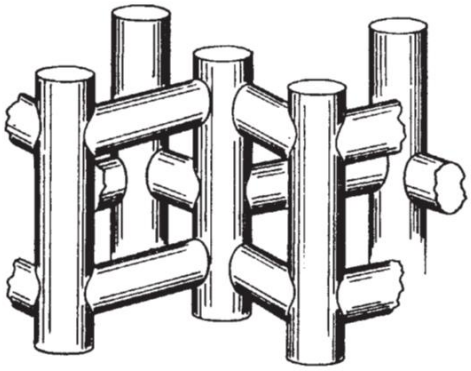

Figure I-5. Schematic three-dimensional channel structure of **MFI** [17].

1.2. Acidity of zeolites

The term "acidity of zeolite" however, is by no means unequivocal as pointed out by Karge [23]. "Acidity" would include three meaning as follows:

(i) the nature of acid sites; Brønsted acid sites or Lewis acid sites

(ii) the number or density of the acid sites

(iii) the acid strength of the acid sites

Acid properties of zeolite can be understood from the concepts of Brønsted acidity (capability of donating proton) and Lewis acidity (capability of accepting electron pair). Zeolite framework containing only SiO_4 tetrahedra would be electrically neutral and no acidity would be developed in the zeolite. Replacing a Si^{4+} site by a trivalent cation, such as an Al^{3+}, a negative charge is created in the lattice. This negative charge is compensated by counter caion, such as metal cation and proton. When the negative charge is compensated by a proton, the proton is attached to an oxygen atom that is connected to neighbor silicon and aluminum atoms. Thus these atoms consist the so-called bridging hydroxyl group. This bridging hydroxyl group has been said to be the origin of the Brønsted acidity of zeolites; the site is attributed to Brønsted acid site (BAS) in zeolites. The schematic

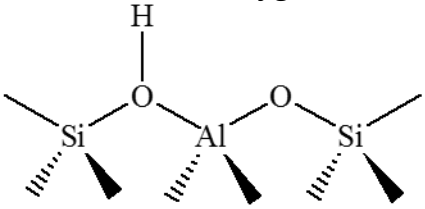

Scheme I-1. A structure model of bridging hydroxyl groups, which act as Brønsted acid sites.

structure of the bridging hydroxyl group is illustrated in Scheme I-1, which was first proposed by Uytterhoeven et al. [25] and was improved afterward [11,24]. The proposition was supported by the two facts that the number of the bridging hydroxyl groups is the same as that of Al^{3+} sites and that the redshift of the ν(OH) band with respect to a terminal silanol (SiOH) from infrared (IR) observation can be explained by the interaction of Si-OH with a neighbor Al^{3+} site [11].

While the Brønsted acidity of zeolites has been extensively studied, the study of the Lewis acidity of zeolites lags behind: the role and nature of Lewis acid sites (LAS) in zeolites is not well understood. It is safe to say that cation sites at as true LAS in the case of metal-cation-exchanged zeolites. On the other hand, it has been well known that LAS in proton-form zeolites are formed by dehydrating the zeolites at elevated temperatures [26]. However, the mechanism of the dehydration has been controversial. Among various proposed mechanism, representative mechanisms are described here. The first dehydrating mechanism was proposed by Uytterhoeven et al. in 1965, which is shown in Scheme I-2 [27]. According to this mechanism, two LAS, which consist of trigonal atoms of Al and Si, are generated at an expense of two BAS. However, this scheme was questioned by Kuhl who was unable to detect experimentally trigonal Al in dehydrated H-Y zeolite using X-ray fluorescence techniques [28]. Hence, it was proposed that the dehydration was followed by a framework dealumination involving the expulsion of the trigonal Al as an extralattice $(AlO)^+$ species and simultaneous saturation of the coordinatively unsaturated Si as shown in scheme I-3. In the mechanism, an extralattice $(AlO)^+$ species was postulated to act as LAS. Thus, one LAS was

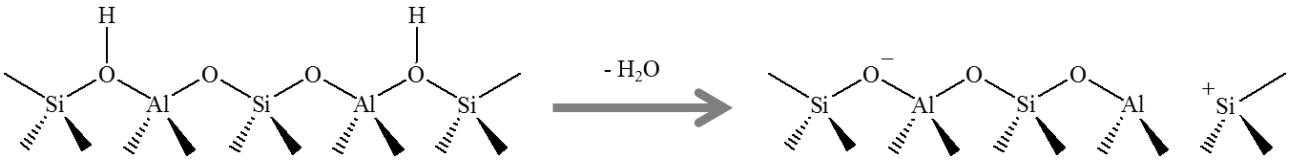

Scheme I-2. Dehydrating mechanism of proton-form zeolite.

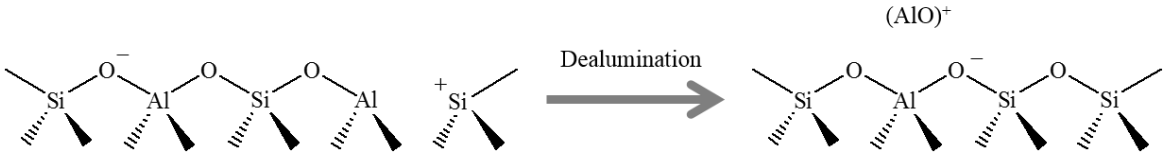

Scheme I-3. Framework dealumination of protom-form following Scheme I-2.

generated at an expense of two BAS. This scheme was also supported by IR [29] and Nuclear Magnetic Resonance (NMR) [30] studies in the case of H-Y zeolite.

A unified scheme was presented by Kazansky [31]; he pointed out that dehydration of high-silica zeolites, such as ZSM-5, follows the mechanism shown in Scheme I-2 although the de hydration is, in the case of low-silica zeolites such as faujasite, followed by the dealumination shown in Scheme I-3 because the zeolite lattice is destabilized by the high negative charge due to the high Al content. This picture was also supported by a quantitative X-ray photoelectron spectroscopy (XPS) study of pyridine adsorption on H-ZSM-5 [32]. However, this scheme has been questioned by Zecchina et al. from IR study of CO adsorption on H-ZSM-5. It was concluded that trigonal Al is the most likely candidate for LAS in H-ZSM-5 and that trigonal Si species are probably not formed [33]. They also proposed a plausible scheme in which not a trigonal Si species but a trigonal Al species is formed though the dehydration. A CP-MAS NMR study suggested the existence of two different sorts of LAS in zeolites: a tetrahedral site and octahedral site in the nonframework aluminium debris [33]. However, the nature and role of LAS is still unclear now.

1.3. Characterization of acidity of zeolite using IR spectroscopy

Because of the importance of the subject, extensive reviews have been published for the characterization of zeolite acidity [11,24,35-44]. Here, outline of the method using IR spectroscopy is described.

The IR spectroscopy is a facile and powerful technique to investigate phenomena taking palace on solid surfaces: it allows one to examine directly the behavior of both adsorbed species and functional groups existing on the surfaces [44]. Fourier-transform (FT) IR spectrometer and semiconductor IR detectors have facile and powerful analytical machine: improvements in sensitivity, signal-to-noise ratio, stability, data-processing system using conventional personal computer, scanning velocity etc.

First observation of IR bands of adsorbed species on solid surface was carried out by Eishens

and Pliskin in 1954: the IR bands of CO adsorbed on supported metal catalysts were observed [46,47]. Since then, transmission IR spectroscopy has been widely used to study adsorptions and reactions on solid surfaces including heterogeneous catalysts. Reviews on the use of the IR spectroscopy for the adsorption and catalysis on solid surfaces have been published. Early IR studies on the adsorption on zeolites have been reviewed in the book written by Little [48], and the works carried out up to 1976 have been extensively reviewed by Ward [49].

The IR spectroscopy is one of powerful and utilized techniques to investigate the zeolite acidity with and/or without probe molecules. Using this technique, one can look directly at the hydroxyl groups that exist on a solid acid catalyst and consequently can see which of them can interact with basic probe molecules and therefore to find out which presents BAS (and/or LAS) and which of them are/are not accessible to base molecules of different sizes [11,50-52]. The strength of the interaction between the hydroxyl groups and frequency shift of the hydroxyl band, and thus the acid strength of the hydroxyl groups can be estimated. Brønsted acidity of solid acid catalyst can be directly examined through the behavior of the hydroxyl groups with/without probe molecules such as H_2, CO, NH_3 etc. On the other hand, Lewis acidity is indirectly characterized from the behavior of the IR bands of probe molecules: the strength of LAS can be scaled by the shift of the bands of, for instance, pyridine or CO coordinatively attached to these sites [24]. As a measure of basicity of probe molecules, proton affinity (PA) [53], as well as their kinetic diameter [54] if available, are tabulated in Table I-1.

Table I-1. Proton affinity (PA) [53] and kinetics diameter [54] of probe molecules.

Probe molecule	PA / kJ mol^{-1}	Kinetic diameter / nm
He	178	0.26
H_2	424	0.286
CO	593	0.376
H_2O	697	0.265
NH_3	853.5	0.26
CH_4	552	0.38
C_2H_4	680	0.39
C_3H_6	751	
CH_3OH	761	
$(CH_3)_2O$	804	
C_2H_5OH	788	
Pyridine	924	

The most widely used probe molecule in IR studies is pyridine that can simultaneously determine the existence and concentration of BAS and LAS. Pioneering works carried out by Pary [55], Basila et al. [56] and Hughes and White [57] demonstrated that the characteristic bands of pyridine protonated by BAS (pyridinium cations) appear at 1545 cm^{-1} (19b, ν(CC(N))) and 1640 cm^{-1} (8a, ν(CC(N)) while the characteristic bands due to the pyridine coordinated to LAS appear at 1450 cm^{-1} (19b, ν(CC(N)) and 1620 cm^{-1} (8a, ν(CC(N)). The IR bands of hydrogen-bonded pyridine also appear at 1440 cm^{-1} (19b, ν(CC(N)) and 1590 cm^{-1} (8b, ν(CC(N)). Ammonia is also used to distinguish between BAS and LAS. NH_3 is also a hard base but its molecular size is so small that can penetrate even into the sodalite cage. The protonated form NH_4^+ gives the bands at ca. 3130 cm^{-1} and 1450 cm^{-1}, and NH_3 coordinated to LAS gives the bands at ca. 3330, 1630 and 1250 cm^{-1} [58].

Table I-2. Assignment of IR bands observed for adsorbed pyridine (Py) [58].

Mode: ν(CC(N))	**Py^P**	**Py^H**	**Py^L**	**Py^B**
8a	1580	1614	1620	1638
8b	1572	1593	1577	1620
19a	1482	1490	1490	1490
19b	1439	1438	1450	1545

Py^P: physically adsorbed Py.

Py^H: adsorbed Py with hydrogen-bonding.

Py^L: Py adsorbed on LAS.

Py^B: Py adsorbed on BAS.

As example of weaker base, a number of IR data for using such as CO and H_2 have been reported [11]. Adsorption of carbon monoxide at low temperature is widely used nowadays as a probe of acid site on solid-acid catalyst: that is owing to the facts that CO is a very weak base with a small molecular size excluding steric hindrance, and that CO is unreactive at low temperature [11]. CO specifically interacts with both acidic hydroxyl groups (BAS) and LAS and gives specific IR bands. CO interacts with acidic hydroxyl groups through hydrogen bonding at low temperatures. The strength of the interaction is considered as a quantitative measure of the acid strength of hydroxyl groups. The hydrogen-bonding formation affect both the hydroxyl groups and CO molecules and this is reflected on the frequency shifts of ν(OH) and ν(CO) bands: ν(OH) band shifts usually from ca. 3600 cm^{-1} to 3300 cm^{-1}, and ν(CO) band of adsorbed CO on BAS is usually observed at ca. 2170-2178 cm^{-1}, while the band of CO in gas phase is at 2143 cm^{-1} [11]. CO is also known to be coordinatively adsorbed on

LAS through a σ-donation of their lone-pair electrons (5s electrons of CO) to LAS (electron accepting). The ν(CO) band of the CO species usually appears above 2195 cm^{-1}. Although it has been said that the extinction coefficient of the ν(CO) band of the adsorbed CO in the 2150-2200 cm^{-1} range is almost constant [59], this is not confirmed.

1.4. Observation of reactions using IR spectroscopy

In-situ infrared spectroscopy can be defined as the observation of catalyst and adsorbed species at reaction temperature in the presence of reactants. For the acid-catalyzed reaction of zeolites, it has been said that the proton transfer from BAS to the adsorbates is crucial. In the case of hydrocarbon-related reactions, different carbocations can be formed depending on the acidity properties of the catalyst and the sort of reaction involved [60]. Among the carbocations, a distinction has to be made between carbonium and carbenium cations [61]. Carbenium cations contains a tricoordinated positively charge carbon atom. the three substituents being alkyl groups or hydrogen atoms. Carbonium cations contains a pentacoordicated positively charged carbon atom, having the same type of substituents while at least one of five substituents should be hydrogen atom. These carbocations can occur according to different mechanisms [61]. The protonation of an olefin by the acidic hydroxyl group leads to formation of an alkylcarbenium cations. On the other hand, when the proton is attached to a saturated molecule, an alkylcarbonium cations is formed. The alkylcarbonium cation by adstraction of an electroneutral molecule such as a paraffin, involving explicitly cracking reactions [61]. For super-acid catalyzed reactions in solution, the reaction mechanism involving these carbocations as an intermediate has been well established [62].

H/D exchange between surface OH groups and adsorbate molecules is a valuable method for the investigation of acid strength of OH groups and the mechanism of acid-catalyzed reactions. Lee et al. investigated the H/D exchange between CH_4, C_2H_6, C_3H_8, and C_6H_{14} with the acidic OH groups of deuterated ferrierite [63]. By comparison of the activation energies of the H/D exchange reaction determined experimentally (130 to 143 kJ mol^{-1}) with data calculated by quantum-mechanical

methods, Lee et al. derived a reaction mechanism which passed through a neutral transition state.

The double-bond migration of butenes has been extensively examined on solid acids (ex. SiO_2-Al_2O_3) and solid bases [64], and the *cis*/*trans* ratio of the 2-butene product from the double-bond migration of 1-butene has been used to determine the acid-base property of the catalysts. Kondo et al. have investigated the mechanism of the double-bond migration of 1-butene on acid forms of mordenite and ZSM-5 zeolite [65-67]. With deuterated zeolites Kondo et al. were able to establish that starting from the π complex of 1-butene at acidic OD groups, a reaction to *cis*- and *trans*-2-butene occurred even at 230 K without an H/D exchange of the acidic OD groups. At temperatures below 230 K, the double-bond migration of 1-butene thus occurs without formation of a protonated intermediate specie such a butylcarbenium cation (Scheme I-4).

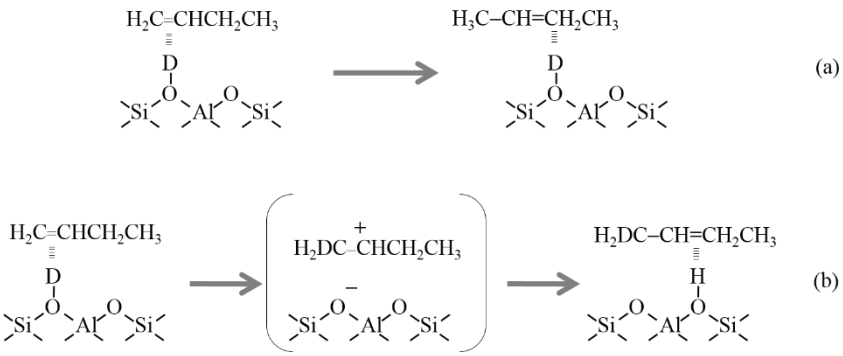

Scheme I-4. Double-bond migration of 1-butene via (a) novel and (b) carbenium cation route [67].

Fluid catalytic cracking (FCC) is the largest and oldest industrial application of zeolite based catalysts, ultra-stable Y zeolite. The FCC unit is still a main conversion unit in many refineries, which is able to process very large amounts of heavy oil fractions. It is able to direct the production preferentially to gasoline and diesel or it can maximize propene, with minor modifications of the unit or in the operating conditions [68]. Dardas et al. studied on the cleavage of heptane on H-Y zeolite under subcritical and supercritical conditions [69,70]. At a pressure of 4 MPa the authors observed an increased concentration of heptane in the pores of the cracking catalyst and a change in the stretching vibrations of the C–H bonds as a result of increased generation of intermolecular hydrogen bonds. Supercritical conditions led to a partial regeneration of the catalysts deactivated in the subcritical range.

Oligomerization of light olefins, such as propene and butenes, is an important industrial route for producing synthetic liquid fuels free of aromatics and sulfur. Bordiga et al. studied the polymerization of acetylene, methylacetylene, and ethylacetylene on H-ZSM-5 catalysts [71]. The authors identified as catalytically active sites bridging OH groups at 3610 cm^{-1}. The bands at 3260 and 1950 cm^{-1} occurring immediately after the adsorption of acetylene were explained by OH and C=C stretching vibrations of the adsorbed complexes bonded through hydrogen bonds. In contrast, ethylacetylene does not form hydrogen-bonded complexes. These molecules were protonated immediately after adsorption. After an increase in the reaction temperature to 420 K, the start and progress of the polymerization of the acetylene could be observed. Additionally, Geobaldo et al. investigated the reaction of propene and the formation of oligomers on mordenite at 100 to 300 K [72]. The weakening of the bands of the bridging OH groups at 3609 cm^{-1} observed with increasing temperature is caused by hydrogen bond formation of these OH groups with propene molecules, which at the same time leads to a shift of the OH band to 3100 cm^{-1} and the appearance of a C=C stretching band of the adsorbate molecule at 1632 cm^{-1}. A band at 1380 to 1366 cm^{-1} is an indication of the existence of saturated hydrocarbons. The formation of oligomer commenced at temperatures above 180 K.

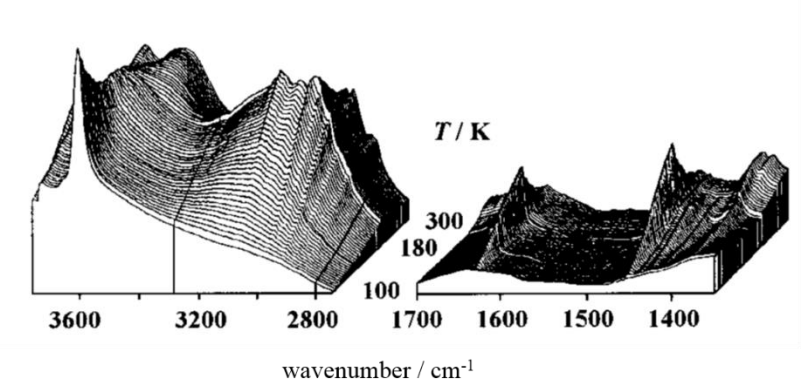

Figure I-6. FTIR spectra of mordenite recorded during the reaction of propene in temperature range of 100 to 300 K [67].

The formation of coke during hydrocarbon transformations over acid zeolite catalysts has important practical consequences for a growing number of industrial processes. Flego et al. investigated the hydrocarbon deposition arising during the alkylation of isobutane with 1-butene on a LaH-Y zeolite [73]. They observed a decrease in oligomerization of 1-butene with an increase in the fraction of isobutane in the reaction mixture. Attempts at desorption of the coke deposition at temperatures above 523 K led to the formation of a band attributable to aromatic compounds at 3050

cm^{-1}.

2. Methanol to hydrocarbons reaction

In the early 1970s, Chang and Silvestri of Mobil Central Research were trying to discover new ways to make high-octane gasoline from methanol and isobutene using Mobil's new catalyst, an acidic aluminosilicate zeolite called ZSM-5. The Mobil workers imagined that methanol would be activated on the catalysts possibly to either the methyl cation (CH_3^+) or carbene ($:CH_2$), and the highly reactive intermediate would then add to the paraffin. They observed some gaseous products and a liquid mixture of paraffins and aromatics similar to high-octane gasoline. Mass balance showed that none of the isobutene was consumed, and the same products were obtained using methanol alone. Reviews on the MTH reaction have been reported [21,74-78]. The MTH process over acid zeolite catalysts has seen renewed interest in recent years both for its ability to grow carbon chains and because methanol can be produced via a syngas intermediate from any gasifiable carbon-based feedstock, such as natural gas [79], coal [80,81] and biomass [82,83]. Methanol or its dehydration product dimethyl ether can be used as a feed to produce several different classes of hydrocarbons, including light olefins (methanol-to-olefins, MTO) [84-86], gasoline-range hydrocarbons (methanol-to-gasoline, MTG) [74], branched alkanes [87,88] and aromatics [89]. The selectivity to any of these classes of compounds is determined both by the zeolite topology and the operating conditions used [75,77].

2.1. Mechanism of MTH reaction

Scheme 1 outlines in a general way, and with little mechanistic insight, the reactions of methanol on solid acids [21,75]. Methanol is first dehydrated to dimethyl ether. The equilibrium mixture formed,

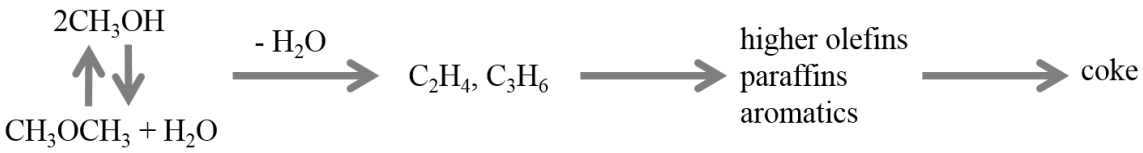

Scheme I-5. Conversion of methanol to hydrocarbons.

consisting of methanol, dimethyl ether and water, is the converted to light olefins. These light olefins react to form higher olefins, paraffins and aromatics by alkylation, oligomerization, cyclization and hydrogen transfer.

Since the discovery of MTH, there has been much debate regarding two aspects of the chemistry: (1) the formation of initial C−C bonds and (2) the mechanism by which MTH proceeds, so-called "hydrocarbon pool mechanism".

2.1.1. The formation of initial C-C bonds in MTH reaction

Initial research focused on possible routes for the formation of initial C-C bonds from C1 units, that is, methanol or dimethyl ether. More than 20 possible mechanisms have been proposed, encompassing a variety of reactive intermediates. Among them are oxonium ylides [90,91], carbocations [92,93], carbenes [74,95,96], and free radicals [97,98]. However, little experimental evidence in favor of any of these proposals has appeared [99,100], and theoretical methods most often yield prohibitively high energy barriers [101‑105].

2.1.1.1. The oxonium ylide mechanism

Van den Berg et al. [90] postulated that dimethyl ether interacts with a Brønsted acid site of the solid catalyst to form a dimethyl oxonium ion, which reacts further with another dimethyl ether or methanol to form a trimethyl oxonium cation. This trimethyl oxonium cation is subsequently deprotonated by a basic site to form a surface associated dimethyl oxonium methyl ylide species. The

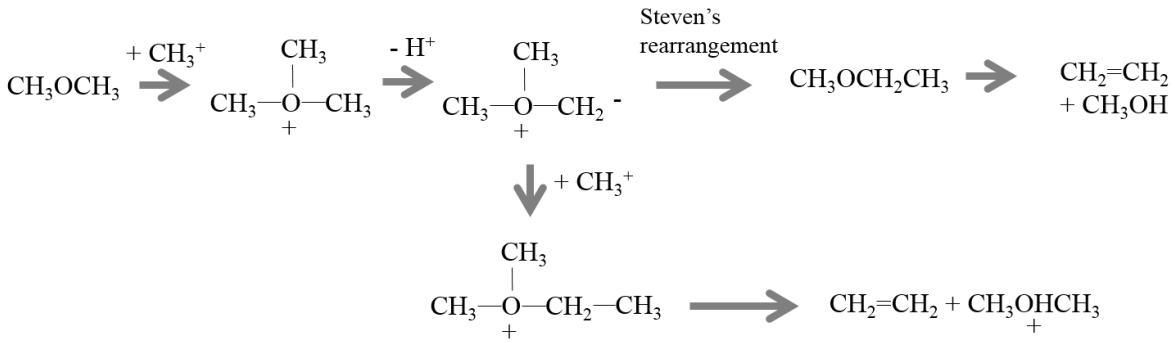

Scheme I-6. The oxonium ylide mechanism [75].

next step is either an intramolecular Stevens rearrangement [106], leading to the formation of methylethyl ether, or an intermolecular methylation, leading to the formation of the ethyldimethyl oxonium cation. In both cases ethylene is formed via β-elimination [107]. Haw et al. reported that the trimethyl oxonium cation did indeed form (at very high loadings), but it reverted to starting material as the temperature was raised [108].

2.1.1.2. The carbocation mechanism

Ono and Mori [93] suggested that surface methoxy groups formed by the reaction of methanol and Brønsted-acid sites could be a possible intermediate. Methoxy species may become be polarizable at high temperature. So, methoxy species were supposed to migrate in the form of methyl cations in a similar manner to the motion of protons of acidic OH groups [109]. Therefore, methoxy species may act as free methyl cations, which adds to the C–H bond of dimethyl ether to form a pentavalent carbonium transition state. Abstraction of a proton completes the reaction, analogous to the proposed 'superacid mechanism' by Olah et al. [110]. The possibility of a reaction pathway of the methoxy groups in methyl unit was considered by Hunger et al. [111,112]. It was reported that methoxy species react as methyl cations with strongly basic molecules to form $(CH_3)nNH_{(4-n)}^+$ (n = 1-4) from ammonia and $C_5H_5N\text{-}CH_3^+$ from pyridine.

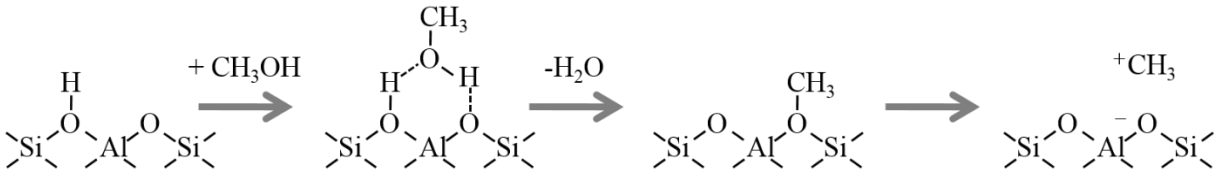

Scheme I-6. The carbocation mechanism.

2.1.1.3. The carbene mechanism

Chang and Silvestril proposed a mechanism of MTH reaction involving a carbene-like intermediate [21,74,95]. Carbene species shown as Figure I-7 are thought to be produced by a concerted a-elimination mechanism involving both Brønsted-acid sites and basic sites, the mechanism being proposed originally by Swabb and Gates [113]. Experimental evidence with respect to the

intermediate carbene formation has been indirect, for example by trapping the reactive C_1 intermediate from ^{13}C labelled methanol decomposition over ZSM-5 using unlabelled propane. The analysis of the product isomer and isotope distributions gave indications that the reactive C_1 intermediate was carbenic and the mode of attack on propane was sp^3 insertion into H–C bonds [114]. Such carbene insertions are indiscriminate in selectivity [115], resulting in a statistical distribution of the butane isomers (*i*:*n* = 1:3). Methylation by a carbocationic C_1 intermediate would, by contrast, result in high isobutane selectivity [110]. However, van Hooff suggested that low *i*/*n*-butane ratios could be explained by hydride transfer between propane and butyl cations. If hydride transfer were slower to *t*-butyl cation than to the secondary cation, low *i*/*n*-butane ratios would result. Van Hooff's proposal also failed to account for the high *i*/*n* ratios observed in the reaction of methanol alone. From the NMR observation of the production of [^{13}C]methylcyclohexane from [^{13}C]methoxy groups and cyclohexane, a carbene-like intermediate for the reaction of methoxy groups is proposed through C-H bond activation of the methoxy group with lattice oxygen by Hunger et al. [111,112].

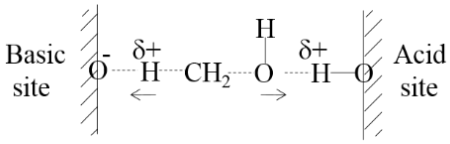

Figure I-7. Formation of carbene [110].

2.1.1.3. The free radical mechanism

The participation of free radicals in the conversion of methanol to hydrocarbons over natural mordenite has been suggested by Zatorski and Krzyzanowski [97], however, without experimental evidence documented in their reported. Later, Clarke et al. recognized that dimethyl ether could be the source of methylradicals when they identified free radicals in the reaction of dimethyl ether over H-ZSM-5 monitored by ESR spectroscopy [98]. Clarke et al. proposed that radicals are formed initially by interaction of dimethyl ether with paramagnetic centers (solid-state defects) in the zeolite and that C–C bond formation results from direct coupling of radicals [95]. However,

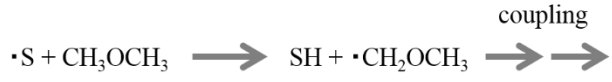

Scheme I-8. The free radical mechanism: S is a surface radical specie [76].

this concept was considered as unlikely because of the probability of radical interaction with the zeolite surface [107].

2.1.2. Hydrocarbon pool mechanism

Lesthaeghe et al. used ONIOM methods to calculate activation energies and rate constants for multiple pathways to form C-C bonds starting from two methanol molecules and found activation energy barriers for direct C-C coupling to be prohibitively high (~200 kJ mol^{-1}) [104,105]. Additionally, experiments using fractionally distilled methanol demonstrated that the catalyst induction period for MTH on ZSM-5 and SAPO-34 is highly sensitive to the impurity concentration in the methanol feed, indicating that if direct C_1 coupling does occur, it operates at a rate significantly slower compared with the rate at which trace impurities initiate the reaction [116]. Direct C−C coupling mechanisms also require C−H bond activation; however, Marcus et al. found that feeding d_3-DME over H/D-SAPO-34 (in which 50% of the acid sites were H^+ and the other 50% were D^+) at 623 K resulted in an effluent containing approximately 25% d_0-DME, 50% d_3-DME, and 25% d_6-DME [117]. The binomial distribution of D atoms in DME showed that C−H activation. Thus, possible routes of direct C-H bond formation are most likely of little practical importance, but remain an intriguing question.

Early work in MTH postulated an autocatalytic mechanism on the basis of the observed catalytic induction period during which increasing the concentration of hydrocarbons greatly increased the rate of methanol/DME conversion. Ono and Mori first studied the co-catalytic, which is so-called "autocatalytic", effect of co-provided ethene and *cis*-2-butene with methanol, and showed that the induction period of MTH reaction was reduced compared with the reaction of methanol alone over H-ZSM-5 at 512 K [93]. Additionally, Langner noted that by co-feeding methanol with higher alcohols that readily dehydrate to linear olefins under reaction conditions on H-ZSM-5, the kinetic induction period could be substantially reduced, indicating the important catalytic role of olefins in MTH [118]. Mole observed a "cocatalytic" effect when he co-fed toluene with methanol on zeolite

HZSM-5 [119]. Dessau and LaPierre outlined a reaction mechanism for MTH based on olefins that are sequentially methylated and subsequently crack to form smaller olefins or participate in hydrogen transfer reactions to form alkanes and aromatics [120,121]. Dahl and Kolboe later showed, using isotopic labeling, that both ethene and propene displayed little reactivity when co-reacted with methanol over H-SAPO-34 [84-86].The low reactivity of olefins in SAPO-34 led Dahl and Kolboe to propose the hydrocarbon pool mechanism, as shown in Scheme I-9. It is now widely agreed upon that MTH proceeds through this hydrocarbon pool mechanism.

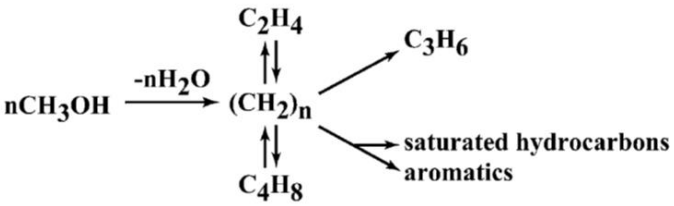

Scheme I-9. The hydrocarbon pool mechanism [77].

Haw et al. investigated the MTH chemistry on an H-ZSM-5 catalyst using solid-state NMR spectroscopy, and it was found that methylated cyclopentenyl cations might also function as reaction centers for alkene formation [76,122-124]. Bjørgen et al. investigated the reactivity of polymethylbenzenes over the large pore zeolite H-beta, and the heptamethylbenzenium cation was identified as a key intermediate [125-128].

Bjørgen et al. on H-ZSM-5 in which ^{12}C-methanol feed is switched with ^{13}C-methanol feed during steady-state reaction showed that ^{13}C incorporation of ethene closely matched that of xylene and/or trimethylbenzenes [129,130]. It was concluded that the aromatics-based hydrocarbon pool

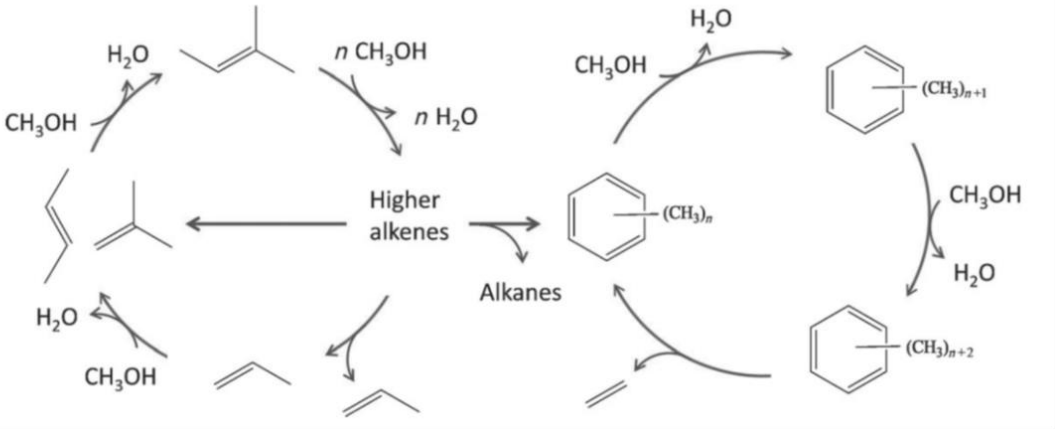

Figure I-8. Suggested dual-cycle concept for the conversion of methanol over H-ZSM-5 [77].

mechanism was the predominant source of ethene over H-ZSM-5. The higher rate of ^{13}C incorporation in the C_{3+} olefins compared to ethene and the most reactive methylbenzenes showed that propene and higher olefins to a considerable extent are formed from alkene methylations and interconversions, such as cracking reactions [129,130]. Thus, it was suggested that two mechanistic cycles run simultaneously during the MTH reaction over H-ZSM-5: ethene (and propene [131]) formation from the lower methylbenzenes followed by re-methylation, and methylation/cracking involving only the C_{3+} olefins (not ethene). The idea was referred to as the dual-cycle concept and is summarized in Figure I-8 [77,129-131].

2.2. Studied on HTH reaction

The influence of topologies (channels/cavity networks and dimensions; window and cavities [21,75-77,133-140]), compositions (strength, number and distribution of acidic sites, defects [141-150]), and morphologies (micro and mesoporosity [151-155]) in MTH reaction has been reported.

2.2.1. Influence of topology

Despite the fact that SAPO-34 and ZSM-5 are the only two zeolites used in industrial MTH processes, a comprehensive screening on a large variety of materials characterized. Figure I-9 shows partial structures for three methanol conversion catalysts and the corresponding chromatograms of the products obtained from methanol on these catalysts at 723 K [76]. The silico-aluminophosphate catalyst SAPO-34 (Figure I-9a) has the chabazite (CHA) structure that features cages ca. 1 nm in dimension that are interconnected through windows that are much smaller, ca. 0.38 nm. Figure I-9b shows that the volatile products of methanol conversion on this catalyst are ethylene, propene, smaller amounts of butanes, and traces of linear paraffins. Figure I-9c shows a view down one of the two sets of intersecting channels in the aluminosilicate zeolite ZSM-5. Figure I-9d shows that there is little apparent similarity between the products on ZSM-5 and SAPO-34 (Figure I-9b). The ZSM-5 catalyst used in the example produced very little olefin; instead it gave methylbenzenes and light alkanes,

especially isobutane and isopentane. The channel intersections of H-ZSM-5 provide enough volume for cyclization reactions and intermolecular hydride transfer reactions by which a mixture of olefins can be converted into alkanes and aromatics. The aluminosilicate zeolite ferrierite (FER topology, Figure I-9e) has an acid strength very similar to that of ZSM-5, but topological differences result in profoundly different product distributions. The ferrierite catalyst produces almost entirely olefins, especially butenes and pentenes (Figure I-9f). The topology of ferrierite is illustrated schematically in Figure I-9e; the structure features 10-ring channels running in one direction that are bridged by

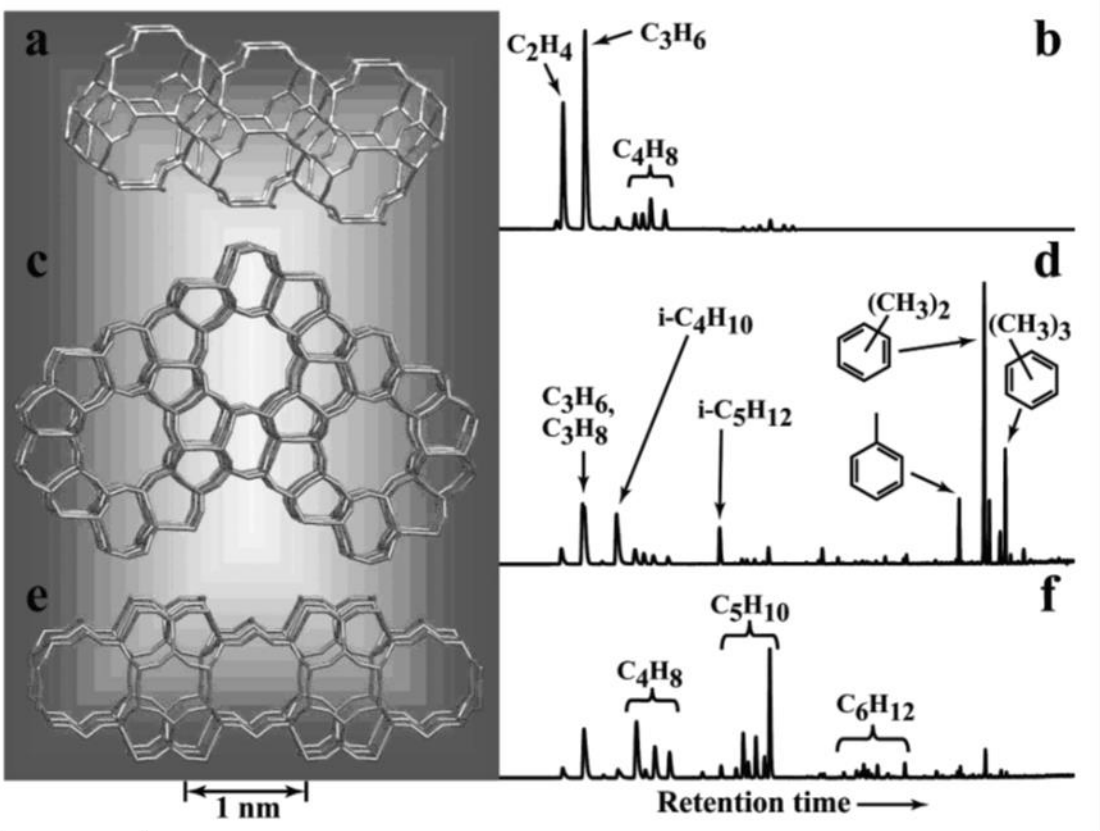

Figure I-9. Three of the methanol conversion catalyst in this contribution and GC-MS total ion chromatograms illustrating product selectivity on these materials [76]: (a) The CHA topology of SAPO-34, (b) The products of methanol conversion over SAPO-34, (c) The MFI structure of ZSM-5, (d) The products of methanol conversion over ZSM-5, (e) The FER topology of ferrierite and (f) The products of methanol conversion over ferrierite. Each experimental used 300 mg of catalyst operated at 723K and products were sampled 1.5 s following pulsed introduction of 10.2 μL of methanol.

cages (ferrierite cages) in a second direction.

Zeolites with the **LEV**, **CHA**, and **AFX** frameworks were used to study the effect of the cage

size on the selectivity toward lower olefins in the MTO reaction by Davis et al. [134]. All these materials had cavities that were accessible through 8-membered ring windows, but with cavities of differing lengths. The aggregate crystal size, primary crystallite size, and the Si/Al ratio were kept constant to study the effect of framework alone. Reaction testing of these catalysts showed that the selectivity toward ethylene increased with a decrease in the cage size. Propylene selectivity was highest with the **CHA** framework. The **AFX** material had the worst carbon yield and catalyst lifetime, but it also had the lowest amount of carbon deposited after complete deactivation, suggesting that there was pore blockage preventing further reaction. This interpretation is consistent with the analysis of the occluded organics, which showed that the **AFX** material formed large three-ring aromatics at maximum propylene selectivity, before the formation of smaller aromatics that filled the GME cage.

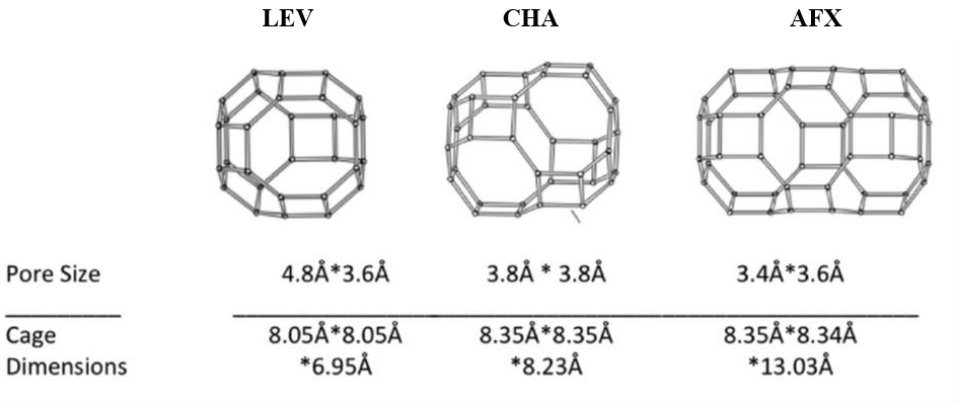

Figure I-10. Cage studied and their dimensions of LEV, CHA and AFX structures [134].

2.2.2 Effects of acid site density and acid strength

Wu and Kaeding reported the distribution of products in MTH reaction over H-ZSM-5 zeolite with silica/alumina ratios [141]. In entry 1 (Table l), where ZSM-5 with the lowest acid site density, the major products observed were low molecular weight olefins. As the acid site density of H-ZSM-5 increased, Run 2 to 6, the aromatic fraction and paraffinic products also increased to finally become large components. Additionally, They et al. reported the effect of increasing the temperature on the product distribution in MTH reaction over H-ZSM-5 [141]. At higher temperatures, the olefin formation is favored with respect to the formation of aromatics [142]. Thermodynamically, the effect

of increasing the temperature over the same range of partial pressures of olefins is to shift the distribution towards the lower olefins [156]. This equilibrium distribution is only approached at low conversions of MTH reaction [157]. Whereas ethylene is most abundant at low temperatures, butene and especially propylene become more important at higher temperatures [158].

Table I-3. Products distribution of MTH reaction over ZSM-5 with various SiO_2/Al_2O_3 ratios [141].

Entry	**1**	**2**	**3**	**4**	**5**	**6**
SiO_2/Al_2O_3	1600	500	298	140	70	35
Product selectivity / wt%						
CO, CO_2, CH_4	3.2	2.1	0.7	1.3	1.0	4.8
C_2H_4	5.2	9.9	7.3	6.4	2.8	2.0
C_3H_6	32.1	20.1	20.1	7.4	3.7	1.5
C_4H_8	22.0	23.9	26.5	26.7	8.0	6.7
C_2H_6	0.1	0.3	0.2	0.4	0.4	1.3
C_3H_8	0.7	1.5	2.9	6.6	8.4	13.9
C_4H_{10}	2.6	3.8	7.8	18.2	21.0	24.6
C5	12.1	17.3	14.2	10.9	12.5	3.7
C6	6.5	4.2	4.0	2.9	4.0	0.5
C7	6.6	6.2	4.1	2.0	3.4	0.2
C8	5.2	3.9	3.9	6.9	15.0	11.8
BTX	3.7	6.8	8.3	20.3	19.7	29.1

Reaction conditions: temperature, 450 ºC, except entry 5 at 400 ºC; WHSV of methanol, 4.0-4.3.

Bleken et al. recently performed a comparative study of two **CHA** analogues, SSZ-13 and SAPO-34, with similar acid site density and crystal size, but with significantly different acid strength [77,159]. SSZ-13 had a higher activity and more rapid deactivation than SAPO-34, in line with its higher acid strength. An interesting observation was that the conversion capacity of SSZ-13 was higher than for SAPO-34 at lower temperatures (Figure I-11), and that the optimum

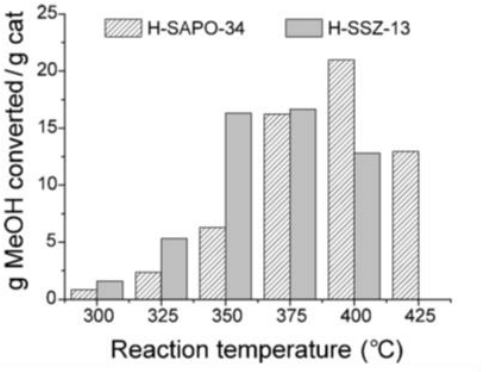

Figure I-11. Methanol conversion capacity in SAPO-34 and SSZ-13 [77].

temperature of reaction was shifted to lower temperatures for this catalyst, thus suggesting that the more acidic SSZ-13 could be an interesting alternative to SAPO-34 as MTO catalyst [77,159].

2.2.3 Coke formation

For the archetypical MTO catalyst SAPO-34, a more complex dependence of product selectivity on deactivation is observed. Several authors have reported an enhanced ethene to propene ratio with increasing time on-stream for this topology [160-163]. On the other hand, deactivation does not affect product selectivity over ZSM-5 [129]. The observed difference in deactivation influence on product selectivity for **MFI** and **CHA** topologies reflects the relative importance of external versus internal coke formation In **MFI**, external coke is concluded to be the major contributor to catalyst deactivation. Bjørgen et al. suggested that it is a plausible rationale for the superior lifetime properties of ZSM-5 in MTH reaction [129]. In the **CHA** topology, however, internal coke is of major importance for catalyst deactivation. Its large cavities are spacious enough for an olefin molecule to pass by even a bi- or polycyclic aromatic compound/coke precursor, thus giving access to active sites at the interior of a coked cavity.

3. Outline of this thesis

The aim of this study is to investigate the mechanism of C-C bond formation during methanol to hydrocarbons reaction over ZSM-5 zeolite using infrared spectroscopy. Main purpose of this study is to clarify the reactivity of surface alkoxy species such methoxy species and ethoxy species on acidic OH groups.

In Chapter II, general experimental bases of this study and a new concept of the estimation of real temperature of sample in IR cell are described.

In Chapter III, the reaction of methoxy species and ethene was investigated as one of elementary step of MTH reaction. I studied whether methoxy groups act as methylation reagents of ethene and reaction mechanism of the methylation of ethene by methylation.

In Chapter IV, the reaction of methoxy species with methanol and dimethyl ether was studied as formation of initial C-C bond in MTH reaction. Products as hydrocarbons in the initial step ofMTH reaction were investigated.

In Chapter V, the kinetics of the methylation of olefins by methoxy species was investigated. Activation energies for the methylation of ethene and propene by methoxy species and the formation of methoxy species from methanol and dimethyl ether were estimated.

In Chapter VI, the oligomerization of ethene over H-ZSM-5 at 303 K was studied as one of elementary step of MTH reaction. I investigated whether ethoxy species act as intermediates in the ethene oligomerization. The mechanism of the decomposition of ethoxy species to ethene was additionally discussed.

Finally, in Chapter VII, summary of this study is presented.

References:

[1] C. Martínez, A. Corma, Coor. Chem. Rev. 255 (2011) 558-1580.

[2] N. V. Choudary, B. L. Newalkar, J. Porous Mater. 18 (2011) 685-692.

[3] B. Yilmaz, U. Müller, Top. Catal. 52 (2009) 888-895.

[4] W. Vermeiren A J.-P. Gilson, Top. Catal. 52 (2009) 1131-1161.

[5] G. Busca, Chem. Rev. 107 (2007) 5366-5410.

[6] Datebase of Zeolite structures, Structure Commission of the International Zeolite Association: http://www.iza-structure.org/databases/

[7] J. M. Thomas, Phil. Trans. R. Lond. A 333 (1990) 173-207.

[8] W. M. Meier, Pure Appl. Chem. 58 (1986) 1323-1328.

[9] Ch. Baerlocher, W. M. Meier, D. H. Olson, Atlas of Zeolite Framework Types, 5th revised Ed. Elsevier 2001.

[10] R. M. Barrer, Pure Appl. Chem. 51 (1979) 1091-1100.

[11] A. Corma, Chem. Rev. 95 (1995) 559-614

[12] A. Corma, M. E. Davis, ChemPhysChem 5 (2004) 304‑313.

[13] C. S. Cundy, P. A. Cox, Chem. Rev. 103 (2003) 663-701.

[14] M. Moliner, F. Rey, A. Corma, Angew. Chem. Int. Ed. 52 (2013) 13880-13889.

[15] R. L. Wadlinger, G. T. Kerr, E. J. Rosinski, US Patent 3,308,069, 1967.

[16] R. J. Argauer, G. R. Landolt, US Patent 3,702,886, 1972.

[17] G. T. Kokotailo, S. L. Lawton, D. H. Olson, W. M. Meier, Nature 272 (1978) 437-438.

[18] D. H. Olson, G. T. Kokotaillo, S. L. Lawton, W. M. Meier, J. Phys. Chem. 85 (1981) 2238-2243.

[19] T. Takahashi, M. Kato, K. Itabashi, Zeolite 15 (1995) 21-32.

[20] S. L. Meisel, J. P. McCullough, C. H. Lechthaler, P. B. Weisz, CHEMTECH 6 (1976) 86-89.

[21] C. D. Chang, Catal. Rev.-Sci. Eng. 25 (1983) 1-118

[22] C. D. Chang, A. J. Silvestri, CHEMTECH 17 (1987) 624-631.

[23] G. J. Kramer, R. A. van Santen, J. Am. Chem. Soc. 97 (1993) 2887-2897.

[24] H. G. Karge, Stud. Surf. Sci. Catal. 65 (1991) 133-156.

[25] J. B. Uytterhoeven, L. G. Christner, W. K. Hall, J. Phys. Chem. 69 (1965) 2117-2126.

[26] J. W. Ward, J. Catal. 11 (1968) 271-273.

[27] J. B. Uytterhoeven, P. Jacob, K. Makay, R. Schoonheydt, J. Phys. Chem. 72 (1968) 1768-1775.

[28] H. Kuhl, J. Phys. Chem. Solids 38 (1977) 1259-1263.

[29] P. A. Jacobs, H. K. Beyer, J. Phys. Chem. 83 (1979) 1174-1177.

[30] D. Freude, T. Frohlich, M. Hunger, H. Pfeifer, G. Scheler, Chem.Phys. Lett. 98 (1983) 263-266.

[31] V. B. Kazansky, Catal. Today 3 (1988) 367-542.

[32] R. Borade, A. Sayari, A. Adnot, S. Kaliaguine, J. Phys. Chem. 94 (1990) 5989-5994.

[33] A. Zecchina, S. Bordiga, G. Spoto, D. Scarano, G. Petrini, G. Leofanti, M. Padovan, C. O. Arean, J. Chem. Soc. Faraday Trans. 88 (1992) 2959-2969.

[34] D. Coster, A. L. Blumenfeld, J. J. Fripiat, J. Phys. Chem. 98 (1994) 6201-6211.

[35] J. A. Rabo, G. J. Gajda, Catal. Rev.-Sci. 31 (1989) 385-430.

[36] W. E. Farneth, R. J. Gorte, Chem. Rev. 95 (1995) 615-635.

[37] J. A. Lercher, C. Grundling, G. Eder-Mirth, Catal. Today 27 (1996) 353-376.

[38] G. Busca, Phys. Chem. Chem. Phys. 1 (1999) 723-736.

[39] C. Lamberti, A. Zecchina, E. Groppo, S. Bordiga, Chem. Soc. Rev. 39 (2000) 4951-5001.

[40] V. Solinas, I. Ferino, Catal. Today 41 (1998) 179-189.

[41] G. Bagnasco, J. Catal. 159 (1996) 249-252.

[42] E. Brunner, Catal. Today 38 (1997) 361-376.

[43] M. Hunger, Catal. Rev.-Sci. 39 (1997) 345-393.

[44] J. F. Haw, T. Xu, Adv. Catal. 42 (1998) 115-180.

[45] H. Boehm, H. Knözinger, In Catalysis – Science and Technology Vol. 4 Springer-Verlag Berlin 1983.

[46] R. P. Eischens, W. A. Plinskin, J. Chem. Phys. 22 (1954) 1786-1787.

[47] R. P. Eischens, W. A. Plinskin, Adv. Catal. 10 (1958) 1-56.

[48] L. H. Little, Infrared Spectra of Adsorbed Species Academic Press. New York 1966

[49] J. W. Ward, In Zeolite Chemistry and Catalysis ACS monograph 171

[50] J. N. Kondo, E. Yoda, H. Ishikawa, F. Wakabayashi, K. Domen, J. Catal. 191 (2000) 275-281.

[51] T. Armaroli, M. Trombetta, A. G. Alejandre, J. R. Solis, G. Busca, Phys. Chem. Chem. Phys., 2 (2000) 3341-3348.

[52] T. Motanari, E. Finocchio, G. Busca, J. Phys. Chem. C, 115 (2011) 937-943.

[53] S. G. Lias, J. F. Liebman, R. D. Levin, J. Phys. Chem. Ref. Data 13 (1984) 695-808.

[54] J. H. C. van Hooff, J. W. Roelofsen, Stud. Surf. Sci. Catal. 58 (1991) 241-283.

[55] E. P. Parry, J. Catal. 2 (1963) 371-379.

[56] M. R. Basila, T. R. Kanter, K. H. Rhee, J. Phys. Chem. 68 (1964) 3197-3207.

[57] T. R. Hughes, H. M. White, J. Phys. Chem. 71 (1967) 2192-2201.

[58] H. Knözinger, Adv. Catal. 25 (1976) 184-271.

[59] A. Zecchina, S. Bordiga, C. Lamberti, G. Spoto, L. Carnelli, C. O. Arean, J. Phys. Chem. 98 (1994) 9577-9582.

[60] G. J. Kramer, R. A. van Santen, J. Am. Chem. Soc. 117 (1995) 1766-1776.

[61] S. R. Blaszkowski, A. P. J. Jansen, M. A. C. Nascimento, R. A. van Santen, J. Phys. Chem. 98 (1994) 12938-12944.

[62] G. Olah, G. K. S. Prakash, J. Sommer, Superacids, John Wiley & Sons, New York 1985

[63] B. Lee, J. N. Kondo, F. Wakabayashi, K. Domen, Catal. Lett. 59 (1999) 51-54.

[64] J. W. Hightower, W. K. Hall, Chem. Eng. Prog. Symp. Ser. 63 (1967) 122.

[65] J. N. Kondo, S. Liquin, F. Wakabayashi, K. Domen, Catal. Lett. 47 (1997) 129-133.

[66] J. N. Kondo, L. Shao, F. Wakabayashi, K. Domen, J. Phys. Chem. B 101 (1997) 9314-9320.

[67] J. N. Kondo, K. Domen, F. Wakabayashi, Microporous Mesoporous Mater. 21 (1998) 429-437.

[68] A. Corma, B. W. Wojciechowski, Catal. Rev. Sci. Eng 27 (1985) 29-150.

[69] Z. Dardas, M. G. Süer, Y. H. Ma, W. R. Moser, J. Catal. 159 (1996) 204-211.

[70] M. G. Süer, Z. Dardas, Y. H. Ma, W. R. Moser, J. Catal. 162 (1996) 320-326.

[71] S. Bordiga, G. Ricchiardi, G. Spoto, D. Scarano, L. Carnelli, A. Zecchina, C. O. Arean, J. Chem. Soc. Faraday Trans. 89 (1993) 1843-1855.

[72] F. Geobaldo, G. Spoto, S. Bordiga, C. Lamberti, A. Zecchina, J. Chem. Soc. Faraday Trans. 93 (1997) 1243-1249.

[73] C. Flego, I. Kiricsi, W. O. Parker, Jr., M. G. Clerici, Appl. Catal. A 124 (1995) 107-119.

[74] C. D. Chang, A. J. Silvestri, J. Catal. 47 (1977) 249-259.

[75] M. Stöcker, Microporous Mesoporous Mater. 29 (1999) 3−48.

[76] J. F. Haw, W.-G. Song, D. M. Marcus, J. B. Nicholas, Acc. Chem. Res. 36 (2003) 317-326.

[77] U.Olsbye, S. Svelle, M. Bjørgen, P. Beato, Ton V. W. Janssens, F. Joensen, S. Bordiga, K. P. Lillerud, Angew. Chem. Int. Ed. 51 (2012) 5810-5831.

[78] S. Ilias, A. Bhan, ACS Catal. 3 (2013) 18-31.

[79] D. A. Hickman, L. D. Schmidt, Science 259 (1993) 343−346.

[80] N. M. Laurendeau, Prog. Energy Combust. Sci. 4 (1978) 221−270.

[81] W. Y. Wen, Catal. Rev. Sci. Eng. 22 (1980) 1−28.

[82] M. Asadullah, S. Ito, K. Kunimori, M. Yamada, K. Tomishige, J. Catal. 208 (2002) 255−259.

[83] D. Sutton, B. Kelleher, J. R. H. Ross, Fuel Process. Technol. 73 (2001) 155−173.

[84] I. M. Dahl, S. Kolboe, Catal. Lett. 20 (1993) 329−336.

[85] I. M. Dahl, S. Kolboe, J. Catal. 149 (1994) 458−464.

[86] I. M. Dahl, S. Kolboe, J. Catal. 161 (1996) 304−309.

[87] J. H. Ahn, B. Temel, E. Iglesia, Angew. Chem. 121 (2009) 3872−3874.

[88] D. A. Simonetti, J. H. Ahn, E. Iglesia, J. Catal. 277 (2011) 277 173−195.

[89] Ø. Mikkelsen, S. Kolboe, Microporous Mesoporous Mater. 29 (1999) 173−184.

[90] J. P. van den Berg, J. P. Wolthuizen, J. H. C. van Hooff, in Proceedings 5th International

Zeolite Conference Heyden London, 1980.

[91] G. A. Olah, Pure Appl. Chem. 53 (1981) 201-207.

[92] G. J. Hutchings, F. Gottschalk, M. V. Michle, R. Hunter, J. Chem. Soc. Faraday Trans. 83 (1987) 571-581.

[93] Y. Ono, T. Mori, J. Chem. Soc. Faraday Trans. 77 (1981) 2209-2221.

[94] D. Kagi, J. Catal. 69 (1981) 242-248.

[95] C. D. Chang, J. Catal. 69 (1981) 244-248.

[96] E. A. Swabb, B. C. Gates, Ind. Eng. Chem. Fund. 11 (1972) 11 540-545.

[97] W. Zatorski, S. Kryzanowski, Acta Phys. Chem. 29 (1978) 347-348.

[98] J. K. A. Clarke, R. Darcy, B. F. Hegarty, E. O'Donoghue, V. Amir-Ebrahimi, J. J. Rooney, J. Chem. Soc. Chem. Commun. (1986) 425-426.

[99] S. Kolboe, Stud. Surf. Sci. Catal. 61 (1991) 413-416.

[100] J. F. Haw, D. M. Marcus, in Handbook of Zeolite Science and Technology, Marcel Dekker, New York, 2003.

[101] J. Sauer, M. Sierka, F. Haase in Transition State Modeling for Catalysis, ACS, Washington, 1999 358.

[102] S. R. Blaszkowski, R. A. van Santen, J. Phys. Chem. 99 (1995) 11728-11738.

[103] S. R. Blaszkowski, R. A. van Santen, J. Am. Chem. Soc. 119 (1997) 5020-5027.

[104] D. Lesthaeghe, V. Van Speybroeck, G. B. Marin, M.Waroquier, Angew. Chem. Int. Ed. 118 (2006) 118 1746-1751.

[105] D. Lesthaeghe, V. Van Speybroeck, G. B. Marin, M.Waroquier, Ind. Eng. Chem. Res. 46 (2007) 46 8832-8838.

[106] G. A. Olah, H. Doggweiler, J. D. Felberg, S. Frohlich, M. J. Grdina, R. Karpeles, T. Keumi, S. Inaba, W. M. Ip, K. Lammertsma, G. Salem, D. C. Tabor, J. Am. Chem. Soc. 106 (1984) 2143-2149.

[107] G. F. Froment, W. J. H. Dehertog, A. J. Marchi, A review of the literature, Catalysis 9 1992 .

[108] E. J. Munson, J. F. Haw, J. Am. Chem. Soc. 113 (1991) 6303-6305.

[109] T. Baba, T. Mori, Y. Ono, H. Sugihara, J. Phys. Chem. B 102 (1998) 804-808.

[110] G. A. Olah, G. Klopman, R. H. Schlosberg, J. Am. Chem. Soc. 91 (1969) 3261-3268.

[111] Y. Jiang, M. Hunger, W. Wang, J. Am. Chem. Soc. 128 (2006) 11679-11692.

[112] W. Wang, M. Hunger, Acc. Chem. Res. 41 (2008) 895-904.

[113] F. A. Swabb, B. C. Gates, Ind. Eng. Chem. Fundament. 11 (1972) 540-587.

[114] C. D. Chang, C. T.-W. Chu, J. Catal. 74 (1982) 203-206.

[115] W. Kirmse, Carbene Chemistry, Academic Press, New York, 1971.

[116] W.-G. Song, D. M. Marcus, H. Fu, J. O. Ehresmann, J. F. Haw, J. Am. Chem. Soc.124 (2002) 3844−3845.

[117] D. M. Marcus, K. A. McLachlan, M. A. Wildman, J. O. Ehresmann, P. W. Kletnieks, J. F. Haw, Angew. Chem. Int. Ed. 45 (2006) 3133−3136.

[118] B. E. Langner, Appl. Catal. 2 (1982) 289−302.

[119] T. Mole, G. Bett, D. Seddon, J. Catal. 84 (1983) 435-445.

[120] R. M. Dessau, J. Catal. 99 (1986) 111−116.

[121] R. M. Dessau, R. B. LaPierre, J. Catal. 78 (1982) 136−141.

[122] J. F. Haw, Phys. Chem. Chem. Phys. 4 (2002) 5431-5441.

[123] P. W. Goguen, T. Xu, D. H. Barich, T. W. Skloss, W. Song, Z. Wang, J. B. Nicholas, J. F. Haw, J. Am. Chem. Soc. 120 (1998) 2650-2651.

[124] J. F. Haw, J. B. Nicholas,W. Song, F. Deng, Z.Wang, T. Xu, C. S. Henghan, J. Am. Chem. Soc. 122 (2000) 4763-4775.

[125] M. Bjørgen, U. Olsbye, S. Kolboe, J. Catal. 215 (2003) 30-44.

[126] M. Bjørgen, U. Olsbye, D. Petersen, S. Kolboe, J. Catal. 221 (2004) 1-10.

[127] M. Bjørgen,U. Olsbye, S. Svelle, S. Kolboe, Catal. Lett. 93 (2004) 37-40.

[128] M. Bjørgen, F. Bonino, S. Kolboe, K.-P. Lillerud, A. Zecchina, S. Bordiga, J. Am. Chem. Soc. 125 (2003) 15863-15868.

[129] M. Bjørgen, S. Svelle, F. Joensen, J. Nerlov, S. Kolboe, F. Bonino, L. Palumbo, S. Bordiga, U. Olsbye, J. Catal. 249 (2007) 195−207.

[130] S. Svelle, F. Joensen, J. Nerlov, U. Olsbye, K.-P. Lillerud, S. Kolboe, M. Bjørgen, J. Am. Chem. Soc. 128 (2006) 14770−14771.

[131] M. Bjørgen, F. Joensen, K. P. Lillerud, U. Olsbye, S. Svelle, Catal. Today 142 (2009) 90-97.

[132] M. Bjørgen, K. P. Lillerud, U. Olsbye, S. Svelle, Stud. Surf. Sci. Catal. 167 (2007) 463-468.

[133] S. Teketel, W. Skistad, S. Benard, U. Olsbye, K. P. Lillerud, P. Beato, S. Svelle, ACS Catal. 2 (2012) 26–37.

[134] Y. Bhawe, M. Moliner-Marin, J. D. Lunn, Y. Liu, A. Malek, M. Davis, ACS Catal. 2 (2012) 2490-2495.

[135] Q. Wang, Z.-M. Cui, C.-Y. Cao, W.-G. Song, J. Phys. Chem. C 115 (2011) 24987-24992.

[136] J. Li, Y. Wei, G. Liu, Y. Qi, P. Tian, B. Li, Y. He, Z. Liu, Catal. Today 171 (2011) 221-228.

[137] Q. Zhu, J. N. Kondo, S. Inagaki, T. Tatsumi, Top. Catal. 52 (2009) 1272-1280.

[138] T. Yokoi, M. Yoshioka, H. Imai, T. Tatsumi, Angew. Chem. Int. Ed. 48 (2009) 9984-9887.

[139] J. W. Park, G. Seo, Appl. Catal. A: Gen. 356 (2009) 180-188.

[140] J. W. Park, J. Y. Lee, K. S. Kim, S. B. Hong, G. Seo, Appl. Catal. A: Gen. 339 (2008) 36-44

[141] M. M. Wu, W. W. Kaeding, J. Catal. 88 (1984) 478-489.

[142] W. O. Haag, R. M. Lago, P. G. Rodewald, J. Mol. Catal. 17 (1982) 161-170.

[143] C. D. Chang, C. T.-W. Chu, R. F. Socha, J. Catal. 86 (1984) 289-296.

[144] W. J. H. Dehertog, G. F. Froment, Appl. Catal. 71 (1988) 155-174.

[145] K. Barbera, F. Bonino, S. Bordiga, T. V. W. Janssens, P. Beato, J. Catal. 280 (2011) 196-205.

[146] S. Zhang, B. Zhang, Z. Gao, Y. Han, Ind. Eng. Chem. Res. 49 (2010) 2103-2106.

[147] S. M. T. Almutairi, B. Mezari, E. A. Pidko, P. C. M. M. Magusin, E. J.M. Hensen, J. Catal. 307 (2013) 194-203.

[148] M. W. Erichsen, S. Svelle, U. Olsbye, J. Catal. 298 (2013) 94-101.

[149] Q. Zhu, J. N. Kondo, T. Yokoi, T. Setoyama, M. Yamaguchi, T. Takewaki, K. Domen, T.

Tatsumi, Phys. Chem. Chem. Phys. 13 (2011) 14598-14605.

[150] J. W. Park, K. S. Kim, M. Seo, S. Y Kim, Y. Sugi, G. Seo, Appl. Catal. A: Gen. 349 (2008) 76-85

[151] W. Dai, G. Wu, L. Li, N. Guan, M. Hunger, ACS Catal. 3 (2013) 588-596.

[152] L. Wu, V. Degirmenci, P. C. M. M. Magusin, N. J. H. G. M. Lousberg. E. J. M. Hensen, J. Catal. 298 (2013) 27-40.

[153] Z. Li, J. Martinez-Triguero, P. Concepcion, J. Yu, A. Corma, Phys. Chem. Chem. Phys. 15 (2013) 14670-14680.

[154] S. Hu, J. Shan, Q. Zhang, Y. Wang, Y. Liu, Y. Gong, Z. Wu , T. Dou, Appl. Catal., A 2012, 445–446.

[155] M. Choi, K. Na, J. Kim, Y. Sakamoto, O. Terasaki, R. Ryoo, Nature 461 (2009) 246–249.

[156] C.T.-W. Chu, C.D. Chang, J. Catal. 86 (1984) 297-300.

[157] I. J. Miller, D. M. Bibby, C. D. Chang, R. F. Howe, Methane Conversion, Elsevier, Amsterdam, 1988.

[158] W. J. H. Dehertog, G. F. Froment, Appl. Catal. 71 (1991) 153-165.

[159] F. Bleken, M. Bjorgen, L. Palumbo, S. Bordiga, S. Svelle, K. P. Lillerud, U. Olsbye, Top. Catal. 52 (2009) 218-228.

[160] W.-G. Song, H. Fu, J. F. Haw, J. Am. Chem. Soc. 123 (2001) 4749-4754.

[161] B. P. C. Hereijgers, F. Bleken, M. H. Nilsen, S. Svelle, K. P. Lillerud, M. Bjorgen, B. M. Weckhuysen, U. Olsbye, J. Catal. 264 (2009) 77-87.

[162] F. J. Keil, Microporous Mesoporous Mater. 29 (1999) 49-66.

[163] D. Chen, K. Moljord, T. Fuglerud, A. Holmen, Microporous Mesoporous Mater. 29 (1999) 191-203.

Chapter II

Experimental

1. Infrared measurement

About 60 mg of the samples were pressed into self-supporting disks (20 mm in diameter). These samples were pressed at the pressure of 200-400 kg cm^{-2}. A sample disk was mounted in a sample holder and placed in a quartz-made infrared (IR) cell as illustrated in Figure II-1. The cell was connected to a closed gas circulation system connected to a vacuum line which was described in Figure II-2. The IR cell can be cooled by flowing liquid nitrogen through a stainless steel tube would around the cell and can be heated by using a heating wire. Sample temperature is monitored by the use of K-type thermocouple set in a hole positioned in close vicinity to the sample from the outside of the cell. CaF_2 plates are used as the IR window of the IR cell. The IR beam from the spectrometer is transmitted through the sample disk via the set of those windows. In order to avoid the breakage of windows by the thermal treatments of the cell, the vicinity of windows are cooled flowing water through a copper tube would around the cell. Gases are introduced to the closed circulation system from the gas handling part is shown in Figure II-2A.

IR spectra are obtained using Jasco FT/IR-4100 spectrometer equipped with a mercury-cadmium-telluride (MCT) detector. The spectral resolution is set in 4 cm^{-1} and 64 scans are averaged. It takes ca. 45 second to collect 64 scans on a spectral resolution of 4 cm^{-1} using the MCT detector.

2. Estimation of the real temperature of samples in IR cell

Abstract:

The peak top frequency of the stretching vibration of OH groups on amorphous silica reversibly changes accompanied by the change of the sample in temperature under the constant concentration. Using this phenomenon, the estimation of the real temperatures of samples in IR cell can be achieved. The temperatures measured from outside the cell are first calibrated to real ones. The OH frequency of silica can be correlated to the real temperature of the sample inside the cell via the calibration of the measured and the real temperatures of samples in each IR cell.

2.1. Introduction

For obtaining of IR spectra of powder catalysts, temperatures of samples are estimated by measuring temperatures of a metal mesh [1], CaF_2 plate [2] or metal mirror [3], where catalyst samples are directly mounted. These set-ups were equipped originally so that correct temperatures can be measured for physicochemical analyses. On the other hand, in IR cells for studies on catalysts, which are widely used recently, the estimation of the real temperature sometimes becomes difficult. This is due to the difficulty in the direct attachment of a thermocouple (TC) to the sample, and to the thermal conductivity from heating or cooling part near the TC to the head of the TC near the sample. So, TCs should be thermally well separated from the temperature controlling part of the cell, but this operation seems to be difficult especially for diffuse reflectance IR measurements.

We have been using quartz made IR cells using transmission method. Even if a TC is placed apart from heating or cooling part as illustrated in Figure II-3(A), the real sample temperature differs from that measured from outside the cell. For this reason, it becomes necessary to calibrate the measured temperature to the real one in the presence and the absence of gaseous molecules for each cell as demonstrated in Figure II-4 (see below for details). Figures II-4(A) and (B) are examples for such calibration curves at low temperature range in the presence and the absence of

gaseous molecules, respectively, during cooling and heating procedures (see below).

It is known that the frequency of the stretching vibration of isolated hydroxyl (OH) groups on amorphous silica reversibly changes depending on the sample temperature in vacuum as long as the concentration is kept constant [4]. Therefore, it becomes possible to estimate the real temperature of the powder samples if the sample holder is first mounted by amorphous silica followed by the observation of the OH stretching frequency under evacuation at various temperatures. For this purpose, we report here, the method employed for the calibration of real temperatures and those measured from outside the cell, and submit the correlation between the real temperatures and the peak top frequencies of OH stretching vibration of amorphous silica.

2.2. Experimental

The amorphous silica (Aerosil 200) was used as obtained from Evonic Industries, which is a hydrophilic fumed silica with 200 m^2 g^{-1} surface area. About 20 mg of the amorphous silica was pressed into a self-supporting disk (20 mm diameter) and placed in a quartz cell connected to a conventional closed gas-circulation system. The sample disk was pretreated at 500 °C with circulating 13 kPa of O_2 gas with a liquid nitrogen trap for 1 h for the elimination of hydrocarbon contaminations [5].

The observation of IR spectra was carried out at a resolution of 4 or 1 cm^{-1} and at a typical averaging of 64 scans using a Jasco FT-IR 6100 spectrometer equipped with an MCT detector. The side view of an IR cell for temperature calibration is shown in Figure II-3(A). For spectra measurements, the temperature is only measured by a TC (1), where any direct thermal contact with either heater or cooling tubes is avoided. Then, a NaCl window is fixed in the place of acryl resin plate in Figure II-3(A) with stainless flanges and o-rings from both sides for obtaining spectra. For measuring the real sample temperature, a heat resisting inorganic plate, which has a hollow at the center to maintain the direct contact with TC (2), is placed as a sample. The TC (2) is stabilized with an acryl resin plate with a hole at the center, where sealing is maintained for evacuation by

epoxy resin. The acryl resin plate is hold only by reduced pressure inside the cell. The temperature controlling rates were 5 and 10 °C min^{-1} below and above room temperature, respectively.

2.3. Results and discussion

The relation between the measured temperature (TC (1)) and the real temperature (TC (2)) with of H_2 (13.3 kPa) in the cell below room temperature is shown in Figure II-4(A). Data were obtained during cooling (open circles) and warming (open triangles) procedures as well as under the steady state conditions (filled circles). Measured temperatures were almost the same as the real one above -50 °C during cooling process but the real temperatures were much cooler than the measured ones below the temperature. Due to the presence of molecules in gas phase, the deviation of the measured temperatures from the real ones were similar in three processes; the real temperature were 20-30 °C lower than the measured ones. On the other hand, measured temperatures during cooling (open circles) and warming (open triangles) procedures were markedly different in vacuum due to the absence of any thermal conductors. From these results it is clear that the temperature of the sample should be corrected by measuring calibration curves under expected conditions. It should be also mentioned that these relations are identical to each IR cell. A calibration curve similar to that in Figure II-4(B) (warming process in vacuum) was measured for a different IR cell starting below -100 up to 500 °C of measured temperatures (Figure II-5). Being different from low temperature range, measured temperatures were coincident to the real ones even under evacuation above room temperature, probably due to the direct heating of the sample by irradiation of the emitted IR light from the heated cell.

It is known by a careful observation of IR spectra that the sharp IR absorption band of surface OH groups on oxide samples reversibly shifts by the temperature variation if the concentration stays unchanged. So, the frequency of OH band on oxide could be a measure to estimate the real temperature. Here, we used amorphous silica as a representative sample. A series of IR spectra in the region of isolated OH groups are arrayed in Figure II-6(A), which were measured between 500

and 25 °C in a cooling process. It is found that the peak top shifted gradually to high frequency side when the temperature was decreased. Figure II-6(B) is a plot of the peak top frequency and the real temperature of the sample. Both sets of data measured with 4 cm^{-1} (open circle) and 1 cm^{-1} (open triangles) resolutions can be plotted on the same line. Therefore, the resolution had no effect on the data scattering. The linear line has an error bar of about ± 25 °C, because the amount of shift is less than 10 cm^{-1} in the large difference of 475 °C in temperature. However, it could be a rough estimate of the real temperature. It should be also reported that the range of data scattering was dependent on the grade of FT-IR machine. A quite new FT-IR with a top grade (28 ° irradiation to a Michelson modulator with a corner cube mirror) was used for data in Figures II-6(A) and (B), but older FT-IR with less S/N ratio and with a different type of Michelson modulator (45 ° irradiation with a corner cube mirror) resulted in exactly the same line as shown in Figure II-6(B) although a different IR cell was attached, but a large scattering of data with an error bar of about ± 50 °C.

There may be better sample oxides, where the shifts of the absorption band are more sensitive. Any contributions to share the experimental knowledge as shown here would be respected and appreciated.

2.4. Conclusions

The peak top frequency of the stretching vibration of OH groups on amorphous silica reversibly changes accompanied by the change of the sample in temperature under the constant concentration. Using this phenomenon, the estimation of the real temperatures of samples in IR cell can be achieved. The temperatures measured from outside the cell are first calibrated to real ones. The OH frequency of silica can be correlated to the real temperature of the sample inside the cell via the calibration of the measured and the real temperatures of samples in each IR cell.

References:

[1] T. Jin, Y. Shou, G. M. Mains, J. M. White, J. Phys. Chem. 91 (1987) 5931-5937.

[2] R. R. Cavanagh, J. T. Yates, Jr., J. Chem. Phys. 75 (1981) 1551-1559.

[3] D. L. Roberts, G. L. Griffin, J. Catal. 95 (1985) 617-620.

[4] B. Lee, J. N. Kondo, K. Domen, F. Wakabayashi, Bull. Chem. Soc. Jpn. 71 (1998) 2149-2152.

[5] The concentration of SiOH groups under the present pretreatment conditions was estimated as 0.346 $mol \cdot g^{-1}$ (1.04 $sites \cdot nm^{-2}$) by pyridine adsorption at 25 ℃.

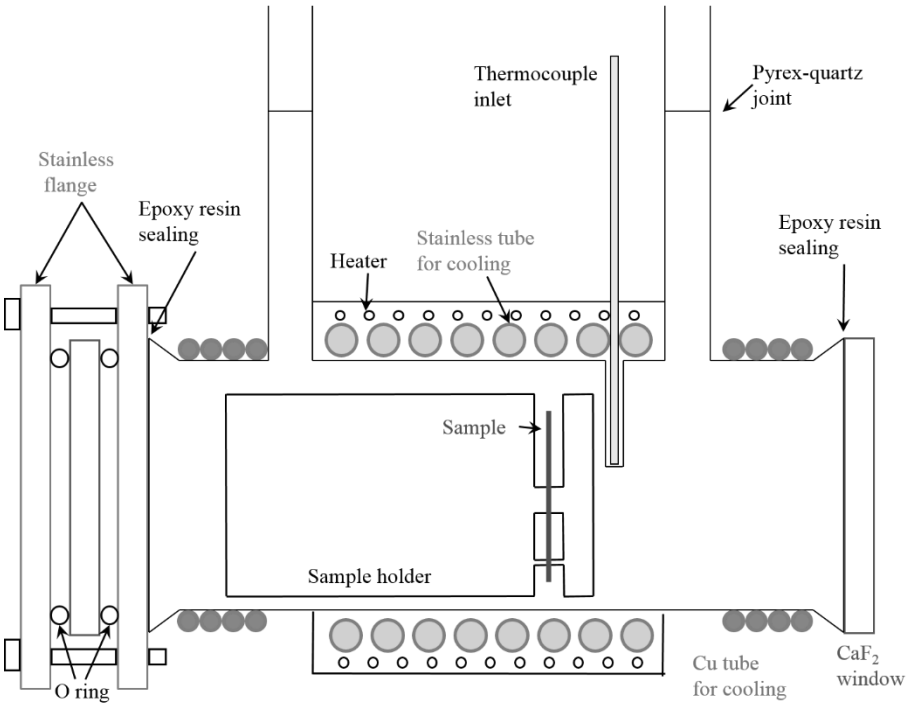

Figure II-1. Infrared cell used in this study.

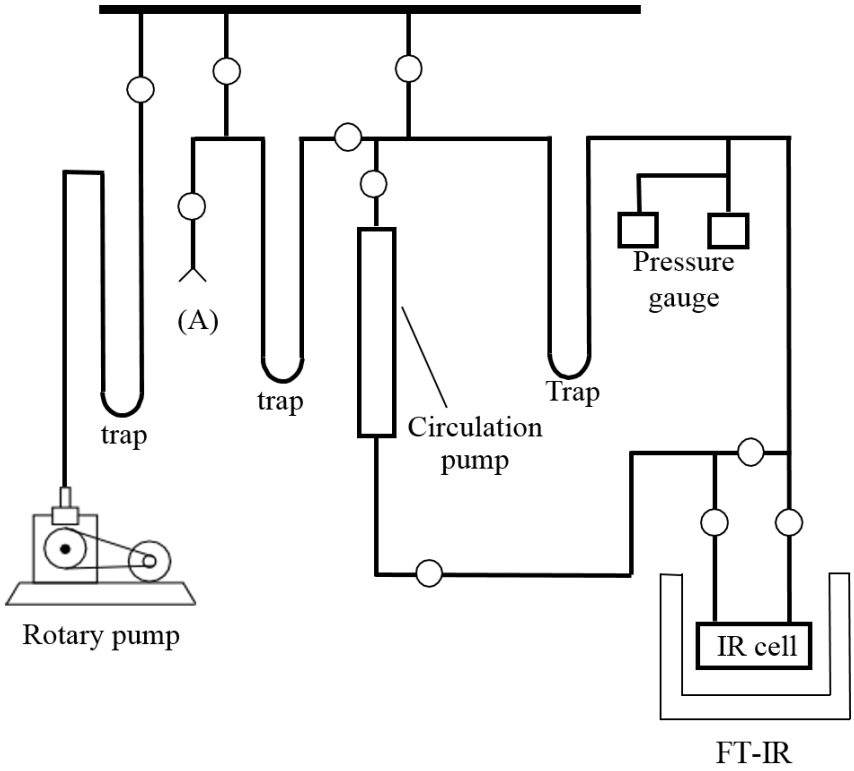

Figure II-2. Closed circulation system used in this study.

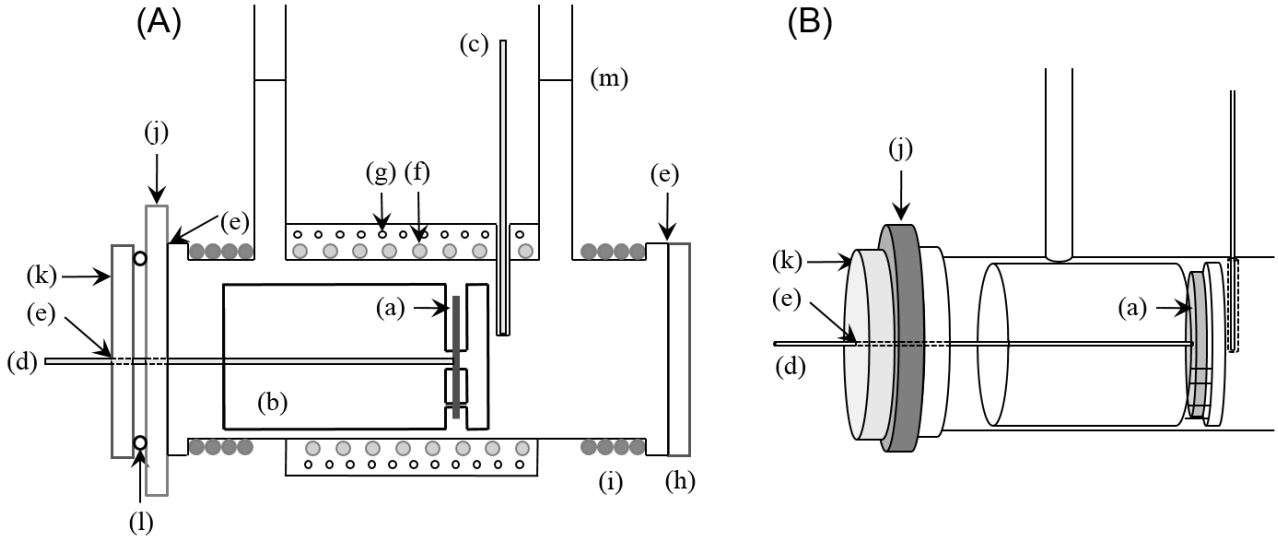

Figure II-3. (A) Side view and (B) schematic illustration of inside of IR cell for temperature calibrations: (a) sample, (b) sample holder, (c) TC (1), (d) TC (2), (e) epoxy resin sealing, (f) cooling tube (liquid nitrogen), (g) heater, (h) NaCl window, (i) cooling tube (water), (j) stainless flange, (k) acryl resin plate, (l) O-ring and (m) Pyrex-quarts joint.

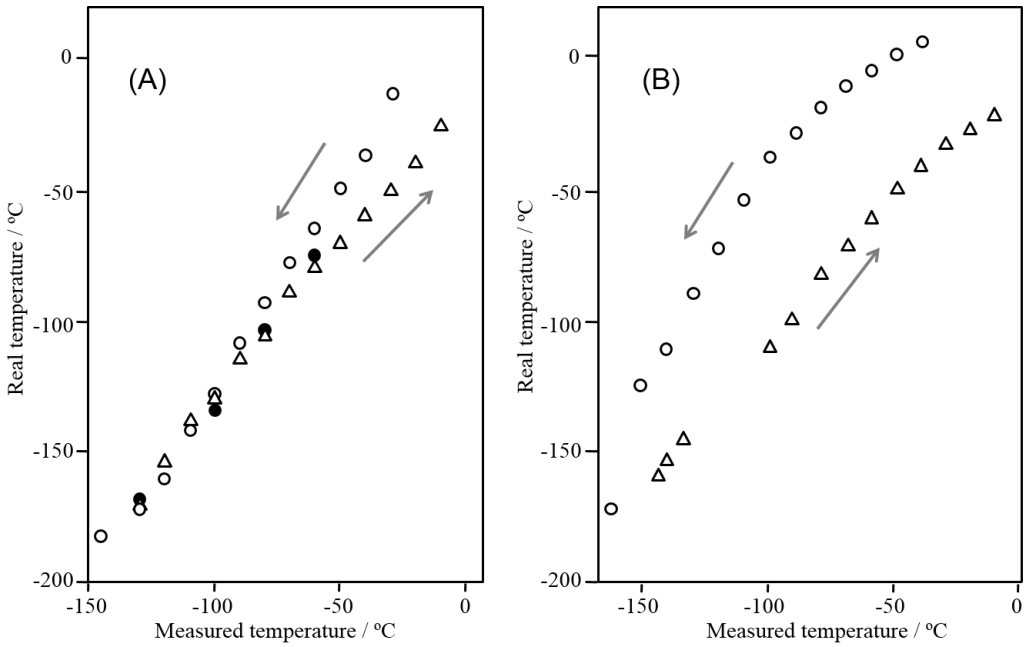

Figure II-4. Calibration curves of the measured and the real temperature (A) in the presence of hydrogen (13.3 kPa) and (B) under evacuation below room temperature: open circle, cooling procedure; open triangle, warming procedure; and filled circle, steady state.

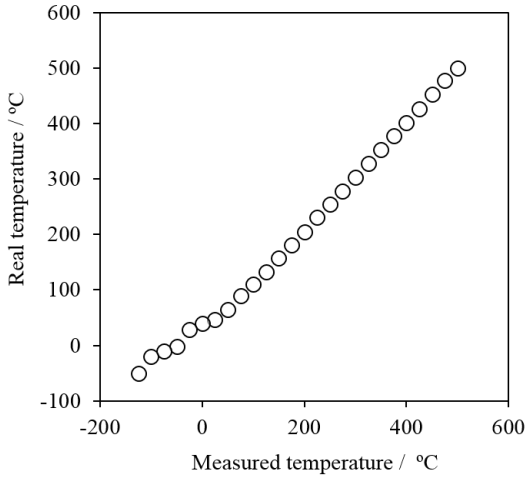

Figure II-5. Calibration curves of the measured and the real temperature under evacuation above room temperature.

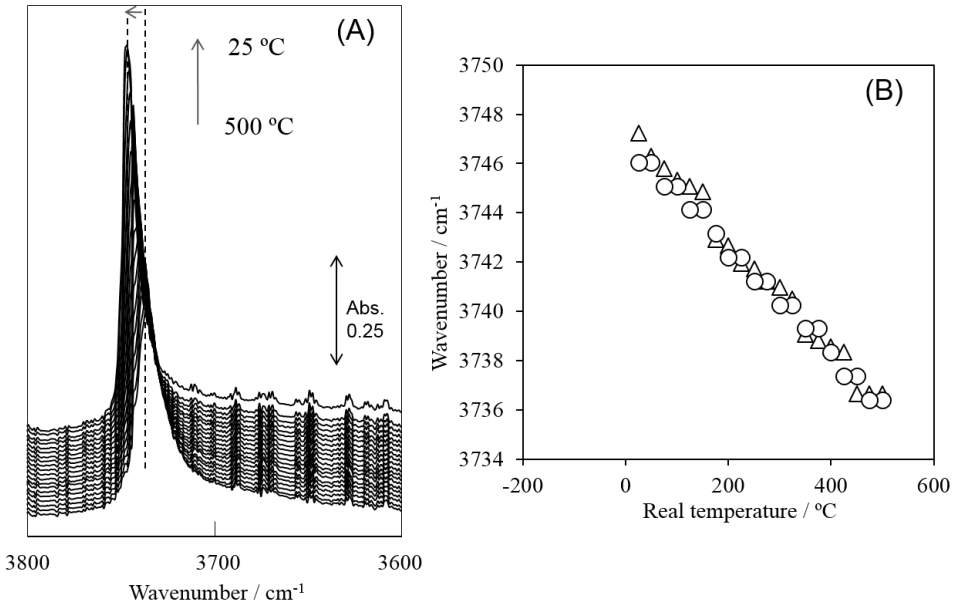

Figure II-6. (A) A series of IR spectra of OH stretching band of isolated silanol groups between 500 and 25 °C, and (B) the relation between the peak top frequency of silanol groups and the real temperature: open circles, data measured with resolution at 4 cm^{-1}; open triangles, those with resolution at 1 cm^{-1}.

Chapter III

Evidence for a "Carbene-like" Intermediate during the Reaction of Methoxy Species with Light Alkenes on H-ZSM-5

Abstract:

The infrared (IR) study on the reaction of methoxy species on ZSM-5 zeolite and ethene was investigated as one of the elementary step of methanol to hydrocarbons reactions. Carbene-like intermediate for the methylation of light olefins by methoxy species was proposed on zeolite, which is based on the IR observation that the recovered acidic hydroxyl groups after the reaction of d_3-methoxy groups with light olefin molecules are all deuterated. This indicates that the reaction of methoxy groups with olefins occur as methylene units but not as methyl units.

1. Introduction

Various discussions have been made on the mechanism of methanol to hydrocarbons (MTH) reaction from pin-point considerations on certain zeolite topologies of **CHA** [1-3], **MFI** [4-7], **BEA** [6], **TON** [8,9] and others to general summaries [10]. One of the main discussions is made on the structure of hydrocarbons in zeolite channels, so-called "hydrocarbon pool (HCP)" [6-12]. Since the selectivity of products formed from cracking of HCP is directly affected by the porous structure of zeolites, the clarification of the structures of HCP in various zeolites is certainly important. On the other hand, less research and discussion have been made on the initial C-C bond formation from a C_1 compound, methanol [1-3,8,9,12,13]. The initial processes of MTH would not be affected by the porous structure due to the small sizes of the products, reaction mechanisms on a single acidic OH group of zeolites should become of significance rather than zeolite topologies.

MTH reaction starts with the activation of methanol. The formation of methoxy species on zeolite upon exposure to methanol was first observed by infrared (IR) spectroscopy by Ono et al.

[14]. Afterward, IR spectra of methoxy species on bridging site of Si and Al and those on external Si sites, compensating for the acidic OH groups and the external silanol groups, respectively, were reported to appear differently [15-18]. Similarly, the formation of ethoxy species from ethanol adsorption on zeolites was confirmed by IR [19] and nuclear magnetic resonance (NMR) [20] spectroscopy. Thus, surface alkoxy species are regarded as the first activated species on zeolites formed from dehydration of alcohols. On the other hand, reports on the mechanism of the first C-C bond formation from methoxy species and the reactivity of them are still limited. Mainly two types of intermediates in mechanisms on the first C-C bond formation with methoxy species have been proposed [10,21]: 1) carbenium cation and 2) carbene-like intermediates. While recent researches focus more in HCP species [22-24] rather than reactions of light hydrocarbons, there is an agreement on the reaction of methoxy species; the first C-C bond formation from methoxy groups to ethene does not occur [4,5,8,9,13]. Under such circumstances, the research group of Hunger has recently been energetically studying the reactivity of methoxy species using solid state NMR spectroscopy and claim that methoxy groups are active species during MTH reaction [25]. They recently report that methoxy groups work as methylation agents of cyclohexane via "carbene-like species" [21]. Since recent developments in experimental techniques allow us to consider various proposals on mechanisms on MTH, the reactivity of methoxy species on H-ZSM-5 as well as other zeolites is investigated by IR spectroscopy using isotopes.

2. Experimental

Proton form of ZSM-5 (JRC-Z5-90H, Catalysis Society of Japan, Si/Al = 45) was pressed into a self-supporting disk (20 mm diameter, 60 mg) and placed in an IR cell attached to a conventional closed gas circulation system. The sample was pretreated by evacuation at 773 K with a liquid nitrogen trap for 1 h. IR spectra were obtained at a resolution of 4 cm^{-1} using a Jasco 4100 FT-IR spectrometer equipped with a mercury cadmium telluride (MCT) detector. A total of 64 scans were averaged for each spectrum. The IR spectra of the clean disk were recorded under evacuation at

various temperatures as background spectra. Background-subtracted IR spectra showing adsorbed species are presented throughout this paper. The gaseous components were analyzed by a GC (GC-14B, SHIMADZU Corporation) and a CG-mass (Agilent Technologies, GC-7890Q and MS-5975C with Triple-Axis Detector) spectrometer with a HP plot column. Ethene (TAKACHIHO CHEMICAL INDUSTRIAL Co. Ltd., 99.9%) and three methanol samples were used; CH_3OH (Wako Pure Chemical Industries, Inc., 99.8%), CD_3OH (Merck & Co., Inc., 99% isotopic purity) and $^{13}CH_3OH$ (Cambridge Isotope Laboratories, Inc., 99% isotopic purity). The amount of methoxy groups was adjusted to be 40 % (8.9×10^{-6} mol on 60 mg sample disk) of the acidic OH groups (2.2×10^{-5} mol on 60 mg sample disk), and ethene (2.2×10^{-6} mol), corresponding to a quarter of methoxy and one tenth of the acidic OH groups, was supplied from gas phase.

3. Results and discussion

Methanol molecules adsorb on the acidic OH groups of zeolites by strong hydrogen-bonding interactions as depicted in Scheme III-1, followed by dehydration to methoxy groups and water at temperatures above 473 K. The formed methoxy groups remain stable after water desorption, while immediate formation and desorption of ethene and water occur in the case of ethanol adsorption [19]. The formed methoxy species are thermally stable under evacuation even at 673 K, and the maximum coverage is about 40 % of the number of the acidic OH groups on H-ZSM-5. IR spectrum of methoxy groups on H-ZSM-5 at 523 K is shown in Figure III-2(a), where a background spectrum measured before methoxy formation is subtracted from that with methoxy groups. Negative peaks in OH stretching region are attributed to silanol (3740 cm^{-1}) and acidic OH (3600 cm^{-1}) groups, which decreased in amount due to methoxy formation. Two types of methoxy groups on silanol and the acidic OH groups show CH stretching bands at slightly different frequencies; at 2980 and 2868 cm^{-1} for methoxy species on the sites of the acidic OH groups, and at lower frequency sides of them for those on silanol sites, respectively. The band at 1457 cm^{-1} is assigned to methyl deformation band of both types of methoxy groups. The distorted baseline between 2000

and 1800 cm^{-1} is due to false feature of combination and overtone bands of zeolite lattice vibrations [26]. Time course of spectra after ethene introduction to methoxy groups at the same temperature are arrayed in (b) – (e), and (f) is a subtracted spectrum of (a) from (e). The decrease of three bands of methoxy groups (dotted lines) and the recovery of the band of the acidic OH groups are clearly observed in Figure III-2(f), indicating that methoxy groups on the sites of the acidic OH groups are consumed by the reaction with ethene.

The products of the reaction in Figure III-1 are listed in Table III-1. The bottom row indicate the absence of any reaction of ethene alone on H-ZSM-5 in the absence of methoxy groups after 60 min. Thus, both methoxy species and ethene molecules do not react individually at 523 K. On the other hand, methoxy species react with ethene first to propene, and carbon chain elongation seems to proceed in the time course: propene molecules react with methoxy species to form C_4 products, and C_5 species are produced by further reaction of C_4 compounds with methoxy species. Experimentally, when propene is reacted with methoxy groups under the same reaction condition [27], gradual carbon chain expansion occur in the time course of reaction products similarly to that in Table 1, and similar IR spectra to those in Figure III-1 are observed. Thus, methoxy groups are regarded as methylation reagents of light olefins in addition to cyclohexane and toluene [28].

To gain insight into the reaction mechanism, deuterated methoxy groups are produced from d_3-methanol (CD_3OH) and reacted with light olefins. The spectrum in Figure III-2(a) is attributed to deuterated methoxy groups formed on H-ZSM-5. Similarly to the case of Scheme III-1, decrease of silanol and the acidic OH groups are noted by negative peaks at 3740 and 3601 cm^{-1}, respectively, and CD stretching bands are observed between 2300 and 2000 cm^{-1} instead of CH stretching bands in Figure III-2. The methyl deformation band is absent in Figure III-2(a) due to the isotope shift below the low-frequency limit of IR spectra of adsorbed species on zeolites [29]. After ethene introduction under the same conditions as those in Figure III-2, CD stretching bands decrease in intensity simultaneously with appearance and the increase in intensity of the acidic OD band at 2655 cm^{-1}. It should be noted that only the acidic OD groups recover, while the acidic OH band at

3600 cm^{-1} is silent in the subtracted spectrum in Figure III-2(f). This indicates that the hydrogen of the acidic hydroxyl groups can be only provided from methoxy groups but no possibility to be given from ethene molecules. In other words, C-C bond formation between d_3-methoxy groups and ethene molecules does not proceed with CD_3 unit. Only two deuterium atoms are involved in the product as CD_2 group, leaving one deuterium atom as an acidic OD group.

The alkoxy groups formed on zeolite surfaces are proposed to react as carbenium cations in transition states in early theoretical studies [30]. In addition, methoxy groups are supposed to migrate as in the form of methyl cations similarly to the motion of protons of acidic OH groups [14,31]. This methyl cation formation from methoxy groups is supported by DFT calculation researches [32,33]. Assuming the carbenium cation mechanism for the reaction observed in this study, where d_3-methoxy species react with ethene as CD_3^+ groups, 2-propyl cation ($CD_3CH^+CH_3$) would be present as an intermediate (Scheme III-2). Otherwise, such cationic form may be the transition state and 2-propoxy group would be the stable form. For the reaction of 2-propyl cation to propene and Brønsted acid site, two possible pathways exist; resulting in the formation of $CD_3CH=CH_2$ with OH group, and $CD_2=CHCH_3$ with OD. Even considering isotope effect between hydrogen and deuterium, the absence of the recovery of the acidic OH groups cannot be explained by the carbenium cation mechanism for the reaction. Another possible root is proposed by a recent theoretical calculations, suggesting the stabilization of 1-propyl cation ($^+CH_2CH_2CH_3$) from the reaction of methoxy groups and ethene [33]. Following this scheme, $^+CH_2CH_2CD_3$ cation is expected to form from d_3-methoxy group and ethene, which results in releasing hydrogen for Brønsted acid site and evolving d_3-propene ($CH_2=CHCD_3$). Thus, methyl carbenium cation mechanism is not understandable in any cases.

From the NMR observation of the production of ^{13}C-methylcyclohexane from ^{13}C-methoxy groups and cyclohexane, carbene-like intermediate for the reaction of methoxy groups is proposed via C-H bond activation of methoxy group with lattice oxygen as depicted in Scheme III-3 [21]. However, carbene-like species is excluded from the possible intermediate for the reaction of

methoxy groups by DFT-based calculations [13]. In the case of present study, the presence of carbene-like intermediate is the most likely reaction mechanism from the fact that deuterium is the origin of the recovered Brønsted acid site (Scheme III-3). This reaction probably proceeds in a concerted manner as proposed by Hunger et al., where lattice oxygen would attract one of the deuterium atoms in the d_3-methoxy group [20,21]. Concurrently, adsorbed ethene in equilibrium with gaseous molecules reacts with the activated d_3-methoxy group. If C=C double bond is directly formed between methoxy groups and ethene molecules, CD_2=$CHCH_3$ would be produced. The other possibility is the CD_2HCH=CH_2 generation if hydrogen transfer occurs from ethene molecules to methoxy groups.

For further understanding of the reaction, ^{13}C-methanol was employed to generate ^{13}C-methoxy groups, where ethene was supplied under the same conditions, to analyze the product by gas chromatograph (GC) mass spectroscopy [34]. The cracking pattern of ethene in the collected sample was exactly the same as that of the pure ethene reference (Figure III-3), while it was not the case for propene: peaks in cracking pattern of propene in product appeared in similar intensity ratios as those of pure propene but increased in mass number by one (Figure III-4, m/e = 36 - 45). This clarifies the involvement of one ^{13}C in propene formed by the reaction between ^{13}C-methoxy groups and ethene. Similarly, the cracking pattern of C_2 component in mass spectrum of produced propene increased in mass number from the pattern of propene reference (Figure III-3, m/e = 26 - 29). The result implies that ^{13}C is in sp^2 environment as a result of cleavage of propene to $^{13}CH_2$=CH and C_1 components, assuming that C-C single bond is split more easily than C=C double bond. (C_1 component could not be analyzed due to their weak signals.) Thus, production of CD_2=CH-CH_3 from d_3-methoxy groups and ethene seems more likely than CD_2H-CH=CH_2 in scheme III-3. H-NMR analysis of propene produced by the reaction of ^{13}C-methoxy groups and ethene was attempted by accumulating products from the reaction more than 10 times, but reliable results were not obtained due to the lack of satisfactory intensity of signals.

The possibility of the reaction pathway of methoxy groups in methyl unit is considered. It is

reported that methoxy species react as methyl cation with strongly basic molecules to form $(CH_3)_nNH_{(4-n)}^+$ (n = 1–4) from ammonia and $C_5H_5N\text{-}CH_3^+$ from pyridine [35,36]. I also confirmed that IR spectra measured after the reaction of methoxy groups and ammonia and those of methylamine adsorption were identical. Thus, methoxy groups react with strong bases in methyl unit, while they react via carbene-like species with light olefins.

Since results above are all obtained using H-ZSM-5 (Si/Al = 45), other zeolites as well as H-ZSM-5 samples with different aluminum contents are compared for the reaction of d_3-methoxy groups and ethene. First, H-ZSM-5 samples (Si/Al = 25 and 150) showed the same IR results with good S/N ratio and similar selectivity as that over silicon to aluminum ratio 45, while yield was dependent on the aluminum content; the higher the aluminum content is, the higher the yield becomes. For H-ZSM-5 with much higher silicon to aluminum ratios (Si/Al = 270 and 350), conversion of ethene was very low and S/N ratio of IR spectra were too low, but the absence and presence of the recovery of OH and OD groups was confirmed, respectively. Similar results were obtained over mordenite (MOR, Si/Al = 45) and SSZ-13 (CHA, Si/Al = 45) at the same temperature range but at slightly higher temperatures over HY (FAU, Si/Al = 5.5) zeolite. Thus, the reaction mechanism shown in Scheme III-3 is experimentally evidenced on various zeolites. Further experiments using methanol isotopes and DFT calculations are under way.

4. Conclusions

Carbene-like intermediate for the reaction of methoxy groups with light olefins is proposed on zeolites, which is based on the IR observation that the recovered acidic hydroxyl groups after the reaction of d_3-methoxy groups with light olefin molecules are all deuterated. This indicates that the reaction of methoxy groups with olefins occur as methylene units but not as methyl units.

References:

[1] B. Arstad, S. Kolboe, J. Am. Chem. Soc. 123 (2001) 8137-8138

[2] W. Song, H. Fu, J. F. Haw, J. Am. Chem. Soc. 123 (2001) 4749-4754

[3] W. Wang, Y. Jiang, M. Hunger, Catal. Today 113 (2006) 102-114.

[4] T.-Y. Park, C. F. Froment, Ind. Eng. Chem. Res. 40 (2001) 4172-4186.

[5] S. Svelle, F. Joensen, J. Nerlov, U. Olsbye, K.–P. Lillerud, S. Kolboe, M. Bjørgen, J. Am. Chem. Soc. 128 (2006) 14770-14771.

[6] M. Bjørgen, F. Joensen, K.-P. Lillerud, U. Olsbye, S. Svelle, Catal. Today 142 (2009) 90-97.

[7] Z.-M. Cui, Q. Liu, S.-W. Bain, Z. Ma, W.-C. Song, J. Phys. Chem. C 112 (2008) 2685-2688.

[8] M. Stöker, Microp. Mesop. Mater. 29 (1999) 3-48.

[9] J. Q. Chen, A. Bozzano, B. Glover, T. Fuglerud, S. Kuisle, Catal. Today 106 (2005) 103-107.

[10] M. Bjørgen, S. Svelle, F. Joensen, J. Nerlov, S. Kolboe, F. Bonino, L. Palumbo, S. Bordiga, U. Olsbye, J. Catal. 249 (2007) 195-207.

[11] D. M. McCann, D. Lesthaeghe, P. W. Kletnieks, D. R. Guenther, M. J. Hayman, V. Van Speybroeck, M. Waroquier, J. F. Haw, Angew. Chem. Int. Ed. 47 (2008) 5179-5172.

[12] D. M. Marcus, K. A. McLachlan, M. A. Wildman, J. O. Ehresmann, P. W. Kletnieks, J. F. Haw, Angew. Chem. Int. Ed. 45 (2006) 3133-3136.

[13] D. Lesthaeghe, V. Van Speybroeck, G. B. Martin, M. Waroquier, Angew. Chem. Int. Ed. 45 (2006) 1714-1719.

[14] Y. Ono, T. Mori, J. Chem. Soc., Faraday Trans. 1 77 (1981) 2209-2221.

[15] T. Forester, R. Howe, J. Am. Chem. Soc. 109 (1987) 5076-5082.

[16] S. Campbell, X. Jiang, R. Howe, Microp. Mesop. Mater. 29 (1999) 91-108.

[17] L. Kubelkova, J. Novakova, K. Nedomova, J. Catal. 124 (1990) 441-450.

[18] F. Wakabayashi, M. Kashitani, T. Fujino, J. N. Kondo, K. Domen, C. Hirose, Stud. Surf. Sci. Catal. 105 (1997) 1739-1746.

[19] J. N. Kondo, K. Ito, E. Yoda, F. Wakabayashi, K. Domen, J. Phys. Chem. B 109 (2005)

10969-10972.

[20] W. Wang, J. Jiao, Y. Jiang, S. S. Ray, M. Hunger, Chem. Phys. Chem. 6 (2005) 1467-1469.

[21] W. Wang, M. Hunger, Acc. Chem. Res. 41 (2008) 895-904.

[22] J. F. Haw, T. Xu, Adv. Catal. 42 (1998) 115-180.

[23] J. F. Haw, J. B. Nicholas, W. Song, F. Deng, Z. Wang, T. Xu, C. S. Heneghan, J. Am. Chem. Soc. 122 (2000) 4763-4775.

[24] C. Lamberti, E. Groppo, G. Spoto, S. Bordiga, A. Zeccchina, Adv. Catal. 51 (2007) 1-74.

[25] M. Hunger, J. Weitkamp, Angew. Chem. Int. Ed. 40 (2001) 2954-2971.

[26] A. Zecchina, F. Geobaldo, G. Spoto, S. Bordiga, G. Ricchiardi, R. Buzzoni, G. Petrini, J. Phys. Chem. 100 (1996) 16584-16599.

[27] This reaction was confirmed using H-ZSM-5 with Si/Al= 150 since the reaction of propene in the absence of surface methoxy groups proceeds over H-ZSM-5 (Si/Al = 45) at about 10 % of conversion of propene with methoxy groups.

[28] W. Wang, A. Buchholz, M. Seiler, M. Hunger, J. Am. Chem. Soc. 125 (2003) 15260-15267.

[29] Si-O stretching bands absorb IR beam below 1300 cm^{-1}, and no information are obtained at the corresponding frequency ranges.

[30] V. B. Kazanski, Catal. Today 51 (1999) 419-434; P. E. Sinclair, A de Vries, P. Sherwood, R. C. A. Catlow, R. A. van Santen, J. Chem. Soc., Faraday Trans. 94 (1998) 3401-3408.

[31] T. Baba, T. Mori, Y. Ono, H. Sugihara, J. Phys. Chem. B 102 (1998) 804-808.

[32] C. M. Zicovich-Wilson, P. Viruela, A. Corma, J. Phys. Chem. 102 (1995) 13224-13231.

[33] T. Maihorn, B. Boekfa, J. Sirijaraensre, T. Nanok, M. Probst, J. Limtrakul, J. Phys. Chem. C 113 (2009) 6654-6662.

[34] About 40 % of acidic OH groups were replaced by 13C-methoxy groups and 5 Pa of ethene was reacted at 523 K. The gaseous compounds were collected by liquid nitrogen at 5 min after the supply of ethene. The injected sample was first separated by a column, and then proceeded to a mass analyzer and GC at the same time. The gas sample was dominated by ethene,

involving a few % of propene under the present conditions.

[35] Y. Jiang, M. Hunger, W. Wang, J. Am. Chem. Soc. 128 (2006) 11679-11692.

[36] T. Jin, Y. Shou, G. M. Mains, J. M. White, J. Phys. Chem. 91 (1987) 5931.

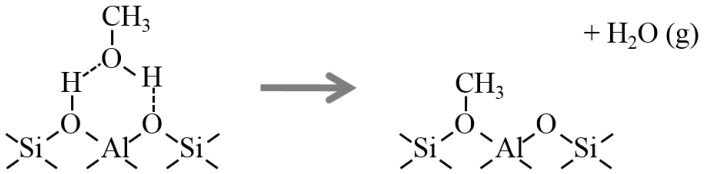

Scheme III-1. Formation of methoxy groups from methanol adsorbed on the acidic OH groups on zeolites.

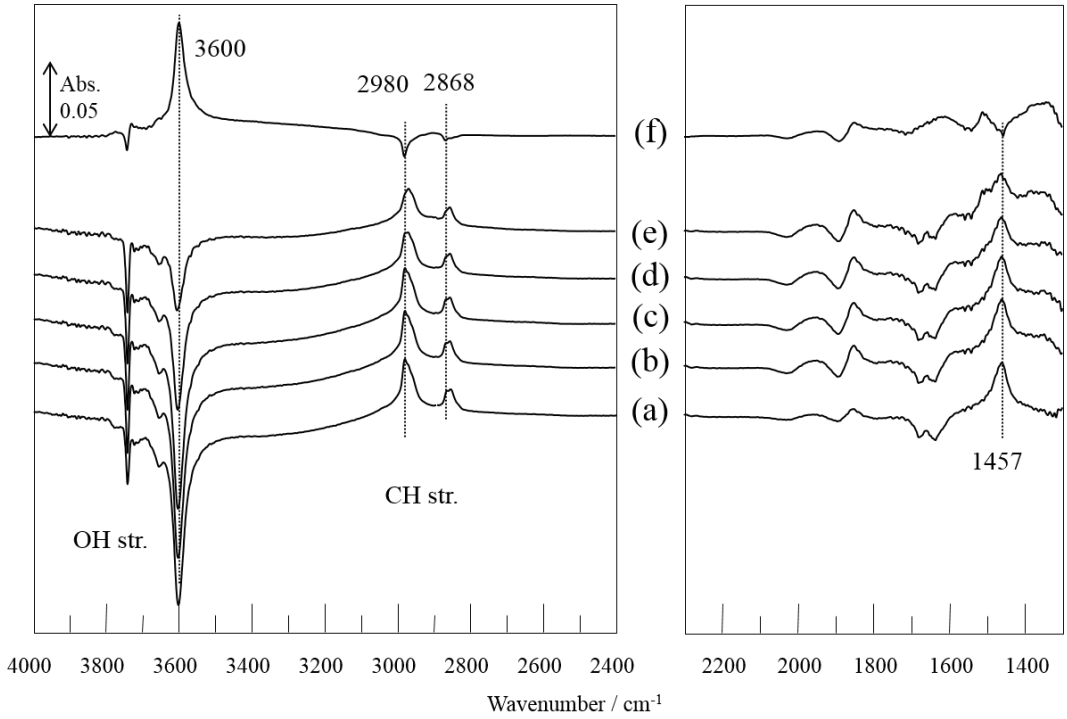

Figure III-1. Time course of IR spectra of surface species during the reaction of methoxy species with ethene at 523 K on H-ZSM-5; (a) before ethane introduction, (b) 5 min, (c) 10 min, (d) 30 min, (e) 60 min, and (f) subtracted spectrum of (a) from (e).

Table III-1. Reaction of ethene with methoxy species on H-ZSM-5 at 523 K

Reaction time / min	Conversion[a] / %	Yield / mol%			
		$C3^{=}$	C4	C5	C6
5	0.8	0.8	0	0	0
10	2.3	1.9	0.4	0	0
30	12.3	8.2	3.4	0.5	0.3
60	16.3	8.3	6.6	1.0	0.3
60[b]	0	-	-	-	-

Reaction conditions: catalyst, 60 mg; ethene, ca.15 Pa; temperature, 523 K.
[a] Conversion of ethene.
[b] No methoxy species present.

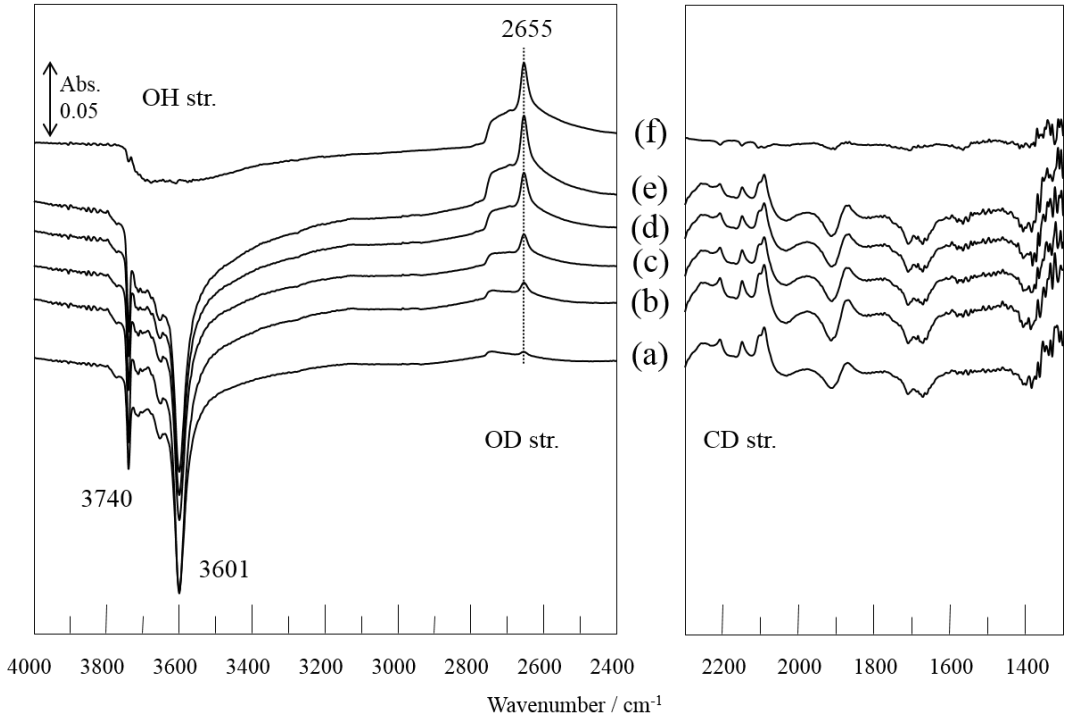

Figure III-2. Time course of IR spectra of surface species during the reaction of methoxy (OCD_3) species with ethene at 523 K on H-ZSM-5; (a) before ethene introduction, (b) 5 min, (c) 10 min, (d) 15 min, (e) 20 min, and (f) subtracted spectrum of (a) from (e).

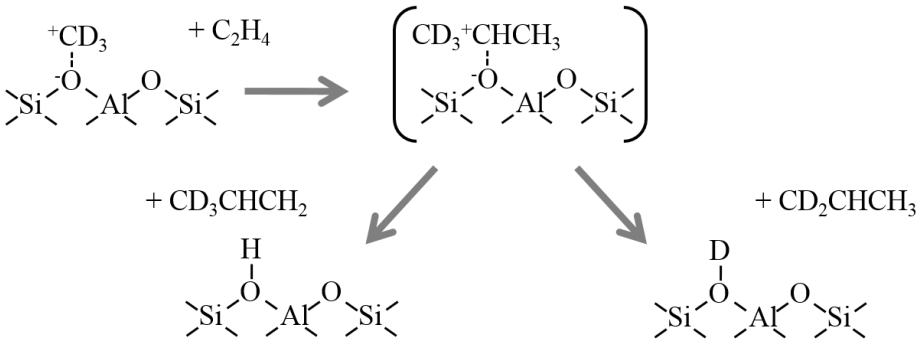

Scheme III-2. Mechanism of the reaction of methoxy group with ethene to propene via iso-propoxy group (or iso-propyl cation).

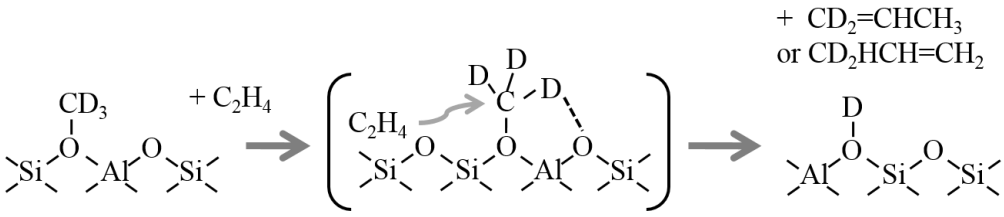

Scheme III-3. Proposed mechanism of the reaction of methoxy group with ethene to propene via carbene-like species.

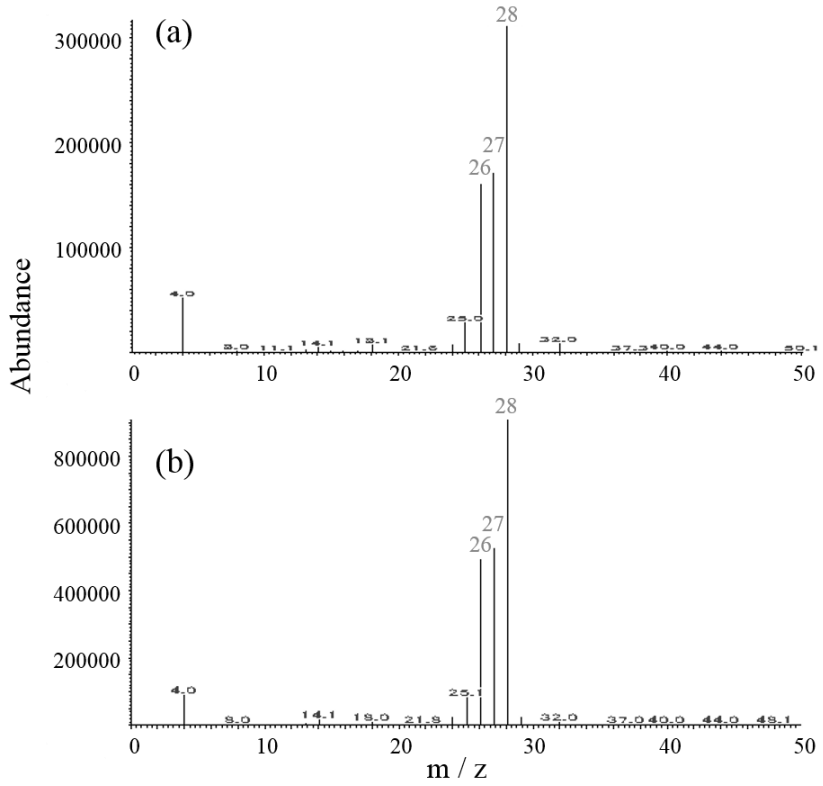

Figure III-3. GC mass spectra of (a) ethene in collected gas from the reaction of ^{13}C-methoxy species and ethene at 523 K for 5 min and (b) pure ethene reference.

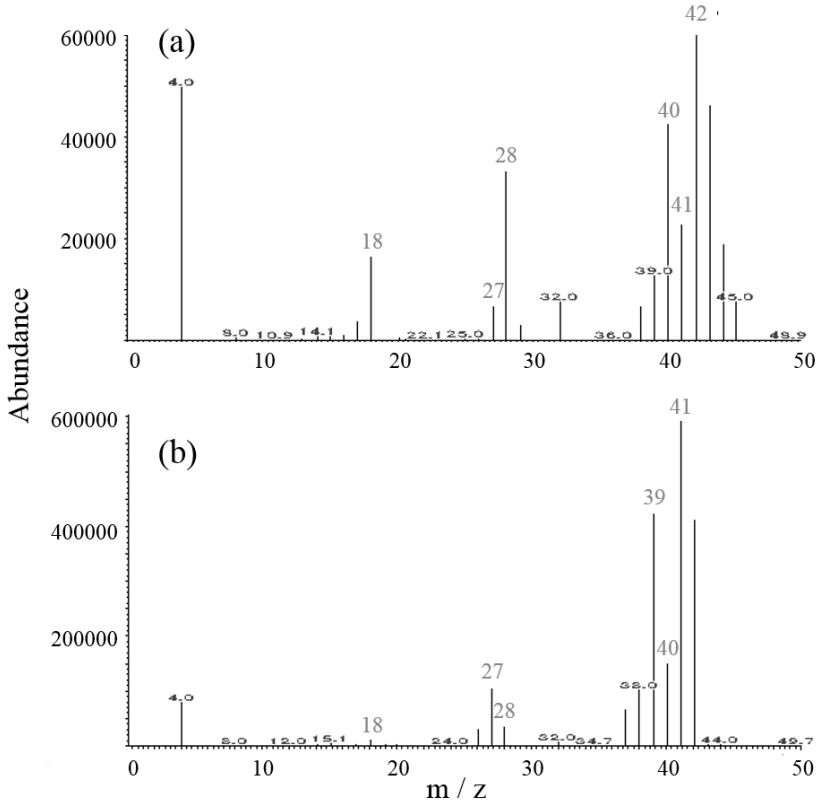

Figure III-4. GC mass spectra of (A) prepene in collected gas from the reaction of ^{13}C-methoxy species and ethene at 523 K for 5 min and (B) pure propene reference. The collection of gaseous molecules were conducted 5 min changing catalyst each time for the accumulation of propene content.

Chapter IV

Direct Production of Propene from Methoxy Species and Dimethyl Ether over H-ZSM-5

Abstract:

The mechanism of the initial C−C bond formation on methanol to hydrocarbon (MTH) reactions were not clarified. In this chapter, the reaction mechanism and the reactivity of methoxy species on H-ZSM-5 zeolite with methanol or dimethyl ether (DME), which is the initial product of MTO and MTH reactions, were observed by infrared (IR) spectroscopy. The direct production of propene from methoxy groups and DME is evidenced on H-ZSM-5 zeolite by isotopic studies of IR observation of surface species and gas chromatograph-mass spectroscopy (GC-MS) analysis of products. Stepwise reactions of DME to ethene and water followed by methylation of ethene by methoxy groups were negligible during the generation of propene by the reaction of methoxy groups and DME.

1. Introduction

Among various olefins produced from the methanol-to-hydrocarbons (MTH) reaction, the demand for propene, which is a vital starting material for petrochemical products, is markedly increasing. A variety of zeolites is explored for the application to the MTH reaction in order to selectively obtain propene, so-called methanol-to-olefins (MTO) [1-5]. The “hydrocarbon pool mechanism” has been long considered as a mechanism of the steady state of the MTO reaction [6,7]. Meanwhile, the initial elemental step of the MTO reaction is found to be the formation of surface methoxy species from methanol [8-10]. The reactivity of methoxy species with amines, cyclohexane, toluene, ethene, and so on has been investigated by infrared (IR) [8,9,11] and nuclear magnetic resonance (NMR) [10] spectroscopies. Accordingly, it was found that methoxy species react with strong bases as a

methyl unit (CH_3-) to form C-N bond [10,11], while they react with light olefins as carbene-like species to generate C-C bond (Scheme IV-1) [11]. While methoxy species were confirmed as active species for carbon chain elongation of olefins [11-15], the essential information on the initial production of light olefins is unprovided. It is well known that dimethyl ether (DME) is the main product at lower reaction temperatures [15-17] and over deactivated catalysts during the MTO reaction. Consequently, DME and water (CH_3OCH_3 + H_2O) are generally considered to be equivalent to 2 molecules of methanol ($2CH_3OH$) [16-17]. While investigating the reactivity of methoxy species in our group, I found that the reaction of methoxy species with DME is faster than that of methoxy species with ethene or methanol. In addition, it is inferred that DME reacts with methoxy species directly to form propene from analysis of IR and gas chromatography-mass spectroscopy (GC-MAS) using isotopes, which is shown below.

2. Experimental

The hydrogen form of ZSM-5 (JRC-Z5-90H, Catalysis Society of Japan, Si/Al = 45) was pressed into a self-supporting disk (20 mm diameter, 60 mg) and placed in an IR cell attached to a conventional closed gas circulation system. The sample was pretreated by evacuation at 773 K for 1 h. IR spectra were obtained at a resolution of 4 cm^{-1} using a Jasco 4100 FT-IR spectrometer equipped with a mercury cadmium telluride (MCT) detector. A total of 64 scans were averaged for each spectrum. The IR spectra of the clean disk were recorded under evacuation at various temperatures as background spectra. Background-subtracted IR spectra showing adsorbed species are presented throughout this paper. The gaseous components were analyzed by a GC (GC-14B, SHIMADZU Corporation) and a GC-MS (Agilent Technologies, GC-7890Q and MS-5975C with Triple-Axis Detector) spectrometer with a HP plot column. Ethene (TAKACHIHO CHEMICAL INDUSTRIAL Co. Ltd., 99.9%), dimethyl ether (Kanto Chemical Industries, Inc., 99.8%) and three methanol samples were used; CH_3OH (Wako Pure Chemical Industries, Inc., 99.8%), CD_3OH (Merck & Co., Inc., 99% isotopic purity) and $^{13}CH_3OH$ (Cambridge Isotope Laboratories, Inc., 99%

isotopic purity). The amount of methoxy groups was adjusted to 40 % (8.8×10^{-6} mol on 60 mg sample disk) of the acidic OH groups (2.2×10^{-5} mol on 60 mg sample disk).

3. Results and discussion

When H-ZSM-5 (Si/Al = 45) was exposed to methanol at 573 K, 40% of the acidic OH groups was replaced by methoxy species [11]. The distributions of the products of the reactions of methoxy species with DME, methanol or ethene at 523 K are shown in Table IV-1. The amount of injected DME, methanol or ethene was adjusted to a molar ratio of a quarter of methoxy species i.e., corresponding to 10% of the acidic OH sites of H-ZSM-5. In the case of the reaction of methoxy species with DME, the conversion of DME at 5 min was 57.1%, and the main product was propene with a small amount of C_4 compounds. The total yield of hydrocarbons (49.0%) was lower than the conversion of DME (57.1%) on a carbon atom basis owing to the production of methanol, which became inconspicuous as the reaction proceeded. Propene was the main product until 10 min, and C_4 compounds became dominant due to the further reaction of the produced propene with methoxy species [11] after 30 min. It should be noted that the formation of ethene was not observed until 30 min. This is in agreement with the conclusion that ethene is not directly formed from the coupling of methoxy species [2,18-21]. The belated production of ethene in the time course may indicate it is formed from the cracking of higher hydrocarbons. However, the absence of ethene at the beginning could be also explained by the rapid reaction of ethene, which was formed from DME, with methoxy species (Scheme IV-2 (a)). Products yield from the reaction of methoxy species with ethene are also shown in Table IV-1. The conversion of ethene was much smaller than that of DME under the same conditions. Furthermore, the yield of propene from methoxy species and ethene was obviously lower than that from methoxy species and DME. Thus, DME would be considered to react with methoxy species directly to form propene (Scheme IV-2 (b)). The propene formation mechanism is discussed below based on IR results using isotopes.

Next, methanol was introduced to react with methoxy species under the same conditions.

Although the initial conversion exceeded 80%, the main product was DME with a small amount of propene detected. The products distribution at 30 min was almost the same as that at 10 min of the reaction of methoxy species with DME. A prolonged reaction time, the products were similar to those of the reaction of methoxy species with DME. This finding is explained by the initial formation of DME from methoxy species and methanol, followed by the further reaction of DME with methoxy species.

Figure IV-1 shows a time course of background-subtracted IR spectra of surface species during the reaction of methoxy species with DME at 523 K, corresponding to results in Table IV-1. Before injection of DME (Figure IV-1 (a)), the presence of methoxy species on the sites of original silanol (3740 cm^{-1}) and acidic OH groups (3602 cm^{-1}) was ascertained by negative OH stretching bands, while methoxy species were identified by upward CH stretching bands (3000-2800 cm^{-1}) and bending (1457 cm^{-1}) bands. The time course of IR spectra after injection of DME to methoxy species are arrayed in Figure IV-1 (b)-(e); Figure IV-1 (f) is a subtracted spectrum of (a) from (e). The decrease of the band of methoxy species in intensity and the concomitant recovery of the acidic OH groups are observed in Figure IV-1 (f). This indicates that methoxy species on the site of acidic OH groups were consumed by the reaction with DME, while those on silanol sites did not participate in the reaction [11]. The IR band of oligomeric species (allylic-type cations [22,23]) also appeared at 1510 cm^{-1} and increased in intensity after 30 min. Therefore, ethene was supposed to be formed from cracking of oligomeric species. Similar spectral changes were observed for the reaction of methoxy species with methanol. It should be noted that considerable amount of propene was already produced (Table IV-1) within 30 min, where only methoxy species exist before the formation of oligomeric compounds (Figure IV-1). This indicates the initial production of propene before the operation of hydrocarbon pool mechanism [18].

For quantitative observation, similar reactions were conducted at lower temperature (473 K) with the carbon numbers of reactants kept constant. Table IV-2 compares the product analysis of the reaction of methoxy species with methanol or DME and water at 473 K with the same atomic moles

of carbon, hydrogen and oxygen. Note that 40% of the acidic OH groups are replaced by the methoxy groups. Although DME reacts more slowly with the methoxy species at 473 K than at 523 K, the initial product was mainly propene. Then, carbon chain growth occurred by the successive reaction of propene with methoxy species without ethene production. Therefore, the presence of water is found not to influence the reaction of methoxy species with DME, and ethene is not formed from direct coupling of methoxy species, which is in agreement with the early proposals [2,18-21]. On the other hand, only DME was produced during the reaction of methoxy species with methanol at this temperature for 60 min. Thus, the reactivity of methanol greatly differs from that of DME in the formation of hydrocarbons. Moreover, the reactivity of ethene (Table IV-2) is much lower than that of DME under similar conditions. These results support the pathway in Scheme IV-2 (b); propene is not produced by the reaction of methoxy species with ethene, which could be formed from dehydration of DME, but by its reaction with DME at initial stage of the reaction.

It is worth noting that an appreciable amount of ethene was formed by the reaction of DME on bare H-ZSM-5 in the absence of methoxy species (Table IV-2). Then, an extreme increases in the conversion of DME and the yield of propene were observed from 30 to 60 min, probably due to the formation of methoxy species from DME and the resulting reaction of DME with methoxy species. Figure IV-2 shows the time course of IR spectra of surface species during the reaction of DME alone on H-ZSM-5 at 473 K, corresponding to the third reaction shown in Table IV-2. The negative band of the acidic OH groups appeared due to the adsorption of DME molecules, and was converted to a broad band (3000-1300 cm^{-1}) assigned to hydrogen-bonded OH groups, so-called ABC trio bands [24,25]. All CH stretching bands are attributable to DME [9]. Thus, it seems that DME adsorbed on acidic OH groups at the initial step. Then, the appearance of CH stretching bands changed in progress of the reaction with the broad hydrogen-bonded band decreased in intensity (indicated by arrows). Additionally, the negative band of the isolated acidic OH band increased in intensity up to 30 min after but decreased 60 min after. Figure IV-3 shows the difference IR spectra of those in Figure IV-2 at time intervals in order to emphasize the changes. The decrease in isolated

acidic OH groups (negative band at 3600 cm^{-1}) due to the conversion to the hydrogen-bonded state (broad band of 2600-1300 cm^{-1}) with DME was observed in Figure IV-3 (a). Negative bands at 3100-2800 cm^{-1} and 2600 to 1300 cm^{-1} in Figure IV-3 (b) indicate the decrease in molecularly adsorbed DME on acidic OH groups. Instead, new CH stretching bands at 2980 and 2866 cm^{-1} with a bending band at 1457 cm^{-1} were observed due to the formation of methoxy species from adsorbed DME (Scheme IV-3 (a)). Then, acidic OH groups recovered accompanied with decrease in the amount of methoxy species in Figure IV-3 (c). As shown in Table IV-2, the initial products of this reaction were ethene and propene. After methoxy species were observed 30 min after the reaction and consumed 60 min after, the main product became propene. Therefore, a small amount of ethene was formed from DME in the absence of methoxy species (Scheme IV-3 (b)), although the reaction of DME with methoxy species is much faster than that of DME alone. In other words, methoxy species are an important immediate for the formation of propene.

The reaction mechanism was investigated in detail by using d_3-methoxy species formed form CD_3OH. Figure IV-4 shows a time course of IR spectra during the reaction of d_3-methoxy species with DME at 473 K. Spectrum IV-4 (a) is attributed to d_3-methoxy species on H-ZSM-5. The decrease in silanol and the acidic OH groups appeared as negative peaks at 3742 and 3602 cm^{-1}, respectively, and CD stretching bands of d_3-methoxy species were observed at 2300-2000 cm^{-1}. After introduction of DME, CH stretching bands at 3010-2800 cm^{-1} appeared in Figure IV-4 (b) due to the adsorption of DME similarly to Figure IV-3 (a). The acidic OD groups at 2656 cm^{-1} appeared at 45 min after the reaction and increased in intensity in Figures IV-4 (e)-(f). In order to specify the spectral changes at each time, the difference IR spectra of those in Figure IV-4 at time intervals are shown in Figure IV-5. The distributions of the products of the reaction of methoxy species with DME at 473 K, corresponding to the experimental procedure in Figure IV-4, are shown in Table IV-3. Figure IV-5 (a) indicates that DME was adsorbed on free acidic OH groups similarly to the case in Figure IV-3 (a), and that the CD stretching bands decreased in intensity, suggesting that d_3-methoxy species reacted with d_0-DME to form d_0-methoxy species and d_3-DME (Scheme IV-4).

Since the adsorbed d_3-DME is in equilibrium with gaseous d_0-DME, it is promptly exchanged by d_0-DME, which is dominant. Then, surface species did not change in difference spectra (b) and (c) in Figure IV-5, while a large amount of propene was formed 30 min after (Table IV-3). If ethene formed from DME reacted with methoxy species to propene, acidic OD groups should be formed from d_3-methoxy species (Scheme IV-1). However, acidic OD groups were not produced until 30 min after. Therefore, it is concluded that in the initial stage of the reaction, propene was not formed via ethene through carbene-like immediate. Thus, it is concluded that methoxy species react with DME as CD_3 groups, not as CD_2 units, to form propene. At the final stage of the reaction (Figures IV-5 (d) and (e)), upward peaks of both acidic OH and OD groups concurrently increased in intensity together with downward CH and CD stretching bands. Increase in acidic OH and OD groups should be explained by the methylation of olefins with d_0- and d_3-methoxy species, respectively. Simultaneously, the IR band of oligomeric species [22,23] at 1510 cm^{-1} appeared and increased in intensity 30 min after. These results indicate that carbon chain growth occurred by consecutive reactions. The absence of ethene as product at the beginning of the reaction is probably due to the low reaction temperature, where cracking of the oligomeric species (1510 cm^{-1}) hardly occurs.

For further understanding of the reaction, ^{13}C-methoxy species are employed and allowed to react with DME under the same condition to analyze the gaseous products 5 min after by gas chromatography-mass spectroscopy (GC-MAS). As shown in Figure IV-6 the cracking pattern of DME in the collected sample was similar to that of DME but the peaks of mass number larger by one appeared (Figure IV-6; m/e = 46-47). The peaks of methanol in the products increased in mass number by one (Figure IV-7; m/e = 30-32). These results confirm that ^{13}C-DME is formed from the exchange reaction of DME with ^{13}C-methoxy species (Scheme IV-4 (a)) and ^{13}C-methanol is formed from the exchange reaction of acidic OH groups with ^{13}C-DME (Scheme IV-4 (b)). Thus, the initial consumption of d_3-methoxy species is explained by the exchange reaction of d_3-methoxy species with DME, and the formation of d_0-methoxy species from DME is interpreted to be due to

the exchange reaction of DME with acidic OH groups.

The clarification of the hydrocarbon pool mechanism is recognized as an important issue because of its existence during the steady state of MTO reaction. The MTO reaction was found to be accelerated after the induction period [18], and was confirmed that co-feeding of toluene expelled the induction period [26]. The phenomena were called “autocatalysis” or “aromatic co-catalysis”, which was verified many detailed examinations and established as hydrocarbon pool mechanism [6,7,27]. The reaction mechanism proposed in the present study, the direct formation of propene from surface methoxy species and DME, can be related to the selective production of propene during the induction period of MTO [18]. Although this is not the mechanism operating during the steady state of MTO, it is of importance to understand the chemistry of zeolite solid acids.

4. Conclusions

In summary, the main product as hydrocarbon in the initial The MTO reaction is propene. The reactivity of methanol greatly differs from that of DME in the formation of hydrocarbons. DME react with methoxy species directly to form propene, although the detailed reaction mechanism is not clear at this moment. The formation of propene does not occur via ethene. Two reasons exist:

1) The reactivity of ethene is lower than that of DME under the same conditions.
2) The formation of propene does not occur via carbene-like immediate.

References:

[1] W. Song, H. Fu, J. F. Haw, J. Am. Chem. Soc. 123 (2001) 4749-4754.

[2] S. Svelle, F. Joensen, J. Nerlov, U. Olsbye, K.-P. Lillerud, S. Kolboe, M. Bjørgen, J. Am. Chem. Soc. 128 (2006) 14770-14771.

[3] M. Bjørgen, F. Joensen, K.-P. Lillerud, U. Olsbye, S. Svelle, Catal. Today 142 (2009) 142 90-97.

[4] M. Stöcker, Microp. Mesop. Mater. 29 (1999) 3-48.

[5] M. Bjørgen, S. Svelle, F. Joensen, J. Nerlov, S. Kolboe, F. Bonino, L. Palumbo, S. Bordiga, U. Olsbye, J. Catal. 249 (2007) 195-207.

[6] I. Dahl, S. Kolboe, J. Catal. 149 (1994) 458-464.

[7] J. F. Haw, W. Song, D. M. Marcus, J. B. Nicholas, Acc. Chem. Res. 36 (2003) 317-326.

[8] Y. Ono, T. Mori, J. Chem. Soc., Faraday Trans. 1 77 (1981) 2209-2221.

[9] T. R. Forester, R. Howe, J. Am. Chem. Soc. 109 (1987) 5076-5082.

[10] W. Wang, M. Hunger, Acc. Chem. Res. 41 (2008) 895-904.

[11] H. Yamazaki, H. Shima, H. Imai, T. Yokoi, T. Tatsumi, J. N. Kondo, Angew. Chem. Int. Ed. 50 (2011) 1853-1856.

[12] V. Van Speybroeck, J. Van der Mynsgrugge, M. Vandichel, K. Hemelsoet, D. Lesthaeghe, A. Ghysels, G. B. Marin, M. Waroquier, J. Am. Chem. Soc. 133 (2011) 888-899.

[13] M. Bjørgen, J. Catal. 275 (2010) 170-180.

[14] M. Bjørgen, U. Olsbye, D. Pertersen, S. Kolboe, J. Catal. 211 (2004) 1-10.

[15] S. Svelle, M. Visur, U. Olsbye, Saepurahman, M. Bjørgen, Top. Catal. 54 (2011) 897-906.

[16] C.D. Chang, Catal. Rev. Sci. Eng. 25 (1983) 1-118.

[17] J. Bandiera, C. Naccache, Appl. Catal. 69 (1991) 139-148.

[18] N. Y. Chen, W. J. Reagan, J. Catal. 59 (1979) 123-129.

[19] D. Lesthaeghe, V. Van Speybroeck, G. B. Marin, M. Waroquier, Angew. Chem. Int. Ed. 45 (2006) 1714-1719.

[20] Z.-M. Cui, Q. Liu, S.-W. Bain, Z. Ma, W.-C. Song, J. Phys. Chem. C 112 (2008) 2685-2688.

[21] D. M. Marcus, K. A. McLachlan, M. A. Wildman, J. O. Ehresmann, P. W. Kletnieks, J. F. Haw, Angew. Chem. Int. Ed. 45 (2006) 3133-3136.

[22] I. Kirisci, H. Forster, G. Tasi, J. B. Nagy, Chem. Rev. 99 (1999) 2085-2114.

[23] S. Yang, J. N. Kondo, K. Domen, J. Phys. Chem. B 105 (2001) 7878-7881.

[24] C. Paz, S. Bordiga, C. Lamberti, M. Salvalaggio, A. Zecchina, G. Bellussi, J. Phys. Chem. B 1201 (1997) 4740-4751.

[25] A. G. Pelmenschikov, J. H. M. C. van Wolput, R. A. van Santen, J. Phys. Chem. 99 (1995) 3612-3617.

[26] T. Mole, J. A. Whiteside, D. Seddon, J. Catal. 82 (1983) 261-266.

[27] T. Mole, G. Bett, D. Seddon, J. Catal. 84 (1983) 435-445.

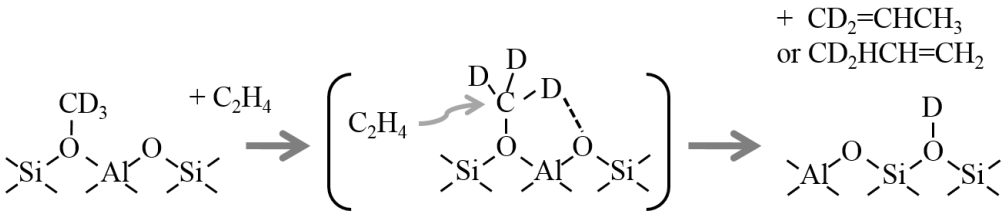

Scheme IV-1. Proposed mechanism of the reaction of methoxy group with ethene to propene via carbene-like species.

Table IV-1. Reactions of various reactants with methoxy species over H-ZSM-5 at 523K.[a]

Reactant	Reaction time / min	Conversion[b] / %	Yield / mol%				
			$C_2^=$	$C_3^=$	C4	C5-C6	Total[c]
DME	5	57.1	0	38.8	10.2	0	49.0
	10	84.6	0	54.3	20.5	6.1	80.9
	30	94.9	2.6	36.6	39.4	9.8	88.4
	60	98.3	3.0	27.9	50.5	14.9	96.3
Ethene	5	0.8	-	0.8	0	0	0.8
	10	2.3	-	1.9	0.4	0	2.3
	30	12.4	-	8.2	3.4	0.8	12.4
	60	16.2	-	8.3	6.6	1.3	16.2
Methanol	5	83.9	0	3.4	0	0	3.4
	10	97.1	0	18.8	5.9	3.4	28.1
	30	97.3	0	54.3	23.8	6.0	74.1
	60	97.1	2.1	38.9	39.3	12.7	83.0

[a] Reaction conditions: catalyst, 60 mg; methoxy species, 8.8×10^{-6} mol; reactant, 2.2×10^{-6} mol; temperature, 523 K.
[b] Conversion of reactant.
[c] Total yield of hydrocarbons.

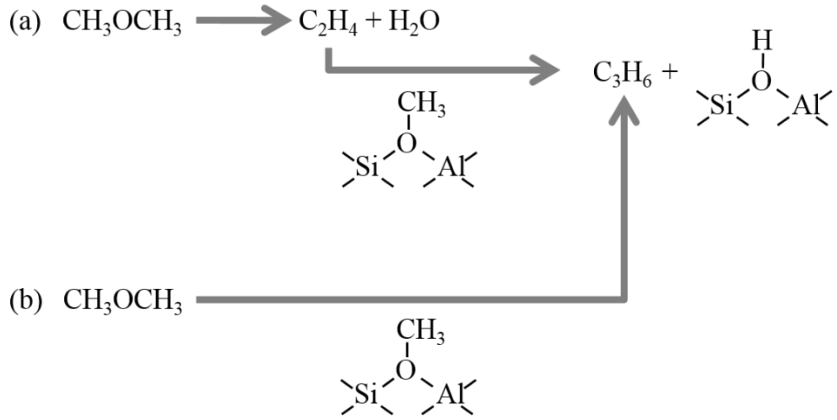

Scheme IV-2. Formation of propene from DME and surface methoxy species on ZSM-5.

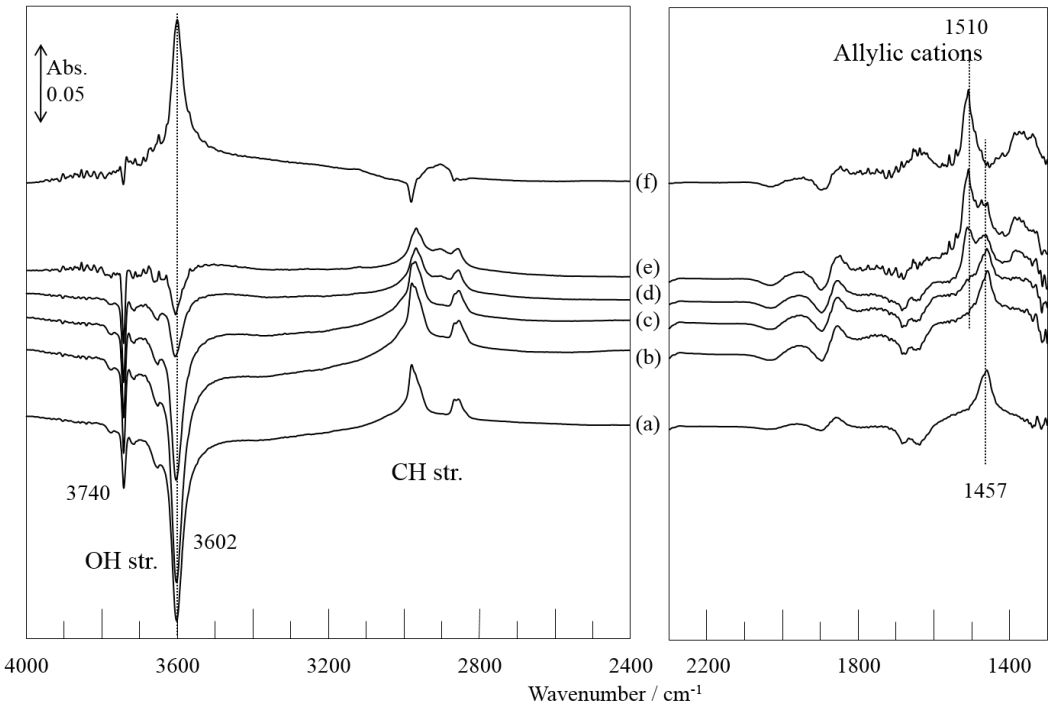

Figure IV-1. Time course of IR spectra of surface species during the reaction of methoxy species with DME at 523 K over H-ZSM-5: (a) before DME introduction and after (b) 5 min, (c) 10 min, (d) 30 min and (e) 60 min; (f) subtracted spectrum of (a) from (e).

Table IV-2. Reactions of various reactants with methoxy species over H-ZSM-5 at 473K.[a]

Reactant	Reaction time / min	Conversion[b] / %	Yield / mol%				
			$C_2^=$	$C_3^=$	C4	C5-C6	Oxygenates[c]
DME + water[d]	5	13.0	0	1.3	0.4	0.2	11.1
	10	12.8	0	3.5	0.3	0.2	8.8
	30	80.8	0	24.7	36.2	14.9	5.0
	60	94.4	0	16.8	47.1	23.3	7.2
Methanol[e]	10	23.1	0	0	0	0	23.1
	30	50.4	0	0	0	0	50.4
	60	58.0	0	0	0	0	58.0
DME[f] (in the absence of methoxy species)	5	9.0	0.3	1.4	0.1	0	7.2
	10	13.7	1.0	3.6	0.4	0.7	7.9
	30	20.5	5.2	4.4	0.3	1.7	9.0
	60	73.1	3.4	32.8	22.4	7.6	6.9
Ethene[f]	10	0	-	-	-	-	-
	30	0.5	-	0.5	0	0	-
	60	2.6	-	1.8	0.8	0	-

[a] Reaction conditions: catalyst, 60 mg; methoxy species, 8.8 x 10^{-6} mol; reactant, [d] 2.2 x 10^{-6} + 2.2 x 10^{-6} mol, [e] 4.4 x 10^{-6} mol, [f] 6.6 x 10^{-6} mol and [g] 2.2 x 10^{-6} mol; temperature, 473 K.
[b] Conversion of reactant.
[c] Methanol or DME.

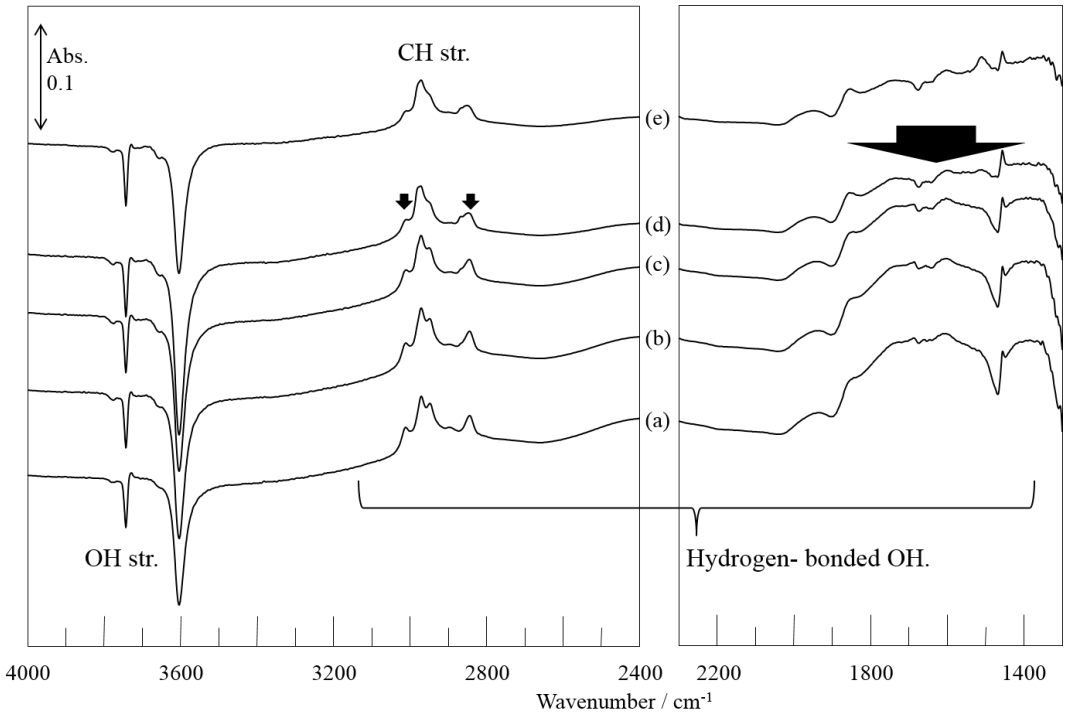

Figure IV-2. Time course of IR spectra of surface species during the reaction of DME at 473 K over H-ZSM-5: after DME introduction at (a) 1 min, (b) 5 min, (c) 10 min, (d) 30 min and (e) 60 min.

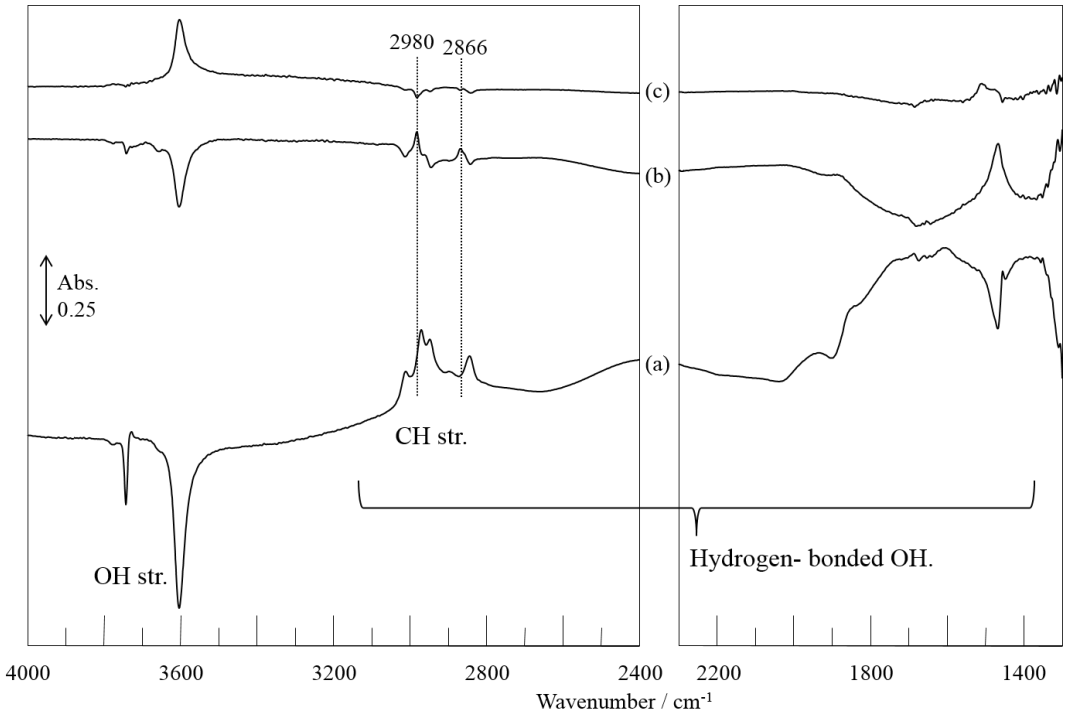

Figure IV-3. Time course of IR spectra of surface species during the reaction of DME at 473 K over H-ZSM-5: subtracted spectra of (a) 0 from 1 min, (b) 1 from 30 min and (c) 30 from 60 min.

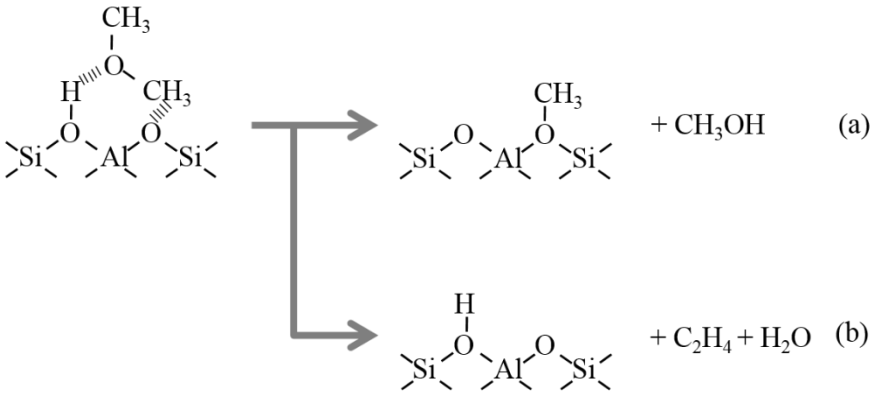

Scheme IV-3. Reaction of DME over acidic OH groups of H-ZSM-5.

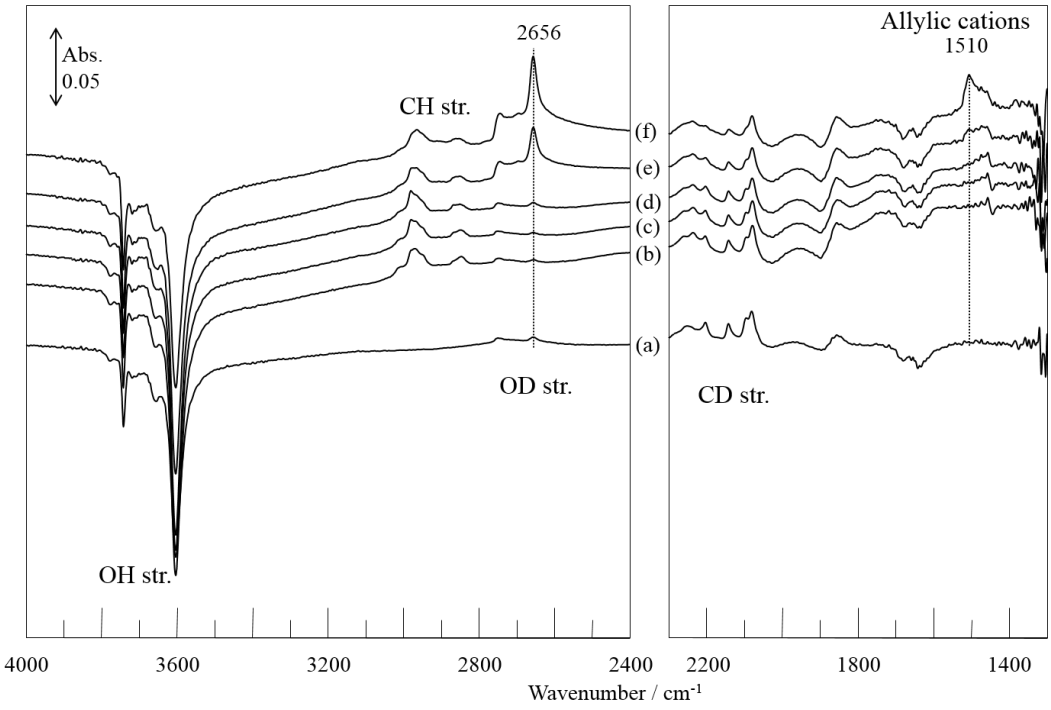

Figure IV-4. Time course of IR spectra of surface species during the reaction of d_3-methoxy species with DME at 473 K over H-ZSM-5: (a) before DME introduction and after (b) 5 min, (c) 10 min, (d) 30 min, (e) 45 min and (f) 60 min.

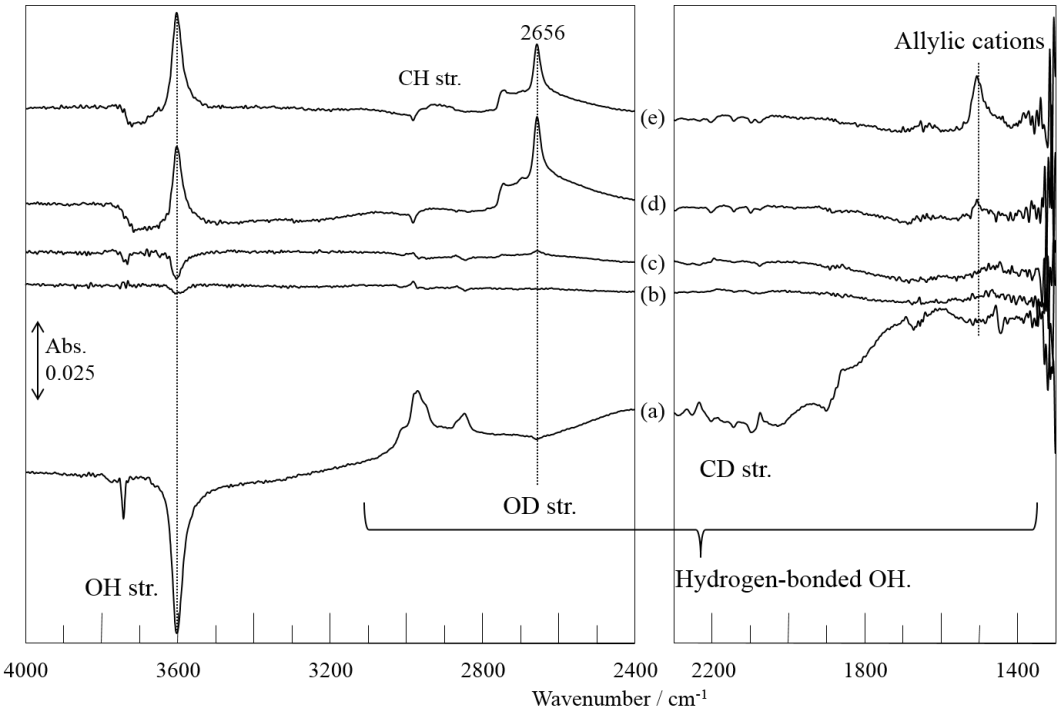

Figure IV-5. Time course of IR spectra of surface species during the reaction of d_3-methoxy species with DME at 473 K over H-ZSM-5: subtracted spectra of (a) 0 from 5 min, (b) 5 from 10 min, (c) 10 from 30 min, (d) 30 from 45 min and (e) 45 from 60 min.

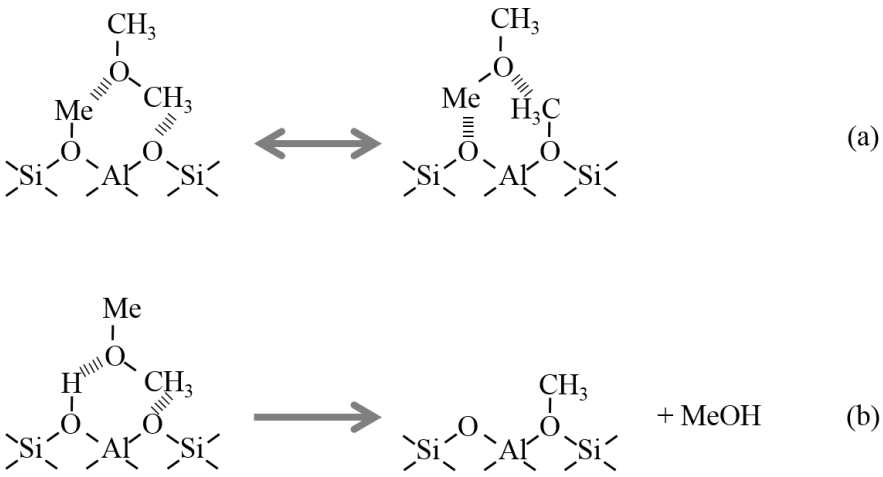

Scheme IV-4. Formation of methoxy species from DME in an initial stage of the reaction of isotope labeled methoxy species and DME (Me = CD3- or 13CH3-):

(a) Isotope exchange of isotope-labeled methoxy species with DME.

(b) Adsorption of isotope-labeled DME on the the acidic OH groups and formation of methoxy species and isotope labeled methanol.

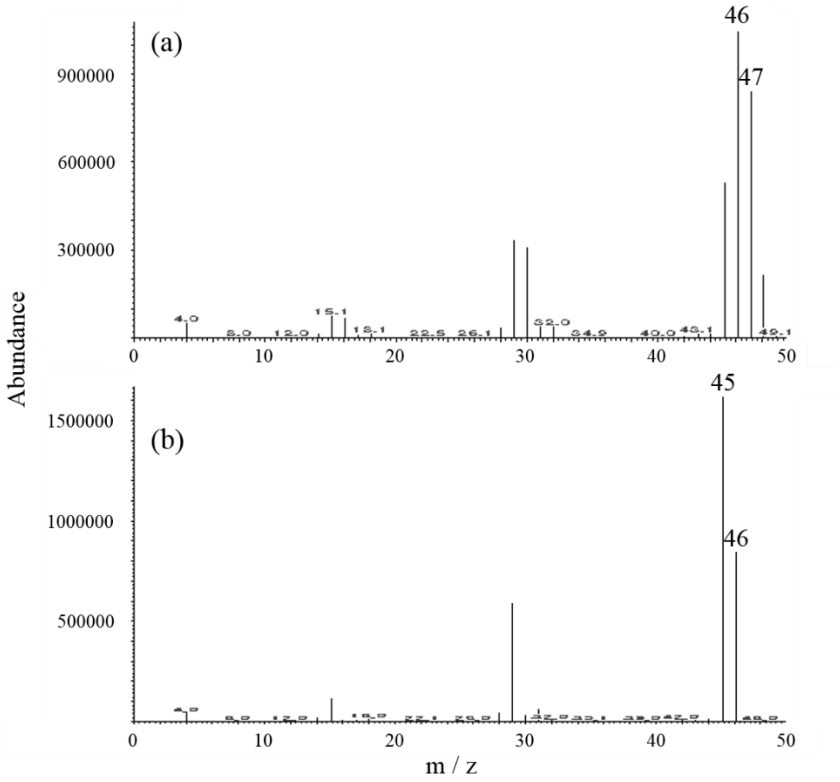

Figure IV-6. GC mass spectra of (a) DME in collected gas from the reaction of ^{13}C-methoxy species and DME at 473 K for 5 min and (b) pure DME reference.

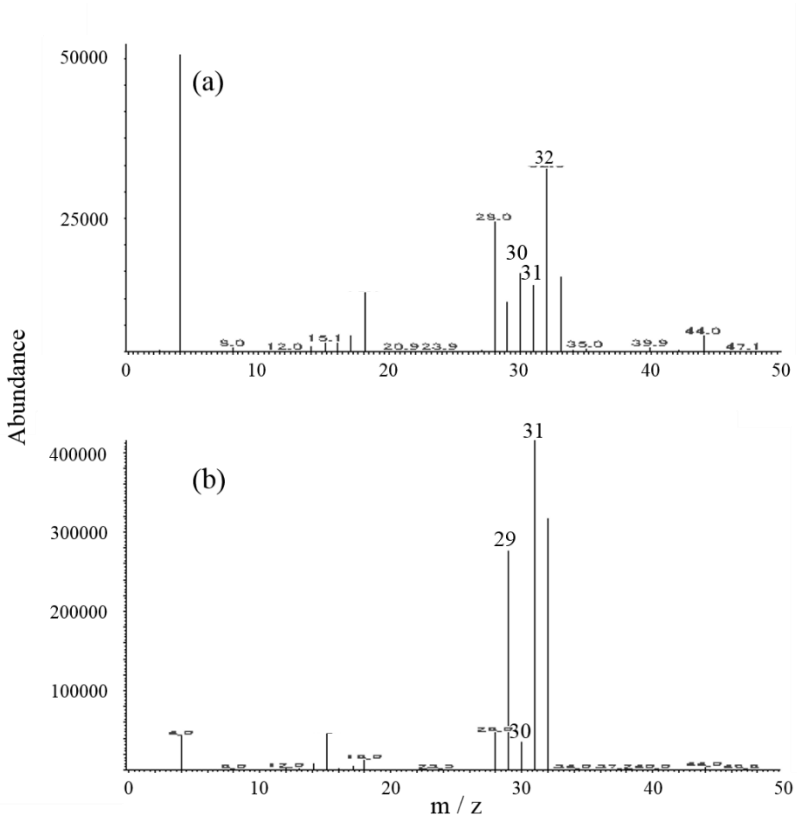

Figure IV-7. GC mass spectra of (a) methanol in collected gas from the reaction of ^{13}C-methoxy species and DME at 473 K for 5 min and (b) pure methanol reference.

Chapter V

Kinetic Study on the Reaction of Methoxy Species and Olefins on H-ZSM5 Zeolite

Abstract:

The kinetics of the methylation of olefins by methoxy species on H-ZSM-5 was investigated using infrared (IR) spectroscopy. Activation energies of the reaction of methoxy species with ethene and propene were estimated at 111 ± 7 and 41 ± 7 kJ mol^{-1} over H-ZSM-5. These activation energies of methylation of olefins by methoxy species decrease with increasing carbon number of olefins. Additionally, the kinetics of the formation of methoxy species on H-ZSM-5 was investigated. Activation energies of the formation of methoxy species from methanol and dimethyl ether were estimated at 95 ± 14 and 69 ± 6 kJ mol^{-1} over H-ZSM-5 zeolite, and that of the formation of dimethyl ether from methanol was obtained at 86 ± 4 kJ mol^{-1}. Dimethyl ether is considered to be the important source of methoxy species.

1. Introduction

The methanol to hydrocarbons (MTH) reaction enables the production of chemicals and synthetic fuels from natural gas, coal and biomass [1-4]. The reaction mechanism of the MTH reaction has not yet become clear due to the presence of various elementary reactions. The hydrocarbon pool mechanism has been generally accepted to operate during the steady state of the MTH reaction, which circulates methylation and cracking of aromatics and olefins [2,5,6]. Since MTH reaction starts with the activation of methanol, methylation, one of the elementary reactions, is concerned to be a key reaction step in MTH reaction. The influence of co-fed reagents with methanol has been studied by experimental and theoretical studies since MTH reaction was reported

by Mobile's researcher [7-37]. Ono and Mori first studied the co-catalytic, which is so-called "autocatalytic", effect of co-provided ethene and **cis**-2-butene with methanol, and showed that the induction period of MTH reaction was reduced compared with the reaction of methanol alone over H-ZSM-5 at 512 K [19]. The importance of the methylation of hydrocarbons by methanol in the MTH was emphasized by Dessau and LaPierre [20,21]. They studied on inference of co-fed olefins and aromatics with ^{13}C-labeled methanol, and proposed a mechanism of the sequential methylation and cracking of the produced olefins in the MTH reaction. Cui et al. studied ^{13}C-labelled methanol reacted with C_2-C_4 olefins and styrene over ZSM-22 [22], whose one dimensional 10-membured ring (MR) zeolites was believed to inhibit both the formation and dealkylation of hydrocarbon species and aromatic [23,24]. They directly observed the methylation of olefins. Additionally, Zhu et al. reported that boron- and aluminum- containing **MFI** zeolite with weak acid sites prevented the formation of ethene oligomers during co-reaction of methanol and ethene, resulting in increasing propene selectivity compared with boron-free **MFI** zeolite [25,26].

For the methylation of olefins, two different mechanisms for olefin methylation have been proposed; stepwise and co-adsorbed mechanisms. In the stepwise mechanism, methanol or dimethyl ether dehydrates to form methoxy species on acid sites that react with olefins [27,29-32,35-37], while a methanol and an olefin molecule are adsorbed on a single acidic site and react at a single site in the co-adsorbed mechanism [15-17,27,29]. I reported that methoxy species react with light olefins as carbene-like species to generate a C-C bond on the basic of the stepwise mechanism (Chapter III) [38]. Accordingly, the kinetics of the formation of methoxy species and methylation of light olefins are reported in this Chapter in order to evaluate the contribution of observed reactions to the while MTH reaction.

2. Experimental

H-ZSM-5, JRC-Z5-90H (Si/Al = 45), was provided by Catalysis Society of Japan. Methanol (99.8%, Wako Pure Chemical Industries, Inc.), ethene (99.9%, Takachiho Chemical Industries, Inc.)

and propene (99.9%, Takachiho Chemical Industries, Inc.) were used. The self-supporting disk of H-ZSM-5 was place in a quartz cell, attached to a conventional closed-gas circulation system. The sample was heated up to 773 K under evacuation and was maintained its temperature for one hour. FT-IR spectra were recorded using a Jasco 4100 FT-IR spectrometer equipped with a mercury cadmium telluride (MCT) detector at a resolution of 4 cm^{-1} and a typical average of 64 scans. FT-IR spectra of the pretreated disk recorded at several temperatures were used as background spectra. Background-subtracted IR spectra showing adsorbed species are presented throughout this paper. The products were analyzed by a GC-MS (Agilent Technologies, GC-7890Q and MS-5975C with Triple-Axis Detector) instrument with a HP Plot column.

3. Results and discussion

3.1. Methylation of ethene by methoxy species

I reported that surface methoxy species on H-ZSM-5 react with ethene to form propene via carbene-like intermediates (Chapter III) [38]. More quantitative analysis were conducted to obtain information on the kinetics. The effect of the number of methoxy species and ethene partial pressure on the rate of the methylation reaction were studied at 573 K. The coverage of methoxy species with acidic OH groups was varied between 0 and 30 % (0 and 6.7 x 10^{-6} mol) with 15 Pa of a partial pressure of ethene (2.2 x 10^{-6} mol). A partial pressure of ethene was varied between 2 and 40 Pa (0.3 and 5.9 x 10^{-6} mol) with 30% coverage of methoxy species (6.7 x 10^{-6} mol). Figure V-1a shows that the conversion of ethene was proportional to the number of methoxy species. Thus, a first-order dependence of the reaction on the number of methoxy species was confirmed. This result is contradictory to reports of the methylation reaction under flow gas conditions [33,35,36], where a zero-order dependence on a partial pressure of methanol was reported. The zero-order dependence on the methylation agent shows that the catalyst surface is saturated with the methylation agent (methanol, dimethyl ether or methoxy species) as reported [33,35,36]]. On the other hand, only a small amount of methoxy species in the present study, which is methylation agent, resulted in a

first-order dependence on the methylation agent. As can be seen from Figure V-1b, the conversion of methoxy species also was dependent of ethene partial pressure, that is, the reaction order to ethene partial pressure is one in the same result of reports obtained under flow gas conditions. [33, 35, 36]

Next, 1the activation energy for the methylation of ethene was estimated. 5 Pa of a partial pressure of ethene (2.2 x 10^{-6} mol), corresponding to a quarter of methoxy and one tenth of the acidic OH groups, was supplied at 523-568 K after the amount of methoxy groups was adjusted to be 40 % of the sites of acidic OH groups (8.9 x 10^{-6} mol). The coverage of methoxy species can be estimated from the integrated intensity of the band of acidic OH groups in Figure V-2A. Thus, by measuring the time course of the recovery of the amount of the isolated acidic OH groups, the rate of methylation of ethene can be obtained. The coverage of methoxy species can be given by the amount of free acidic OH groups in the background ($[OH]_0$) and that of methoxy species-covered surface ([OH]) in the following equation

$$\theta = \frac{[OH]_0 - [OH]}{[OH]_0} \ .$$

Assuming the first-order dependence of the methylation of ethene coverage of methoxy species on the coverage (θ), the rate constant k (s^{-1}) can be expressed as

$$\theta = \theta_0 \exp(-k\mathrm{t}),$$

where t and θ_0 are reaction time and initial coverage of methoxy species, respectively, leading to the following equation

$$\ln\theta = \ln\theta_0 - kt.$$

Then, the activation energy (Ea) for the methylation of ethene is provided from the following equation:

$$\ln k = \ln A - \frac{E_a}{RT},$$

where A, R and T represent pre-exponential factor, gas constant and temperature, respectively.

The time courses of a natural logarithm of coverage (ln θ) at temperatures between 523 and

568 K. The Arrhenius plot using the rate constants obtained in Figure V-2B was fit to a linear correlation, and the activation energy was estimated as 111 ± 7 kJ mol^{-1}. This value agrees with the analytical data as reported by Svelle et al. [33]. Hence, the methylation of ethene by methylation agents may proceed via methoxy species as carbene-like intermediates in gas flow conditions of MTH reaction. By measuring the time course of the recovery of the amount of the isolated acidic OH groups (Figure V-3A), the activation energy of the methylation of propene was also obtained in a similar manner as above. The Arrhenius plot using the rate constants obtained in Figure V-3B was fit to a linear correlation, and the activation energy of methylation of propene was estimated as 41 ± 7 kJ mol^{-1}. This result is contradictory to a report of the methylation reaction of propene (69 kJ mol^{-1}) under flow gas conditions [33]. In flow conditions, the activation energy for the formation of methoxy species is higher than that for methylation of propene, resulted in estimation of the activation energy for the formation of methoxy species (commented in Chapter V-3.2). All elementary reactions simultaneity occur in the flow conditions.

3.2. Formation of methoxy species

I reported that the reactivity of methanol greatly differs from that of dimethyl ether in the formation of hydrocarbons in Chapter IV. In this Chapter, I proposed that dimethyl ether reacts with methoxy species to form propene, and that methoxy species are important immediate for the formation of propene. Therefore, kinetics of the formation of methoxy species were investigated, which are important intermediates for the methylation of olefins and the formation of propene. Methoxy species can be formed on acidic OH groups from methanol and dimethyl ether (Scheme V-2). Methanol and dimethyl ether are adsorbed on acidic OH groups with hydrogen-bond interactions. Methanol react with acidic OH groups to form methoxy species and water, while dimethyl ether to methoxy species and methanol.

The time courses of IR spectra of methanol and dimethyl ether molecules adsorption on H-ZSM-5 zeolite at 473 K are shown in Figure V-4. There spectra were measured under evacuation

after methanol with half moles or dimethyl ether with one-quarter moles equivalent to the number of acidic OH groups was supplied. Since a background spectrum measured before the adsorption of methanol and dimethyl ether is subtracted, a negative band appeared at around 3600 cm^{-1} due to the conversion of isolated acidic OH groups (< 3200 cm^{-1}) to hydrogen-bonded ones on H-ZSM-5 as observed in spectra A-1 and B-1 of Figure V-4. The band of hydrogen-bonded OH groups of H-ZSM-5 extends from 3000 to below 1300 cm^{-1} (known as ABC trio band) [41, 42]. Briefly, the stretching band is perturbed by negative bands of two overtone bending modes (2δ and 2γ). Bands attributable to the adsorbed methanol are observed in Figure V-4(A-1) at 3600-3400 cm^{-1} (stretching of OH groups interacted with acidic OH groups of H-ZSM-5) and at 3000-2800 cm^{-1} (stretching of CH_3 groups). The CH bending modes are too weak to be detected clearly. Similarly, bands of adsorbed dimethyl ether are observed in spectrum V-4(B-1) at 3000-2800 cm^{-1} (stretching of CH_3 groups) and at 1456 cm^{-1} (bending of CH_3 groups). In addition, as the dimethyl ether has higher proton affinity than methanol, spectrum in Figure V-4(B-1) is characterized by stronger absorption of C band at 2000-1300 cm^{-1} compared with that of A and B band at 3000-2000 cm^{-1}. The decrease in intensity of hydrogen-bonded OH groups and the increase of the band of CH bending region of methoxy groups at 1472 cm^{-1} were observed in spectra A-3 and B-3 of Figure V-4 with progress of time. This suggests the conversion of methanol or dimethyl ether to methoxy species and water or methanol. The produces water and methanol molecules were desorbed from the sample under evacuation.

Next, the activation energy for the formation of methoxy species from methanol and dimethyl ether was estimated. The amounts of methoxy species can be estimated from the integrated intensity of the band of CH bending mode, which can be determine the rate of formation of methoxy species. In case of dimethyl ether, the amount of methoxy species was estimated from the height of CH bending of methoxy species due to the overlapped CH bending bands of methoxy species and dimethyl ether. The Arrhenius plots of the rate of formation of methoxy species from both methanol and dimethyl ether are shown Figure V-5. The linear correlation led to the activation energies

estimated as 95 ± 14 and 69 ± 6 kJ mol^{-1} for methanol and dimethyl ether. The difference between methanol and dimethyl ether in the activation energy for the methoxy formation is probably attributable to the formation mechanism; proton of zeolite is transformed to O atom of oxygenates, and methyl groups combine to O atom of zeolite (Scheme V-2). Dimethyl ether is connected to methoxy species and methanol by concertedly attaching of proton to oxygen of dimethyl ether and combining of carbon and oxygen of zeolite due to the exchange reaction of dimethyl ether with acidic OH groups as shown in Scheme V-2(b). On the other hand, it is necessary for methanol to take the dehydration (Scheme V-2(a)). Therefore, it was thought that activation energy for the formation of methoxy species from dimethyl ether is lower than that from methanol.

3.2. Formation of dimethyl ether from methanol

An activation energy for the formation of dimethyl ether, which is an important source of methoxy species, from methanol was estimated. Methoxy species are thermally stable under evacuation even at 673 K [38]. Additionally, as methanol with the 0.1 moles introduced to methoxy species covered 0.4 moles of the number of acidic OH groups at 473 K, almost methanol adsorbed on acidic OH groups and formed to small amount of dimethyl ether [44]. Therefore, dimethyl ether is probably formed form two methanol molecules adsorbed on an acidic OH group [45]. The time course of spectra of methanol adsorbed on H-ZSM-5 zeolite at 473 K without evacuation treatment is shown in Figure V-6. Methanol with half moles equivalent to the number of acidic OH groups was supplied. Immediately after injection of methanol, CH stretching bands of methanol at 2959 and 2857 cm^{-1} were observed in spectrum A-1 of Figure V-6. Additional CH stretching bands of dimethyl ether appeared at 3010, 2970 and 2843 cm^{-1} and increased in intensity (spectra A-2, 3 and 4 of Figure V-6). The band at 3010 cm^{-1}, which is not overlapped with CH stretching bands of methanol, was accordingly used for estimating the rate of formation of dimethyl ether from methanol. The activation energy obtained from the Arrhenius plot in Figure V-6B was 86 ± 4 kJ mol^{-1}. Thus, the activation energy of the formation of methoxy species from methanol were 95 ± 14

or 86 ± 4 kJ mol^{-1} (Scheme V-3). These values are higher than the activation energy of the methylation of propene by methoxy species. Therefore, in flow conditions, it is probably considered the estimation of the activation energy of the formation of methoxy species and not that of the methylation of propene.

From a standpoint of methoxy species and dimethyl ether as important intermediates (ChapterIV) [44], it is possible that propene in initial production of MTH reaction form via an oxonium ylide mechanism [1]. In this mechanism, propene is formed from methylpropyl ether, which is preformed from ethylmethyl ether and methoxy species. Therefore, we studied the reaction of methoxy species and ethylmethyl ether (Table V-1). However, instead of the methylation of ethylmethyl ether, the formation of ethene and methoxy species form ethylmethyl ether occurred. Therefore, the mechanism of the formation of propene in initial period of MTH reaction is not yet clear.

4. Conclusions

Activation energies of the reaction of methoxy species with ethene and propene were estimated at 111 ± 7 and 41 ± 7 kJ mol^{-1} over H-ZSM-5 zeolite using IR spectroscopy. These activation energies of methylation of olefins by methoxy species decrease with increasing carbon number of olefins. Activation energies of the formation of methoxy species from methanol and dimethyl ether were estimated at 95 ± 14 and 69 ± 6 kJ mol^{-1} over H-ZSM-5 zeolite, and that of the formation of dimethyl ether from methanol was obtained at 86 ± 4 kJ mol^{-1}. Dimethyl ether is considered to the important source of methoxy species.

References:

[1] M. Stöcker, Microporous and Mesoporous Materials 29 (1999) 3-48.

[2] U. Olsbye, S. Svelle, M. Bjørgen, P. Beato, T. V. W. Janssens, F. Joensen, S. Bordiga, K. P. Lillerud, Angew. Chem. Int. Ed. 51 (2012) 5810-5831.

[3] G. A. Olah, Angew. Chem. Int. Ed. 44 (2005) 2636 –2639.

[4] G. A. Olah, A. Goeppert, G. K. S. Prakash, J. Org. Chem. 74 (2009) 487–498.

[5] I. M. Dahl, S. Kolboe, Catal. Lett. 20 (1993) 329-336.

[6] J. F. Haw, W.-G. Song, D. M. Marcus, J. B. Nicholas, Acc. Chem. Res. 36 (2003) 317-326.

[7] B. E. Langner, Appl. Catal. 2 (1982) 289-302.

[8] M. M. Wu, W. W. Kaeding, J. Catal. 88 (1984) 478-489.

[9] T. Behrsing, T. Mole, P. Smart, R. J. Western, J. Catal. 102 (1986) 151-159.

[10] L.-M. Tau, A. W. Fort, S. Bao, B. H. Davis, Fuel Process. Technol. 26 (1990) 2009-2019.

[11] D. Lesthaeghe, B. De Sterck, V. Van Speybroeck, G. B. Marin, M. Waroquier, Angew. Chem. Int. Ed. 46 (2007) 1311-1314.

[12] D. M. McCann, D. Lesthaeghe, P. W. Kletnieks, D. R. Guenther, V. Van Speybroeck, M. Waroquier, J. F. Haw, Angew. Chem. Int. Ed. 47 (2008) 5179-5182.

[13] K. Hemelsoet, A. Nollet, M. Vandichel, D. Lesthaeghe, V. Van Speybroeck, M. Waroquier, ChemCatChem 1 (2009) 373-378.

[14] D. Lesthaeghe, J. Van der Mynsbrugge, M. Vandichel, M. Waroquier, V. Van Speybroeck, ChemCatChem, 3 (2011) 208-212.

[15] V. Van Speybroeck, J. Van der Mynsbrugge, M. Vandichel, K. Hemelsoet, D. Lesthaeghe, A. Ghysels, G. B. Marin, M. Waroquier, J. Am. Chem. Soc. 133 (2011) 888-899.

[16] S. Svelle, C. Tume, X. Rozanska, T. Kerber, J. Sauer, J. Am. Chem. Soc. 131 (2009) 816-825.

[17] S. Svelle, M. Bjørgen, J. Phys. Chem. A 114 (2010) 12548-12554.

[18] A. M. Vos, X. Rozanska, R. A. Schoonheydt, R. A. van Santen, F. Hutschka, J. Hafner, J. Am.

Chem. Soc. 123 (2001) 2799-2809.

[19] Y. Ono, T. Mori, J. Chem. Soc., Faraday Trans. 77 (1981) 2209-2221.

[20] R. M. Dessau, R. B. LaPierre, J. Catal. 78 (1982) 136-141.

[21] R. M. Dessau, J. Catal. 99 (1986) 111-116.

[22] Q. Zhu, J. N. Kondo, T. Tatsumi, A. Inagaki, R. Ohnuma, Y. Kubota, Y. Shimodaira, H. Kobayashi, K. Domen, J. Phys. Chem. C 114 (2007) 5409-5415.

[23] Z.-M. Cui, Q. Liu, W.-G. Song, L.-J. Wan, Angew. Chem. Int. Ed. 45 (2006) 6512-6515.

[24] Z.-M. Cui, Q. Liu, Z. Ma, S.-W. Bian, W.-G. Song, J. Catal. 258 (2008) 83-86.

[25] Q. Zhu, J. N. Kondo, T. Setoyama, M. Yamaguchi, K. Domen, T. Tatsumi, Chem. Commun. (2008) 5164-5166.

[26] Q. Zhu, J. N. Kondo, T. Yokoi, T. Setoyama, M. Yamaguchi, T. Takewaki, K. Domen, T. Tatsumi, Phys. Chem. Chem. Phys. 13 (2011) 14598-14605.

[27] A. Corma, G. Sastre, P. M. Viruela, J. Mol. Catal. A 100 (1995) 75-85.

[28] I. I. Ivanova, A. Corma, J. Phys. Chem. B 101 (1997) 547-551.

[29] Saepurahman, M. Visur, U. Olsbye, M. Bjorgen, S. Svelle, Top. Catal. 54 (2011) 1293-1301.

[30] T. R. Forester, R. F. Howe, J. Am. Chem. Soc. 109 (1987) 5076-5082.

[31] W. Wang, A. Buchholz, M. Seiler, M. Hunger, J. Am. Chem. Soc. 125 (2003) 15260-15267.

[32] W. Wang, M. Hunger, Acc. Chem. Res. 41 (2008) 895-904.

[33] S. Svelle, P. O. Rønning, U. Olsbye, S. Kolboe, J. Catal. 224 (2004) 115-123.

[34] S. Svelle, P. O. Rønning, U. Olsbye, S. Kolboe, J. Catal. 234 (2005) 385-400.

[35] I. M. Hill, S. A. Hashimi, A. Bhan, J. Catal. 285 (2012) 115-123.

[36] I. M. Hill, S. A. Hashimi, A. Bhan, J. Catal. 291 (2012) 155-157.

[37] I. M. Hill, Y. S. Ng, A. Bhan, ACS Catal. (2012) 1742-1748.

[38] H. Yamazaki, H. Shima, H. Imai, T. Yokoi, T. Tatsumi, J. N. Kondo, Angew. Chem. Int. Ed. 50 (2011) 1853-1856.

[39] A. G. Permenschikov, R. A. van Santen, J. Phys. Chem. 97 (1993) 10678-10680.

[40] S. R. Blaszkowski, R. A. van Santen, J. Phys. Chem. 99 (1995) 11728-11738.

[41] C. Pazé, S. Bordiga, C. Lamberti, M. Salvalaggio, A. Zecchina, G. Bellussi, J. Phys. Chem. B 101 (1997) 4740-4751.

[42] C. M. Z.-Wilson, P. Viruela, A. Corma, J. Phys. Chem. 99 (1995) 13224-13231.

[43] P. E. Sinclair, C. R. A. Catlow, J. Chem. Soc., Faraday Trans. 92 (1996) 2099-2105.

[44] H. Yamazaki, H. Shima, T. Yokoi, T. Tatsumi, J. N. Kondo, J. Phys. Chem. C 116 (2012) 24091-24097.

[45] S. R. Blaszkowski, R. A. van Santen. J. Am. Chem. Soc. 118 (1996) 5152-5153.

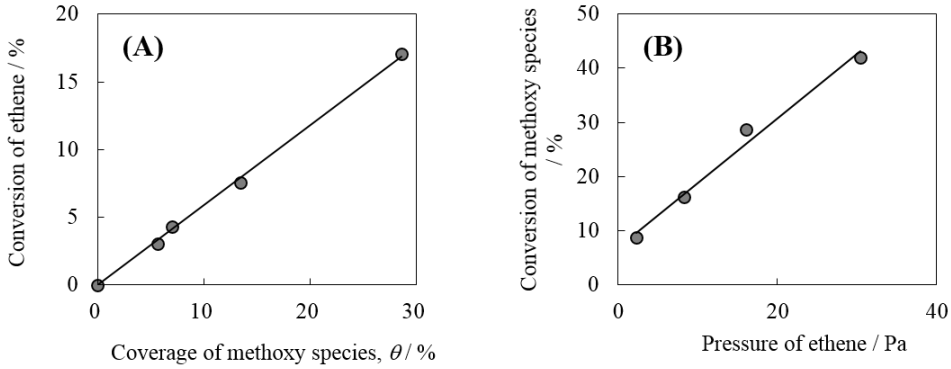

Figure V-1. Dependence of methylation rate on (A) amount of methoxy species and (B) ethene partial pressure at 573 K.

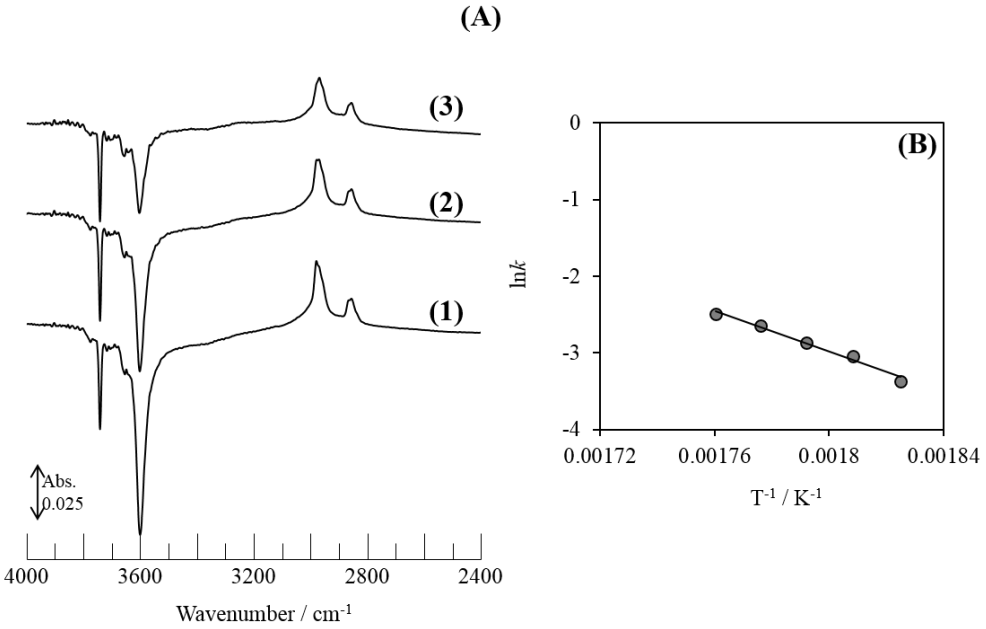

Figure V-2. Time course of IR spectra of surface species during the reaction of methoxy species with ethene at 573 K on H-ZSM-5 and (B) an Arrhenius plot for the reaction of methoxy species and ethene; (1) before ethene introduction and after (2) 5 min and (3) 10 min.

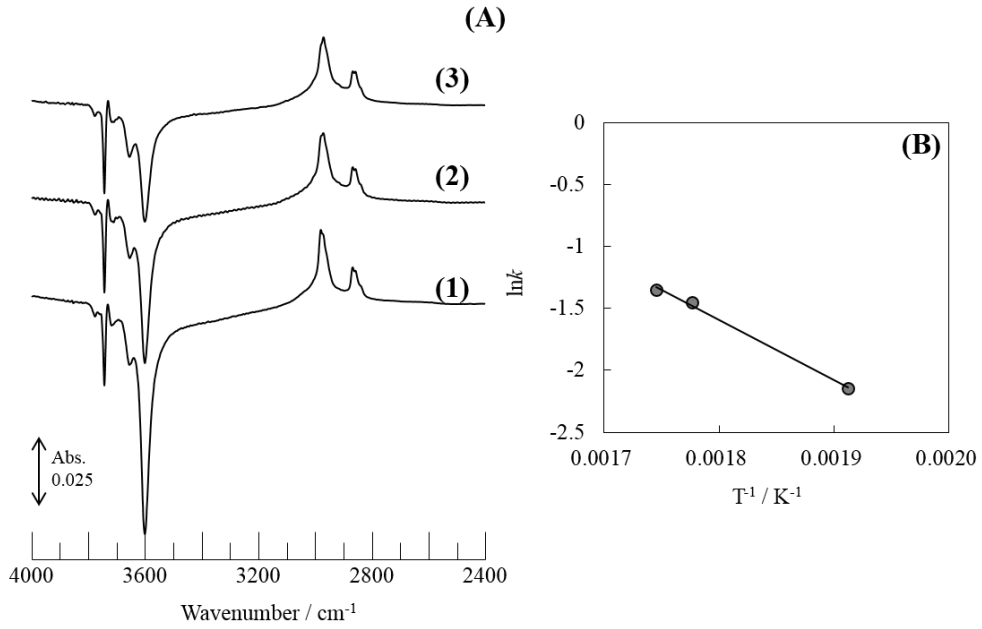

Figure V-3. Time course of IR spectra of surface species during the reaction of methoxy species with propene at 573 K on H-ZSM-5 and (B) an Arrhenius plot for the reaction of methoxy species and propene; (1) before propene introduction and after (2) 1 min and (3) 2 min.

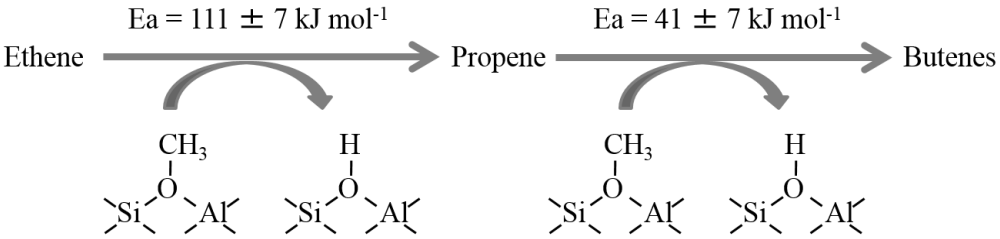

Scheme V-1. Methylation of olefins by methoxy species.

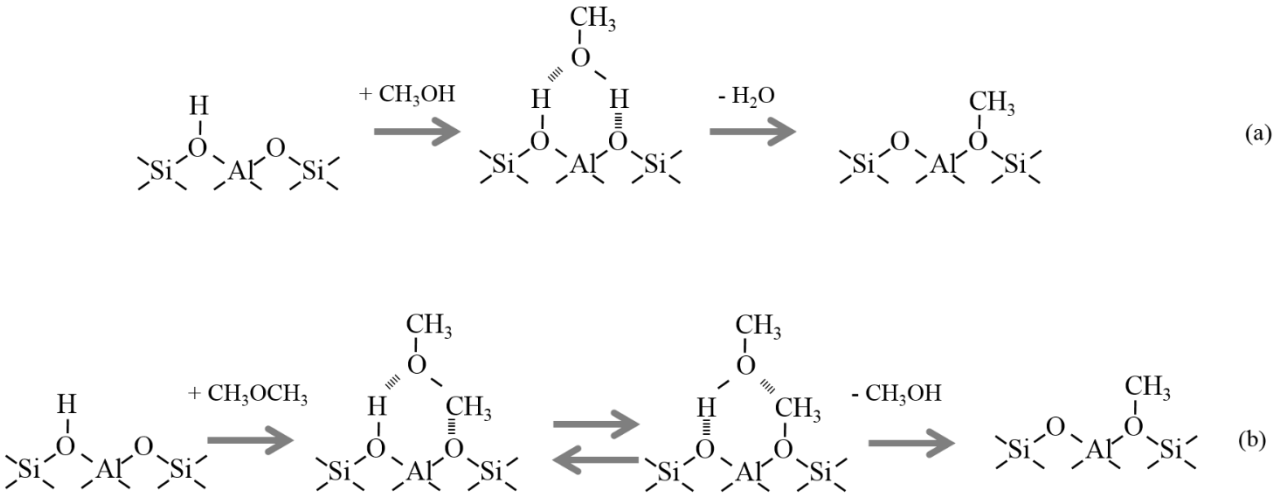

Scheme V-2. Formation of methoxy species from (a) methanol and (b) dimethyl ether.

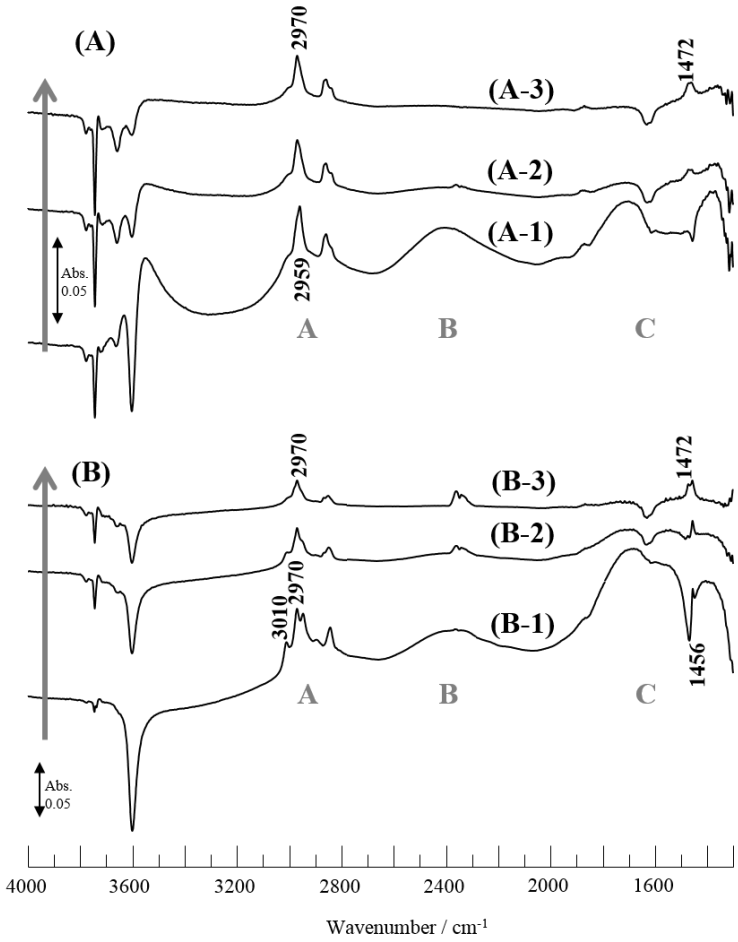

Figure V-4. Time course of IR spectra of H-ZSM-5 interacted with (A) methanol and (B) dimethyl ether under evacuation at 473 K; after methanol introduction for (A-1) 1 min, (A-2) 5 min and (A-3) 10 min; after dimethyl ether introduction for (B-1) 1 min, (B-2) 20 min and (B-3) 30 min.

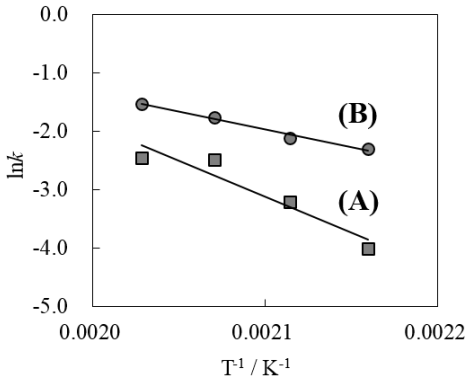

Figure V-5. Arrhenius plots for the formation of methoxy species from (A) methanol and (B) dimethyl ether on H-ZSM-5.

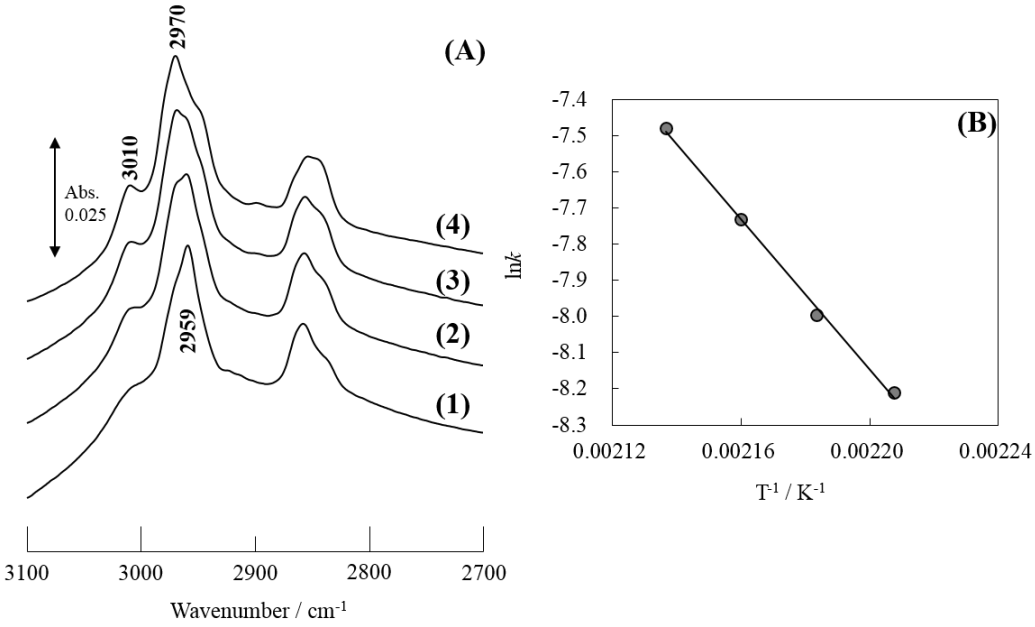

Figure V-6. (A) Time course of IR spectra of H-ZSM-5 interacted with methanol at 473 K and (B) an Arrhenius plot for the formation of dimethyl ether from methanol; after methanol introduction for (1) 1 min, (2) 5 min, (3) 10 min and (3) 30 min.

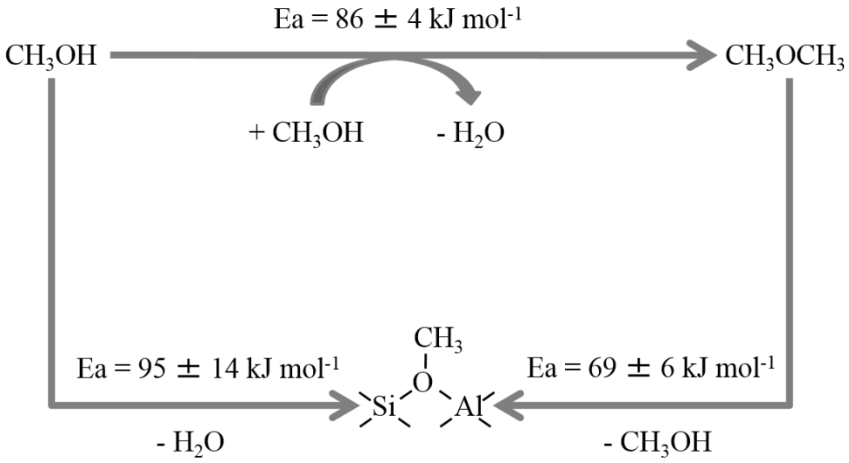

Scheme V-3. Formation of methoxy species from methanol and dimethyl ether.

Table V-1. Reaction of ethylmethyl ether (EME) with presence/absence of methoxy species on H-ZSM-5 at 473 K [a].

	Reaction time / min	Conversion / %	Yield / mol%					
			$C_2^=$	$C_3^=$	C4	C5-C6	DME	MeOH
Methoxy species + EME [b]	5	99.5	90.5	0.2	0	0	6.9	1.8
	10	99.9	92.5	0.4	0	0	4.8	2.2
	30	100	93.2	2.2	0	0	3.9	0.7
	60	100	86.0	10.1	2.1	1.2	0.6	0
EME [c]	5	97.8	96.2	0	0	0	1.6	0
	10	98.6	97.2	0	0	0	1.4	0
	30	99.0	98.5	0	0	0	0.5	0
	60	100	98.8	0.8	0	0	0.4	0

[a] Reaction conditions: catalyst, 60 mg; methoxy species, 8.8 x 10^{-6} mol; EME, [b] 1.5 x 10^{-6} mol, [c] 4.4 x 10^{-6} mol; temperature, 473 K.

Chapter VI

Infrared Study on the Behavior of Ethoxy Species on H-ZSM-5: Oligomerization of Ethene and Decomposition of Ethoxy Species

Abstract:

The oligomerization of ethene over H-ZSM-5 at 303 K was studied as one of the elementary step of methanol to hydrocarbon (MTH) reactions using infrared (IR) spectroscopy. I investigated whether ethoxy species act as intermediates in the ethene oligomerization. Ethene oligomerization at 303 K proceeds on the basis of a concerted mechanism, and not by a stepwise mechanism as the reaction of ethoxy species and ethene. The mechanism of the decomposition of ethoxy species to ethene was additionally discussed. The decomposition of ethoxy species also occurred on the basis of a concerted mechanism, not a carbenium cation mechanism. Therefore, the importance of lattice oxygen atoms, which act as base sites, was made clear.

1. Introduction

Dimerization and oligomerization of light olefins are available routes for the production of liquid fuels [1-5], and elementary reactions in methanol to hydrocarbons (MTH) reaction [6,7]. The initiation of reactions ethene on zeolite was first discussed using theoretical calculation methods [8,9]. It was suggested that protonated ethene did not exist as free carbenium cations, but rather as surface ethoxy species. However, no experimental evidences of the formation of alkoxy species from light olefins, such as ethene, propene and butenes, have been so far provided either by infrared (IR) spectroscopy nor Nuclear Magnetic Resonance (NMR). Many studies have been carried out on the olefin dimerization and oligomerization over zeolites by experimental and theoretical approaches [10-18]. Svelle et al. theoretically explored the ethene dimerization through two different mechanisms using 4T cluster; stepwise and concerted mechanisms (Scheme VI-1) [16]. In

the stepwise mechanism, surface ethoxy specie is formed through the protonation of an adsorbed ethene on an acidic OH group, and then C-C bond is formed between the ethoxy specie and another ethene molecule. On the other hand, in a concerted mechanism, an adsorbed ethene on an acidic OH group is simultaneously activated and reacted with another adjacent ethene. On the basis of the calculated activated barriers, the concerted reaction was concluded to be favorable in the ethene dimerization. Namuangruk et al. also investigated ethene dimerization by using 84T FAU zeolite model [17]. In this case, the activation energy of the rate-determination step, which is the formation of ethoxy species from ethene, assuming the stepwise mechanism was lower than that of the concerted mechanism. Chu et al. calculated the influence of Brønsted acid strength and pore confinement on the ethene dimerization [18], and concluded that the concerted mechanism was preferred on weak acid site, but that two mechanisms became competitive with strong acid sites. In this manner, the mechanism of ethene dimerization have been controvertibly discussed by theoretical methods with little information from experimental results [10].

The formation of ethoxy species from ethene has not been observed so far due to the rapid oligomerization of ethene, while ethoxy species were observed from the dehydration of ethanol over acidic OH groups by using IR spectroscopy and NMR [19-21]. Accordingly, a simple question arises: whether ethoxy species act as intermediates in the ethene dimerization and oligomerization. In order to clarify this point, I studied on ethene adsorption and reactions including other olefins in detail. The mechanism of the decomposition of ethoxy species to ethene is also discussed.

2. Experimental

H-ZSM-5, JRC-Z5-90H (Si/Al = 45), was provided by Catalysis Society of Japan. Silica (Aerosil 200, Evonik) was provided by Aerosil Japan. Ethene (99.9%, Takachiho Chemical Industries, Inc.) and two ethanol; CH_3CH_2OH (99.8%, Wako Pure Chemical Industries, Itd.) and CH_3CD_2OH (98%, Sigma-Aldrich Co. LLC.), were used. The self-supporting disk of H-ZSM-5 was place in a quartz cell, attached to a conventional closed-gas circulation system. The sample was

heated up to 773 K under evacuation and was maintained its temperature for one hour. FT-IR spectra were recorded using a Jasco 4100 FT-IR spectrometer equipped with a mercury cadmium telluride (MCT) detector at a resolution of 4 cm^{-1} and a typical average of 64 scans. FT-IR spectra of the pretreated disk recorded at several temperatures were used as background spectra. Background-subtracted IR spectra showing adsorbed species are presented throughout this paper. The products were analyzed by a GC-MS (Agilent Technologies, GC-7890Q and MS-5975C with Triple-Axis Detector) instrument with a HP Plot column.

3. Results and discussion

3.1 Oligomerization of ethene over H-ZSM-5 at 303 K

First, I observed the oligomerization of ethene at 303 K by IR spectroscopy as reported previously [10, 25]. Time course of spectra measured after introduction of ethene to H-ZSM-5 zeolite at 303 K are arrayed in Figure VI-1. There spectra were measured after the exposure to ethene with the same moles equivalent to the number of acidic OH groups. Since a background spectrum measured before their molecules adsorption is subtracted, a negative band due to the isolated acidic OH groups, appeared at around 3612 cm^{-1}, which converted to hydrogen-bonded ones (3207 cm^{-1}). IR spectra of adsorbed ethene on acidic OH groups are observed at 3100 and 2900 cm^{-1} (stretching of CH groups), 1612 cm^{-1} (stretching of C=C bond) and 1442 cm^{-1} (bending of CH group). It should be noted that the C=C stretching of ethene is IR inactive but appeared due to the direct involvement to adsorption. In addition, a band at 2989 cm^{-1} is attributed to CH stretching band of gaseous ethene (spectra (a) and (b)). Both the shift to the OH stretching band and the C=C stretching band (Raman band of gaseous ethene at 1623 cm^{-1}) suggests the interaction of the π-electron of ethene with acidic OH groups. The formation of saturated methyl and methylene groups was confirmed by the appearance and increase of bands associated to $\nu(CH_3)$ at 2959 cm^{-1} and $\nu(CH_2)$ at 2936 and 2862 cm^{-1} with progress time. Two δ(CH) in saturated hydrocarbon were also observed at 1469 and 1382 cm^{-1}. These results suggest that the protonation and oligomerization

from ethene molecular occurs at 303 K. The negative band of acidic OH groups almost recovered after evacuation of gaseous ethene because of the removal of mono-molecular ethene adsorption. However, it did not completely recovered due to the consumption of some sites by the formation of oligomers, which is probably surface alkoxy species. Therefore, it was confirmed that the oligomerization of ethene proceed rapidly at 303 K.

3.2 Reaction of ethoxy species and ethene on H-ZSM-5 at 303 K

Next, I studied the reactivity of ethoxy species for the ethene oligomerization. This confirms the presence or absence of the stepwise mechanism. Ethene was injected at 303 K after ethoxy species were produced from ethanol at 473 K [19,20]. Figure VI-2(a) shows the spectrum of ethoxy species formed on H-ZSM-5. Decrease of isolated silanol and acidic OH groups is shown by negative peaks at 3747 and 3612 cm^{-1}, respectively, and CH stretching bands of ethoxy species were observed at 3000-2850 cm^{-1}. Bands at 1447 and 1395 cm^{-1} is attributed to CH bending bands of ethoxy species [19,20]. The coverage of ethoxy species in Figure VI-2(a) is 30 % of the number of the acidic OH groups on H-ZSM-5. Ethene with 0.7 moles equivalent to the number of acidic OH groups corresponding to the number of vacant acidic OH groups, was supplied to ethoxy species at 303 K. In Figures VI-2(b) and VI-2(c), isolated acidic OH groups is converted to hydrogen-bonded OH groups with ethene after injection of ethene in the same manner as that in Figure VI-1. No evident spectral changes were formed by comparing spectra (b) and (d) in Figure 2 during the time course for 60 min after ethene supply. Therefore, a subtracted spectrum was calculated to the difference. The spectrum 2(c) for 60 min is the same as the spectrum 2(b) for 1 min after ethene introduction. In spite of conditions for oligomer formation, the amount of ethoxy species was not changed, which was found by the absence of any negative bands of ethoxy species in Figure VI-2(e). This result implies that ethoxy species do not act as intermediates for ethene oligomerization at 303 K. In other words, ethene oligomerization at 303 K proceed mot via stepwise mechanism but via concerted mechanism. Additionally, the formation of ethoxy species from ethene was not observed

either in Figure VI-1 or VI-2. These results indicate that the activation barrier of the oligomerization is lower than that of the formation of ethoxy species from ethene. In the same manner, the formation of C_3 and C_4 alkoxy species from propene and butenes have not been observed due to the formation of oligomers from propene [11] and dimers from butenes [25]. In this study, I studied the formation of C_5 and C_6 alkoxy species from 1-penten and 1-hexane (Figure VI-3 and VI-4). 1-Pentene and 1-hexene were adsorbed on all acidic OH groups at 198 K (Figure VI-3a and VI-4a). The adsorbed 1-pentene and 1-hexene on acidic OH groups are identified by bands at 3078 and 3075 cm^{-1} (stretching of unsaturated CH groups) and at 1643 and 1642 cm-1 (stretching of C=C bond), respectively. These spectra resemble to those spectra of adsorbed 1-pentene and 1-hexene on SiO_2 (Figure VI-3c and VI-4c), 1-pentene and 1-hexene are regarded as on adsorbed molecularly at 198 K on acidic OH groups with hydrogen-bond interaction. IR spectra of adsorbed 1-pentene and 1-hexene heated to 223 K under evacuation without supplying of gaseous molecules are shown in Figure VI-3b and VI-4b. Bands of stretching of unsaturated CH groups and C=C bond were disappeared in the absence of the recovery of acidic OH groups. Therefore, C_5 and C_6 olefins, which cannot be dimerize in pore of H-ZSM-5, produced C_5 and C_6 alkoxy species at 223 K.

3.3 Decomposion of ethoxy species on H-ZSM-5 at 473 K

Nevertheless, the stepwise mechanism cannot be ruled out. Methoxy species, which is lower reactivity than ethoxy species, react with ethene at above 473 K [26]. Therefore, ethoxy species can react with ethene. This is implied by suggesting by Chu et al. that the concerted mechanism is preferred on weak acid sites, and the two mechanism become competitive on strong acid sites [18]. Therefore, it is possible that ethoxy species as intermediates react with ethene to butenes and oligomers at high temperature.

Our groups reported that ethoxy species decompose into ethene and acidic OH groups at above 453 K [19, 20]. Therefore, it is experimentally difficult to observe of the reaction of ethoxy species and ethene at above 453 K. In this study, to gain insight into the decomposition mechanism,

[D_2]ethoxy species (CH_3CD_2O-) were produced from ethanol-1,1-d_2. Assuming the carbenium cation mechanism for the decomposition of ethene in this study, ethyl cation, which is stabilized by CH combination of methyl group and C-C combination, would be present as a transition state (Scheme VI-2(a)). For the conversion of ethyl cation to ethene and acidic hydroxyl groups, two possible pathways exist: on results in the formation of CD_2=CH_2 and an OH group, and the other CHD=CH_2 and an OD group. Another possible route is a concerted mechanism like methoxy species act as carbene-like intermediates (Scheme VI-2(b)) [26]. A lattice oxygen atom would attract one of the hydrogen in methyl group. Concurrently, a combination of carbon atom of methylene group and oxygen atom of zeolite dissociates. Therefore, the CD_2=CH_2 and an OH group are formed in this manner.

Figure VI-5(a) shows the spectra of adsorbed species and H-ZSM-5 under evacuation for 5 min after CH_3CD_2OH with the same moles equivalent to the number of acidic OH groups was supplied at 473 K. Negative bands of silanol and acidic OH groups appeared at 3743 and 3602 cm^{-1}, respectively, and CH_3 stretching and bending bands are observed at 3000-2800 cm^{-1} and 1500-1300 cm^{-1}. Additionally, CH_2 stretching bands are observed at 2300-2100 cm^{-1}. These bands of [D_2]ethoxy species (CH_3CD_2O-) decrease and acidic OH groups increase in intensity with progress time such form Figure VI-5(b) to (d). It should be noted that only the acidic OH groups recover, whereas the acidic OD band at 2658 cm^{-1} is negligible in the subtracted spectrum in Figure VI-5(e). This result indicates that the hydrogen atom of the acidic hydroxyl groups can be only provided by methyl groups and not methylene groups of [D_2]ethoxy species (CH_3CD_2O-). Further products from the decomposition of ethoxy species was analyze by GC-MS. The cracking pattern of ethene in the products appeared in similar intensity ratios as those of pure ethene but increased in mass number by two. This results clarified the involvement of two D atom in ethene formed from [D_2]ethoxy species (CH_3CD_2O-). Therefore, the decomposition of ethoxy species probably proceeds in the concerted manner due to experimental evidences obtained using IR spectroscopy and GC-MS.

Thus, ethoxy species decompose into ethene and acid hydroxyl groups not via ethyl cations at

above 453 K. Therefore, it is experimentally difficult to observe of the reaction of ethoxy species and ethene at above 453 K. Nevertheless, it is an important matter the part of lattice oxygen atoms, which are act as base sites, due to the decomposition of ethoxy species and the oligomerization of ethene in the concerted manner.

4. Conclusions

I studied on the mechanism of oligomerization of ethene and decomposition of ethoxy species using IR spectroscopy and GC-MS. Ethene oligomerization at 303 K proceed on basis of a concerted mechanism, and not a stepwise mechanism as the reaction of ethoxy species and ethene. The decomposition of ethoxy species also occurred on basic of a concerted mechanism, not a carbenium cation mechanism. Therefore, the importance of lattice oxygen atoms, which are act as base sites, was made clear.

References:

[1] S. A. Tabak, F. J. Krambeck, W. E. Garwood, AIChE J. 32 (1986) 1526‑1531.

[2] R.J. Quann, L.A. Green, S.A. Tabak, F.J. Krambeck, Ind. Eng. Chem. Res. 27 (1988) 565-570.

[3] S. Rossini, Catal. Today 77 (2003) 467–484.

[4] C. Martinez, A. Corma, Coord. Chem. Rev. 255 (2011) 1558–1580.

[5] M. Golombok, J. de Bruijn, J. Ind. Eng. Chem. Res. 39 (2000) 267-271.

[6] M. Stocker, Microporous Mesoporous Mater. 29 (1999) 3-48.

[7] D. M. Bibby, R. F. Howe, G. D. McLellan, Appl. Catal. A 93 (1992) 1-34.

[8] V. B. Kazansky, Acc. Chem. Res. 24 (1991) 379-383.

[9] R. A. Van Santen, G. J. Kramer, Chem. Rev. 95 (1995) 637-660.

[10] G. Spoto, S. Bordiga, G. Ricchiardi, D. Scarano, A. Zecchina, E. Borello, J. Chem. Soc., Faraday Trans. 90 (1994) 2827−2835.

[11] F. Geobaldo, G. Spoto, S. Bordiga, C. Lamberti, A. Zecchina, J. Chem. Soc., Faraday Trans. 93 (1997) 1243−1249.

[12] S. Jeong, K. J. Fisher, R. F. Howe, G. D. Willett, Microporous Mesoporous Mater. 22 (1998) 369-377.

[13] M. Bjørgen, K.-P. Lillerud, U. Olsbye, S. Bordiga, A. Zecchina, J. Phys. Chem. B 108 (2004) 7862-7870.

[14] A. N. Mlinar, P. M. Zimmerman, F. E. Celik, M. Head-Gordon, A. T. Bell, J. Catal. 288 (2012) 65-73.

[15] A. Corma, C Martínez, E. Doskocil, J. Catal. 300 (2013) 183-196.

[16] S. Svelle, S. Kolboe, O. Swang, J. Phys. Chem. B 108 (2004) 2953−2962.

[17] S. Namuangruk, P. Pantu, J Limtrakul, ChemPhysChem 6 (2005) 1333−1339.

[18] Y. Cui, A. Bhan, A. Zheng, F. Deng, J. Phys. Chem. C 116 (2012) 12687-12695.

[19] J. N. Kondo, K. Ito, E. Yoda, F. Wakabayashi, K. Domen, J. Phys. Chem. B 109 (2005)

10969-10972.

[20] J. N. Kondo, D. Nishioka, H. Yamazaki, J. Kubota, K. Domen, T. Tatsumi, J. Phys. Chem. C 114 (2010) 20107-20113.

[21] W. Wang, J. Jiao, S. S. Ray, M. Hunger, ChemPhysChem 6 (2005) 1467-1469.

[22] B.-T. L. Bleken, L. Mino, F. Giordanino, P. Beato, S. Svelle, K. P. Lillerud, S. Bordiga, Phys. Chem. Chem. Phys. 15 (2013) 13363-13370.

[23] S. R. Blaszkowski, R. A. van Santen, J. Phys. Chem. 99 (1995) 11728-11738.

[24] C. Pazé, S. Bordiga, C. Lamberti, M. Salvalaggio, A. Zecchina, G. Bellussi, J. Phys. Chem. B 101 (1997) 4740-4751.

[25] J. N. Kondo, K. Domen, J. Mole. Catal. A 199 (2003) 27–38.

[26] H. Yamazaki, H. Shima, H. Imai, T. Yokoi, T. Tatsumi, J. N. Kondo, Angew. Chem. Int. Ed. 50 (2011) 1853-1856.

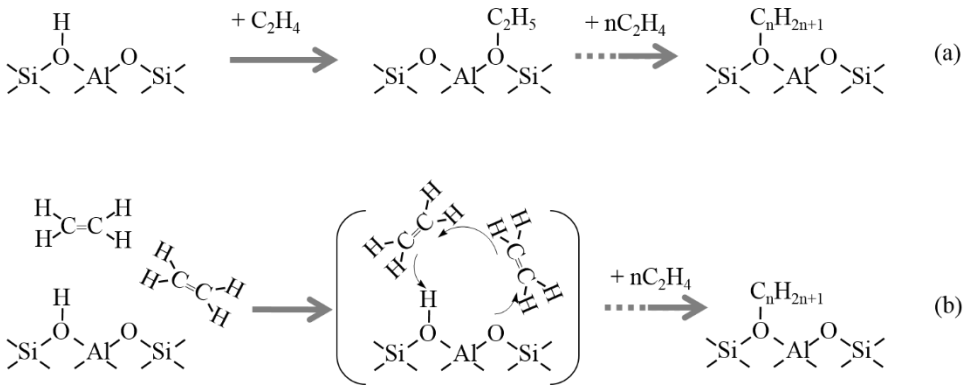

Scheme VI-1. Ethene oligomerization on basic of (a) the stepwise and (b) the concerted mechanism.

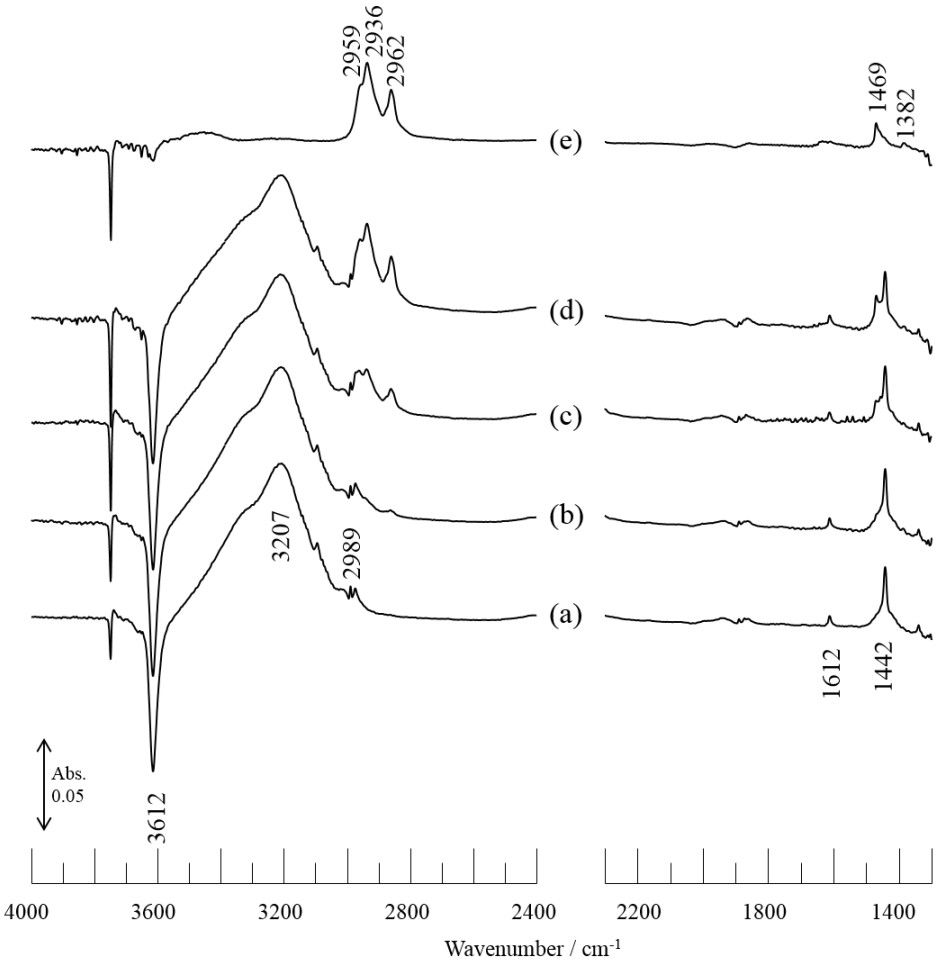

Figure VI-1. Time course of IR spectra of H-ZSM-5 interacted with ethene at 303 K; after ethene introduction for (a) 1 min, (b) 10 min, (c) 30 min and (d) 60 min, and (e) after evacuation of gaseous phase.

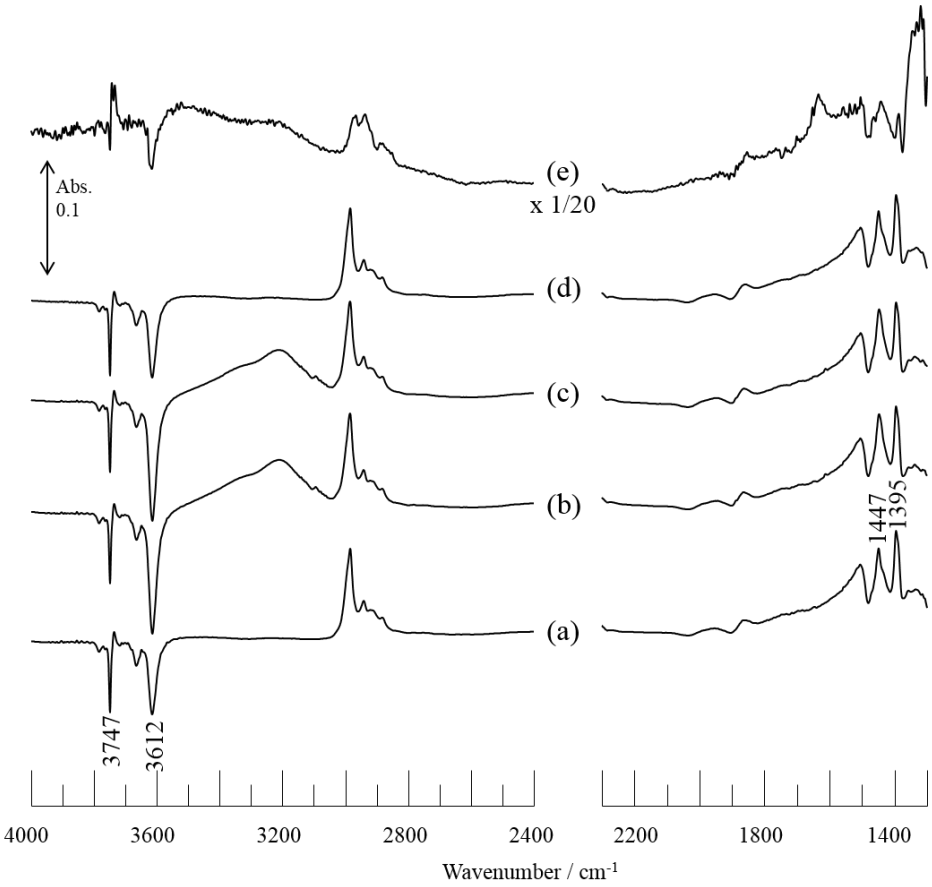

Figure VI-2. Time course of IR spectra of ethoxy species on H-ZSM-5 interacted with ethene at 303 K; (a) before ethene introduction, after ethene introduction for (b) 1 min and (c) 60 min, and (d) after evacuation; (e) subtracted spectrum of (a) from (d).

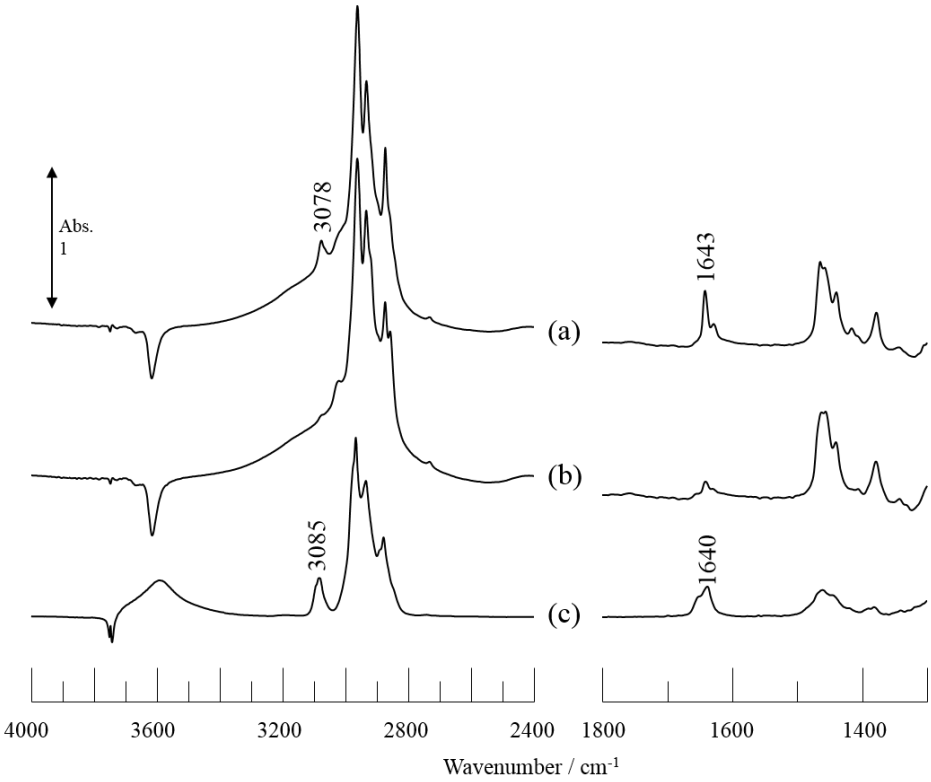

Figure VI-3. IR spectra of H-ZSM-5 introduced 1-pentene at (a) 198 and (b) 223 K, and silica introduced 1-pentene at 303 K.

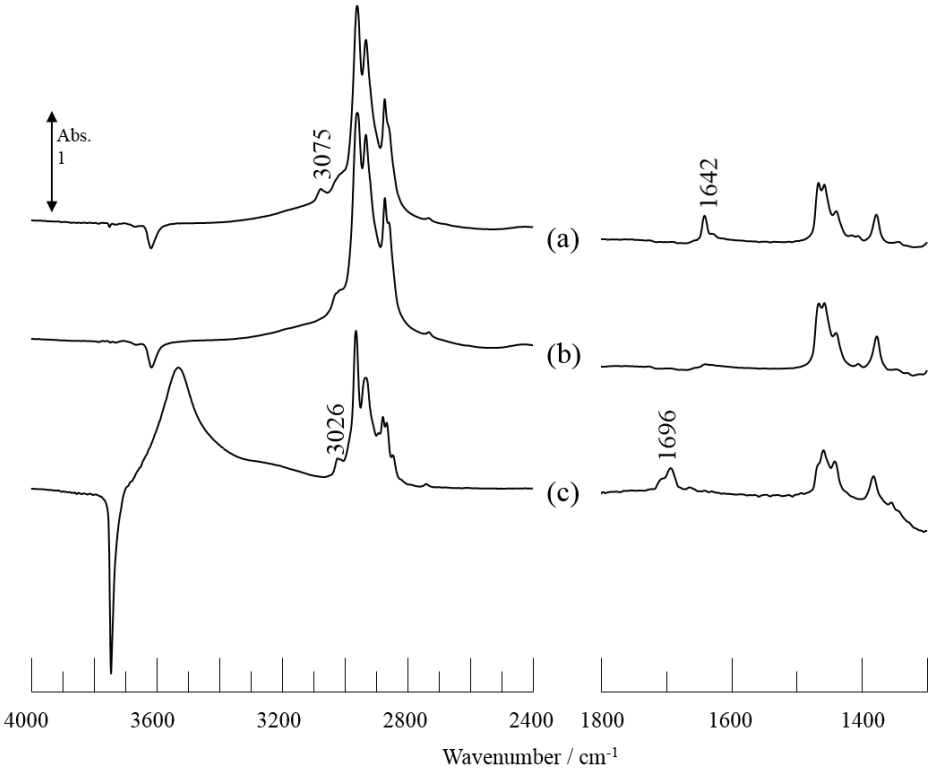

Figure VI-4. IR spectra of H-ZSM-5 introduced 1-hexene at (a) 198 and (b) 223 K, and silica introduced 1-hexene at 303 K.

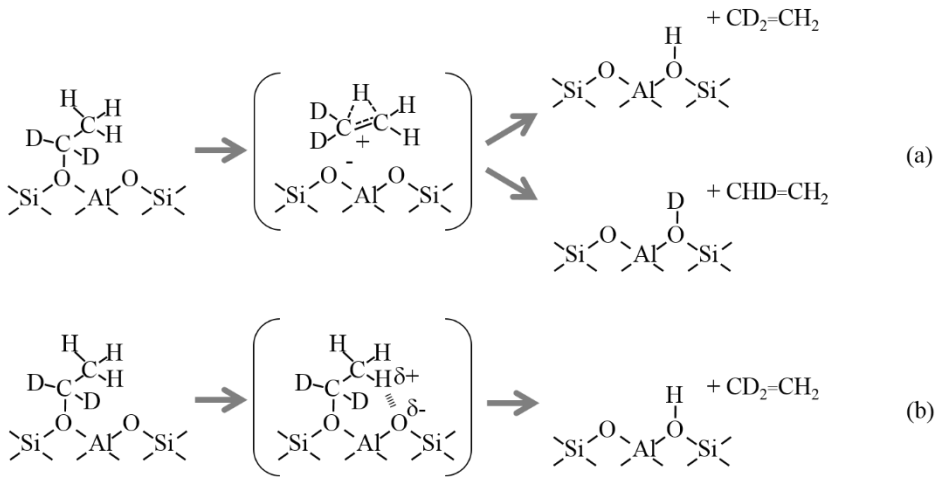

Scheme VI-2. Decomposition of [D_2]ethoxy spceies on basic of (a) the carbenium cation and (b) the concerted mechanism.

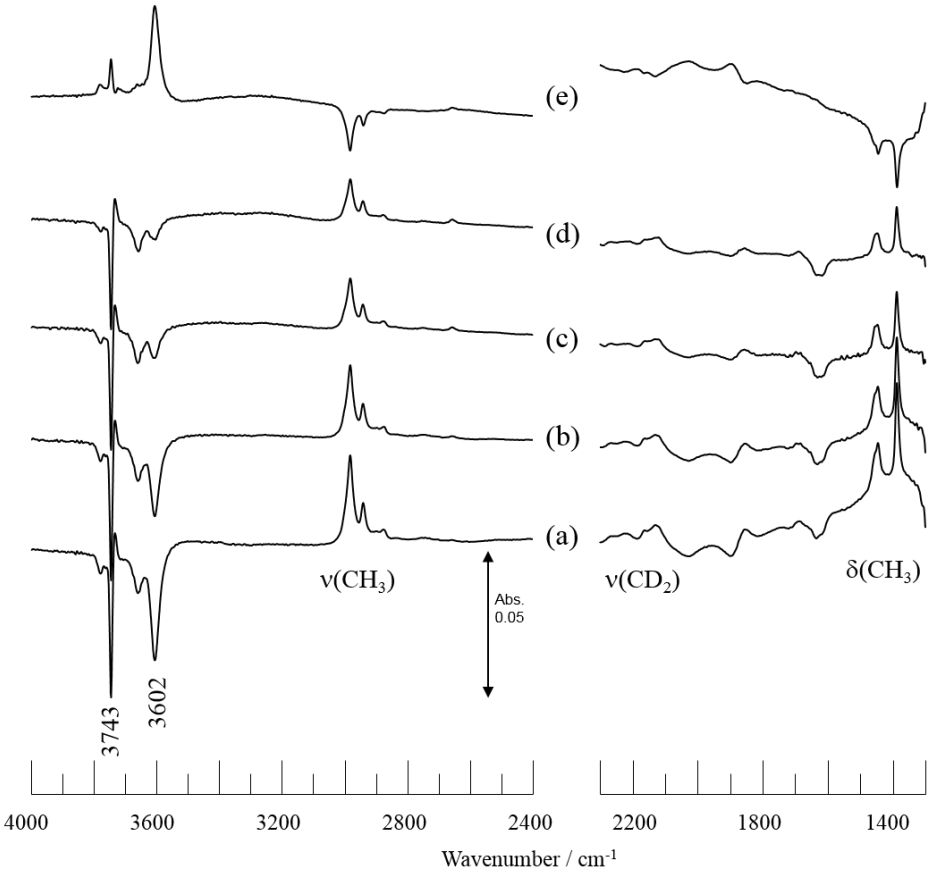

Figure VI-5. Time course of IR spectra of H-ZSM-5 injected CH_3CD_2OH at 473 K; after [D_2]ethanol introduction for (a) 5 min, (b) 10 min, (c) 30 min and (d) 60 min, and (e) subtracted spectrum of (a) from (d).

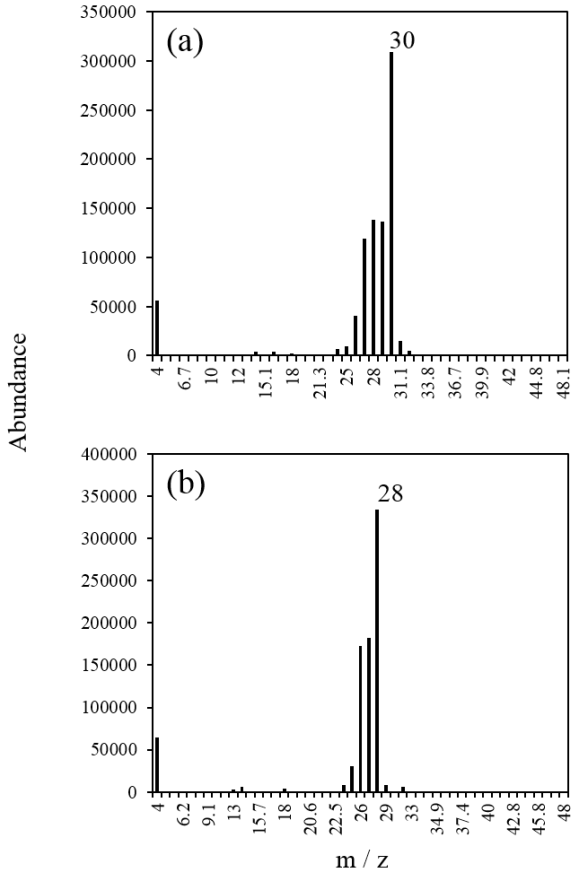

Figure VI-6. GC mass spectra of (a) ethene in collected gas from the decomposition of [D_2]ethoxy species at 523 K and (b) [D_0]ethene reference.

Chapter VII

Summary

The aim of this study is to investigate the mechanism of C-C bond formation during methanol to hydrocarbons reaction over ZSM-5 zeolite using infrared (IR) spectroscopy. Main purpose of this study is to clarify the reactivity of surface alkoxy species such methoxy species and ethoxy species on acidic OH groups.

In Chapter I, the introduction of zeolite chemistry and methanol to hydrocarbons reaction is described.

In Chapter II, experimental apparatus in this study and a new concept of the estimation of real temperature of sample in IR cell are described. The peak top frequency of the stretching vibration of OH groups on amorphous silica reversibly changes accompanied by the change of the sample in temperature under the constant concentration. Using this phenomenon, the estimation of the real temperatures of samples in IR cell can be achieved.

Chapter III – VI constitute the main part of this thesis.

In Chapter III, the reaction of surface methoxy species on ZSM-5 and ethene was investigated as one of the elementary step of MTH reactions. The formed methoxy species on acidic sites of ZSM-5 are thermally stable under evacuation even at 673 K. Methoxy groups are regarded as methylation reagents of light olefins form IR observation and GC-MS analysis. Carbene-like intermediate for the methylation of light olefins by methoxy species was proposed on zeolite, which is based on the IR observation that the recovered acidic hydroxyl groups after the reaction of d_3-methoxy groups with light olefin molecules are all deuterated.

In Chapter IV, the reaction of methoxy species with methanol and dimethyl ether was studied to in relation to the initial C-C bond formation in MTH reaction. In other words, products as hydrocarbons in the initial step of MTH reaction were investigated. The direct production of propene from methoxy groups and DME is evidenced on H-ZSM-5 zeolite by isotopic studies of IR

observation of surface species and gas chromatograph-mass spectroscopy (GC-MS) analysis of products. Stepwise reactions of DME to ethene and water followed by methylation of ethene by methoxy groups were negligible during the generation of propene by the reaction of methoxy groups and DME.

In Chapter V, the kinetics of the methylation of olefins by methoxy species was investigated. Activation energies of the reaction of methoxy species with ethene and propene were estimated at 111 ± 7 and 41 ± 7 kJ mol^{-1} over H-ZSM-5. Activation energies of methylation of olefins by methoxy species decrease with increasing carbon number of olefins. Additionally, the kinetics of the formation of methoxy species on H-ZSM-5 was investigated. Activation energies of the formation of methoxy species from methanol and dimethyl ether were estimated at 95 ± 14 and 69 ± 6 kJ mol^{-1} over H-ZSM-5 zeolite, and that of the formation of dimethyl ether from methanol was obtained at 86 ± 4 kJ mol^{-1}. Dimethyl ether is considered to be the important source of methoxy species.

In Chapter VI, The oligomerization of ethene over H-ZSM-5 at 303 K was studied as one of the elementary step of MTH reactions using IR spectroscopy. Ethene oligomerization at 303 K proceeds on the basis of a concerted mechanism, and not by a stepwise mechanism as the reaction of ethoxy species and ethene. The mechanism of the decomposition of ethoxy species to ethene was additionally discussed. The decomposition of ethoxy species also occurred on the basis of a concerted mechanism, not a carbenium cation mechanism. Therefore, the importance of lattice oxygen atoms, which act as base sites, was made clear.

List of Publications

[1] J. N. Kondo, D. Nishioka, **H. Yamazaki**, J. Kubota, K. Domen and T. Tatsumi
"Activation Energies for the Reaction of Ethoxy Species to Ethene over Zeolites"
J. Phys. Chem. C 114 (2010) 20107-20113.

[2] **H. Yamazaki**, H. Shima, H. Imai, T. Yokoi, T. Tatsumi and J. N. Kondo
"Evidence for a "Carbene-like" Intermediate during the Reaction of Methoxy Species with Light Alkenes on H-ZSM-5"
Angew. Chem. Int. Ed. 50 (2011) 1853-1856. (Chapter III)

[3] **H. Yamazaki**, H. Shima, H. Imai, T. Yokoi, T. Tatsumi and J. N. Kondo
"Direct Production of Propene from Methoxy Species and Dimethyl Ether over H-ZSM-5"
J. Phys. Chem. C 116 (2012) 24091-24097. (Chapter IV)

[4] K. Shimizu, K. Kon, M. Seto, K. Shimura, **H. Yamazaki**, J. N. Kondo
"Heterogeneous Cobalt Catalyst for Accepterless Dehydrogenation of Alcohols"
Green Chem. 15 (2013) 418-424.

[5] S. Inagaki, S. Shinoda, Y. Kaneko, K. Takechi, R. Komatsu, Y. Tsuboi, **H. Yamazaki**, J. N. Kondo, Y. Kubota
"Facile Fabrication of ZSM-5 Zeolite Catalyst with High Durability to Coke Formation during Catalytic Cracking of Paraffins"
ACS Catal. 3 (2013) 74-78.

[6] K. Shimizu, K. Kon, W. Onodera, **H. Yamazaki**, J. N. Kondo
"Heterogeneous Ni Catalyst for Direct Synthesis of Primary Amines from Alcohols and Ammonia"
ACS Catal. 3 (2013) 112-117.

[7] Y. Matsunaga, **H. Yamazaki**, T. Yokoi, T. Tatsumi, J. N. Kondo
"IR Characterization of Homogeneously Mixed Silica−Alumina Samples and Dealuminated Y Zeolites by Using Pyridine, CO, and Propene Probe Molecules"
J. Phys. Chem. C 117 (2013) 14043-10450.

[8] H. Yamazaki, H. Shima, E. Yoda, J. N. Kondo
"Estimation of the real temperature of samples in IR cell using OH frequency of silica"
In preparation. (Chapter II)

[9] H. Yamazaki, T. Yokoi, T. Tatsumi, J. N. Kondo
"Kinetic study on the reaction of methoxy species and olefins on H-ZSM-5 zeolite"
In preparation. (Chapter V)

[10] H. Yamazaki, T. Yokoi, T. Tatsumi, J. N. Kondo
"Infrared study on the behavior of ethoxy species on H-ZSM-5: ethene oligomerization and decomposition of ethoxy species"
In preparation. (Chapter VI)

Acknowledgments

It is a great pleasure for the author to express his sincere gratitude to Professor Takashi Tatsumi and Associate Professor Junko N. Kondo for their helpful, fruitful guidance and discussions, and encouragement throughout the course of this study.

The author is grateful to Assistant Professor Toshiyuki Yokoi for their fruitful and constructive suggestions, and supporting various things at a laboratory.

He is also grateful to Professor Seitaro Namba for his fruitful and constructive advices.

The author is grateful to Associate Professor Yusuke Yoshinaga for teaching knowledge and techniques for study and introducing me to the Tatsumi-Nomura laboratory.

The author is grateful to his contemporaries, Mr. Ryoichi Otomo, Mr. Hiroshi Mochizuki and Mr. Min Liu for working hard together and encouragement.

Thanks are due to Ms. Kazuko Iwane, Dr. Masato Yoshioka, Lecturer Hiroyuki Imai, Dr. Hisashi Shima and all members in Tatsumi-Nomura laboratory for encouragement a lot.

Finally, the author expresses sincere gratitude to his parents, Mr. Yuji Yamazaki and Mrs. Mayumi Yamazaki, and his brothers, Mr. Takao Yamazaki and Mr. Shinsuke Yamazaki, for heartfelt encouragement during the study and his life up to now.

March 2014

Hiroshi Yamazaki

Appendix I

Intra-molecular H/D Exchange of Ethanol Catalyzed by Acidic OH Groups on H-ZSM-5 Zeolite

1. Introduction

Zeolites are crystalline microporous silicates and are well known as a representative family of solid acid catalysts when some Si sites are substituted by Al. Active sites of zeolite catalysts originate from Brønsted acidic OH groups bridging to Si and Al, and zeolites are of practical importance especially in the field of petrochemistry [1]. Acidic OH groups on zeolites are directly observable by infrared (IR) spectroscopy [2] and nuclear magnetic resonance (NMR) [3]. So far, various types of interactions with hydrocarbons, oxygenate compounds and so on have been investigated as well as their behaviour alone. Among a series of IR studies, we have examined adsorption of alcohol and formation of alkoxy species accompanied by dehydration on acidic OH groups of zeolites [4]. Alcohols interact with zeolite OH groups by forming hydrogen-bonding as illustrated in Figure 1. In case of ethanol, it first adsorbs molecularly (Figure 1), and dehydration in vacuum at temperatures approximately above 453 K generates an ethoxy group [4]. Ethoxy species finally decompose to ethane leaving one of hydrogen atoms to regenerate surface hydroxyl groups [5]. As a whole, the dehydration of ethanol to ethane is catalyzed by acidic OH groups. During our effort for the clarification of the detailed mechanism above using isotope-labeled ethanol, the occurrence of intra-molecular H/D isotope exchange reaction from CD_3CH_2OH to CHD_2CH_2OD on acidic OH groups on zeolites was found, which is explained below.

2. Experimental

H-ZSM-5, JRC-Z5-90H (Si/Al = 45), was provided by Catalysis Society of Japan. Ethene (99.9%, Takachiho Chemical Industries, Inc.) and two ethanol; CH_3CH_2OH (99.8%, Wako Pure

Chemical Industries, Itd.) and CH_3CD_2OH (98%, Sigma-Aldrich Co. LLC.), were used. The self-supporting disk of H-ZSM-5 was place in a quartz cell, attached to a conventional closed-gas circulation system. The sample was heated up to 773 K under evacuation and was maintained its temperature for one hour. FT-IR spectra were recorded using a Jasco 4100 FT-IR spectrometer equipped with a mercury cadmium telluride (MCT) detector at a resolution of 4 cm^{-1} and a typical average of 64 scans. FT-IR spectra of the pretreated disk recorded at several temperatures were used as background spectra. Background-subtracted IR spectra showing adsorbed species are presented throughout this chapter.

3. Results and discussion

Ethanol molecules are adsorbed no acidic OH groups on zeolites by forming hydrogen-bond at two adjacent places as illustrated in Figure 1 (CD_3CH_2OH and CH_3CD_2OH) [4,5], where OH groups of ethanol and zeolites are regarded as equivalent and exchangeable at room temperature [6]. Adsorption of both CD_3CH_2OH and CH_3CD_2OH will be accompanied by dehydration (H_2O) at temperatures higher than 423 K in evacuation to form CD_3CH_2O and CH_3CD_2O ethoxy species, respectively (Figure 1). The time course of spectral change of ethanol molecules adsorbed on H-ZSM-5 zeolite at 323 K is shown in Figure 2. These spectra were measured under evacuation after CD3CH2OH was supplied. Since a background spectrum measured before ethanol adsorption is subtracted, a negative band appeared at around 3600 cm^{-1} due to the decrease of isolated acidic OH groups of H-ZSM-5. Alternatively, an extremely broad band ranging from 3200 to 1400 cm^{-1} and below was observed, which is attributed to the hydrogen-bonded OH groups of the zeolite [7]. The other OH band at 3600-3400 cm^{-1} is assigned to OH groups of ethanol. Other bands attributed to CD_3 and H_2 groups of adsorbed CD_3CH_2OH molecules were also observed at 2400-2200 cm^{-1} and 3000-2800 cm^{-1}, respectively. The occupancy of OH groups of H-ZSM-5 was estimated as about 90 % by the decrease of the isolated acidic OH band. At the beginning absorption region of OD groups (2800-2400 cm^{-1}) was silent, but a new band appeared and increased in intensity in the

time course (dotted line in Figure 2). The top spectrum was obtained by subtraction of a spectrum measured at 5 min and that at 60 min after CD_3CH_2OH adsorption, which emphasizes the spectral change from 5 to 60 min. The increase of CH and OD stretching bands in intensity is recognized as well as the decrease of CD and OH stretching bands, indicating the conversion of CD and OH to CH and OD. The frequency of the generated OD band corresponds to OH band of ethanol. Therefore, intra-molecular isotope exchange from CD_3CH_2OH to CHD_2CH_2OD seems to proceed. However, it should be reminded that hydroxyl groups of alcohols and zeolites are exchangeable in structures of alcohol adsorption (Figure 1). Thus, OH groups on H-ZSM-5 should be also exchanged to OD in equivalent amount to that of ethanol (Figure 3). A careful look at the top spectrum in Figure 2 notifies the decrease of the broad band at around 1600 cm^{-1} in intensity, which is attributed to the hydrogen-bonded OH groups of H-ZSM-5. The resultant hydrogen-bonded OD band is expected to appear at 2300-1000 cm^{-1} in stronger intensity at lower frequency region. Such a band overlaps with IR absorption of zeolite (SiO_2), and is not evident, although the slight upward band (around 1400 cm^{-1}) in the subtracted spectrum in Figure 2 may reflect the presence of OD band of D-ZSM-5. Therefore, the apparent intra-molecular isotope exchange reaction can be regarded as mediated by the acidic OH groups of H-ZSM-5 zeolite.

In order to get insight of the apparent intra-molecular isotope exchange reaction of ethanol on acidic OH groups of zeolite, adsorption of CH_3CD_2OH was conducted. CH_3CD_2OH was adsorbed at 323 K followed by evacuation at the same temperature. Similarly to spectra in Figure 2, background-subtracted spectra are arrayed in the time course in Figure 4. A broad band due to the hydrogen-bonded OH groups of H-ZSM-5 was observed at 3200-1400 cm^{-1} and below was observed, in addition to OH, CH_3 and CD_2 stretching and CH_3 deformation bands of CH_3CD_2OH adsorbed on OH groups of H-ZSM-5 as indicated in Figure 4. These bands are resulted from the adsorption structure in Figure 1 (bottom scheme). No spectral changes were evident during the time course for 60 min, as clearly confirmed by the subtracted spectrum of that at 5 min from that at 60 min in Figure 4. Accordingly, only a-hydrogen was found to be isotope-exchanged with OH groups

of zeolite, followed by that with OH groups of the adsorbed ethanol. The absence of H/D isotope exchange during adsorption of CD_3OH and successive methoxy (CD_3O) formation [5] on zeolites supports the above conclusion.

While detailed reaction mechanism is not yet clear, it is most probably proceed via the concerted mechanism as depicted in Figure 5. One of the a-D atoms has the interaction with a lattice oxygen next to Al, accompanied by a simultaneous interaction of a-carbon with the acidic H. Then, isotope exchange of CD and OH of the acid site first occur to CH and OD, followed by the equilibrium of the adsorption of CHD_2CH_2OH on OD and CHD_2CH_2OD on OH (two structure in Figure 5). The isotope exchange of CD_3CH_2OH to CHD_2CH_2OD via intra-molecular dehydration and re-hydration of ethene is one of the candidates.

CD_3CH_2OH –> $CD_2=CH_2$ + HDO –> CHD_2CH_2OD

However, experimental facts exclude the possibility. First, ethanol adsorbs on zeolites only molecularly at temperatures below 373 K [4,7]. Further heating at above 423 K results in dehydration between ethanol molecules and acidic OH groups to form surface alkoxy groups [4,8]. Then, ethane is evolved at slightly higher temperatures than dehydration [4]. Therefore, the first step of the above reaction scheme (intra-molecular dehydration) does not occur under the present experimental conditions. Furthermore, ethene adsorption at 323 K results in oligomerization [9] even in the co-presence of water (Not shown for simplicity). Accordingly, "intra-molecular dehydration and rehydration mechanism" for the present isotope exchange reaction from CD_3CH_2OH to CHD_2CH_2OD on H-ZSM-5 is disqualified.

Acidic OH groups bridging to Si and Al are essential for this reaction because it did not proceed over silicatlite nor a TS-1 titanoshilicate, which have the same zeolite topology. In addition, since such a reaction did not take place over amorphous silica-aluminas, zeolite structure was found to play an important role. Next, the adsorption and the behavior of CD_3CH_2OH were observed on Al-containing H-form zeolites with various topologies as listed in Table 1. Among the zeolites tested only BEA structure allowed the apparent intra-molecular isotope exchange reaction from

CD_3CH_2OH to CHD_2CH_2OD on acidic OH groups in addition to **MFI** (H-ZSM-5). It is known that the acid strength of zeolites with **FER**, **MFI**, **MOR** and **CHA** is strong, while that with **BEA**, **RTH** and **FAU** is weak [11]. Thus, the strong acidity cannot be the origin of the reaction. It is noticed from Table 1 that both zeolites with **MFI** and **BEA** topologies have similar maximum pore diameters and the same pore dimension (3D). Therefore, suitable zeolitic structures seem to be necessary for the present isotope exchange reaction, although details are still under investigation.

4. Conclusions

IR observation of ethanol adsorption clarified the presence of the apparent intra-molecular isotope exchange from CD_3CH_2OH to CHD_2CH_2OD on acidic OH groups of H-ZSM-5 zeolite. This reaction did not proceed with CD_3OH nor CH_3CD_2OH, implying that the β-hydrogen of alcohol had interaction with the lattice oxygen adjacent to Al, and that the reaction was mediated by isotope exchange of CD_3 groups and OH groups on zeolite.

References:

[1] W. Vermeiren, J.-P. Gilson, Top. Catal. 52 (2009) 1131.

[2] G. Busca, Chem. Rev. 107 (2007) 5366.

[3] W. Wang, A. Buchholt, M. Seiler, M. Hunger, J. Am. Chem. Soc. 125 (2003) 15260.

[4] H. Yamazaki, H. Shima, H. Imai, T. Yokoi, T. Tatsumi, J. N. Kondo, Angew. Chem. Int. Ed. 50 (2011) 1853.

[5] J. N. Kondo, D. Nishioka, J. Kubota, K. Domen, J. Phys. Chem. C 114 (2010) 20107.

[6] F. Haase, J. Sauer, *J. Am. Chem. Soc.* 1995, **117**, 3780.

[7] C. Paz, S. Bordiga, C. Lamberti, M. Salvalaggio, A. Zecchina, G. Bellussi, J. Phys. Chem. B 101 (1997) 4740.

[8] W. Wang, J. Jiao, S. S. Ray, M. Hunger, ChemPhysChem. 6 (2005) 1467.

[9] G. Spoto, S. Bordiga, G. Ricchiardi, D. Scarano, A. Zecchina, E. Borello, J. Chem. Soc., Faraday Trans. 90 (1994) 2827-.

[10] Database of Zeolite Structure, Structure Comission of the International Zeolite Association; http://www.iza-structure.org/databases/.

[11] K. Suzuki, T. Noda, N. Katada, M. Niwa, J. Catal. 250 (2007) 151-.

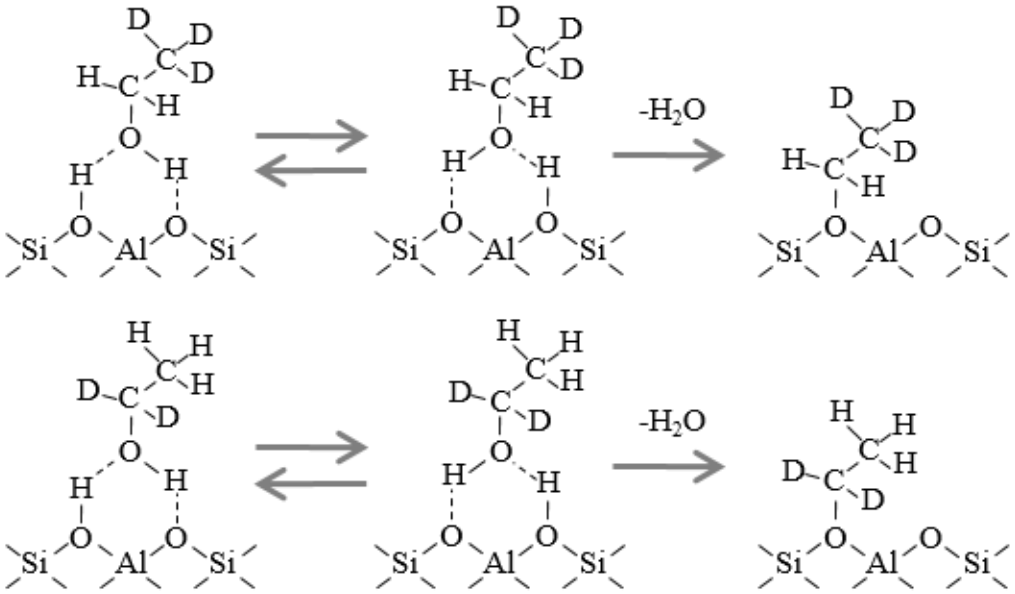

Figure 1. Adsorption structures of CD_3CH_2OH and CH_3CD_2OH and formation of ethoxy species on H-ZSM-5.

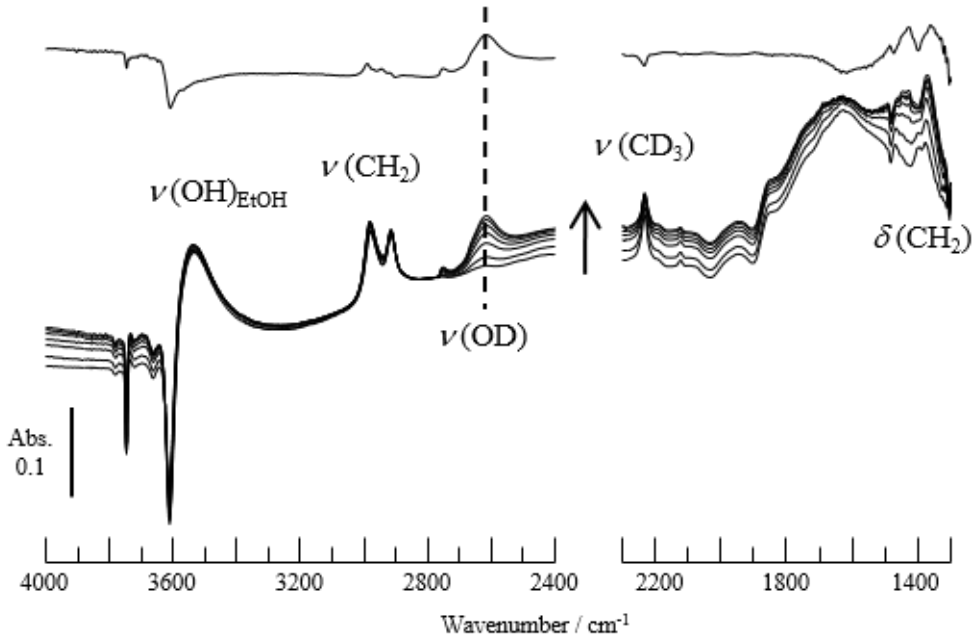

Figure 2. Time course of subtracted IR spectra of CD_3CH_2OH on H-ZSM-5 from 5 to 60 min at 323 K under evacuation. The upper spectrum is obtained by subtraction of spectrum at 5 min from that at 60 min.

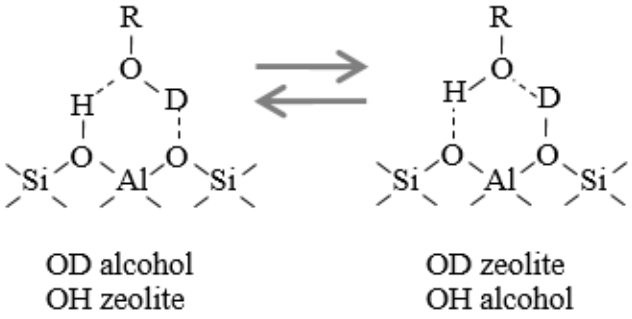

Figure 3. Isotope exchange of hydroxy groups of alcohol and zeolite.

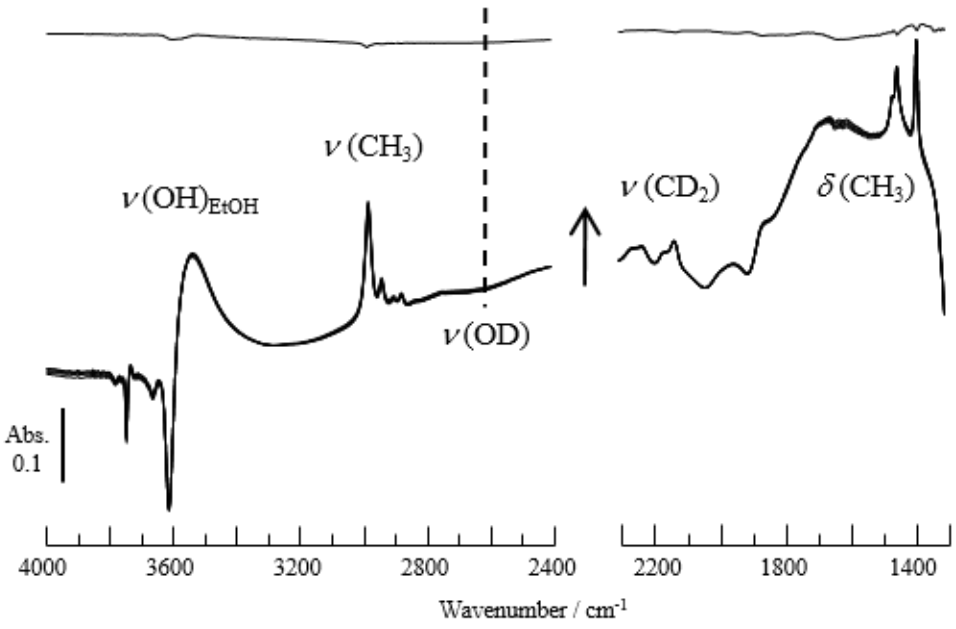

Figure 4. Time course of subtracted IR spectra of CH_3CD_2OH on H-ZSM-5 from 5 to 60 min at 323 K under evacuation. The upper spectrum is obtained by subtraction of spectrum at 5 min from that at 60 min.

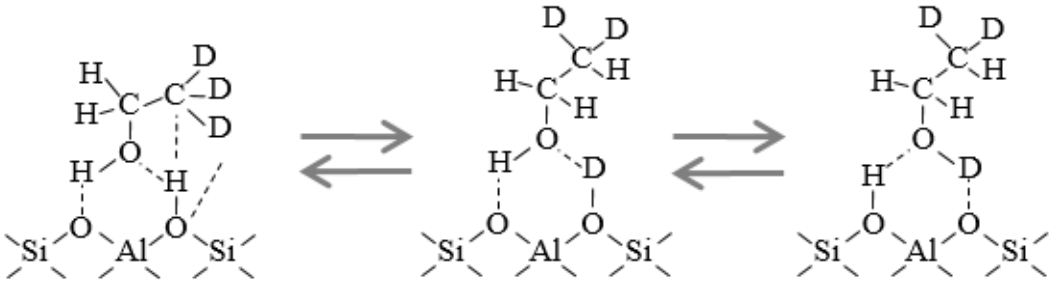

Figure 5. Proposed mechanism of isotope exchange of CD_3CH_2OH to CDH_2CH_2OD on the acidic OH group on H-ZSM-5.

Table 1. Comparison of structure of zeolites with different topologies [10].

Topology	Maximum pore diameter /Å	Ring size	Pore dimension	Si/Al ratio
FER	6.31	10, 8, 6, 5	2D	10
MFI	6.36	10, 6, 5, 4	3D	45
BEA	6.68	12, 6, 5, 4	3D	12.5
MOR	6.70	12, 8, 5, 4	1D	45
CHA	7.37	8, 6, 4	3D	46
RTH	8.18	8, 6, 5, 4	2D	50
FAU	11.24	12, 6, 4	3D	2.8